Ministry for Primary Industries
Manatū Ahu Matua

Abundance and distribution of ECSI Hector's dolphin – Supplementary material

New Zealand Government

Growing and Protecting New Zealand

Requests for further copies should be directed to:

Publications Logistics Officer
Ministry for Primary Industries
PO Box 2526
WELLINGTON 6140

Email: brand@mpi.govt.nz
Telephone: 0800 00 83 33
Facsimile: 04-894 0300

This publication is also available on the Ministry for Primary Industries websites at:
http://www.mpi.govt.nz/news-resources/publications.aspx
http://fs.fish.govt.nz go to Document library/Research reports

TABLE OF CONTENTS

OVERVIEW

This report contains supplementary material for MacKenzie, D.I.; Clement, D.M. (2014). Abundance and distribution of ECSI Hector's dolphin. *New Zealand Aquatic Environment and Biodiversity Report No. 123*. 79 p. It contains further details on the methods of analysis and results that are summarised in the main report. It also contains a comparison of sighting rates around Banks Peninsula with those of Rayment (2008) and responses to independent peer-reviews of the report.

References

Rayment, W. (2008). Distribution and ranging of Hector's dolphins: implications for protected area design. PhD Dissertation. University of Otago, Dunedin, New Zealand. 221 p.

SECTION A

Statistical details of mark-recapture distance sampling method

Background

Mark-recapture distance sampling (MRDS) is a technique that can be used to estimate abundance by having (at least) two observers survey for individuals and recording the distance (and other potential covariates) to the detected individuals. Following the survey the records are compared to determine which individuals have been detected by either or both observers. Determination of which individual was detected by each observer is a form of a mark-recapture experiment, with the recorded distance information providing additional information on the capture, or detection, probability with an expectation that it would generally decline with distance. See Laake & Borchers (2004) or Buckland et al. (2010) for a fuller description.

The MRDS analysis used to estimate abundance of Hector's dolphin within 20 nmi along the east coast of the South Island (ECSI) involve two extensions of the general set of methods. The first is due to the survey design where not all distances are observable from the two observer positions inside the aircraft. Therefore, there are some distances for which the detection probability is zero for one or the other observer. Theoretically this is not a huge extension, although common methods of analysis (e.g., Program DISTANCE and the MRDS *R* package) are not designed for such a situation hence custom code needed to be developed.

The second extension is in how potential lack of independence between observers can be incorporated into the modelling. A lack of independence can be caused by observers responding to cues from other observers in the aircraft (e.g., if the rear observer notices movement from the forward observer when they have detected a group, the rear observer may search harder), or due to detection heterogeneity that is unexplained in the model.

Unaccounted for, a lack of independence can result in underestimates of abundance. Laake & Borchers (2004; and references therein) suggest an approach where a conventional distance sampling (CDS) model is specified for the probability of an individual (or group) being detected by at least one observer, and a second component is separately specified for the mark-recapture element of the data to model the detection probability for the individual observers. Taking such approach allows for 'point independence' where detections of the individuals are independent at a distance of 0, but have some form of dependence between the detection at greater distances. However, given the novel aspect of the sampling design noted above, such an approach is more difficult to implement. Buckland et al. (2010) took an alternative approach by noting that if $p_F(d_i)$ is the probability of the forward observer detecting the *i*th group at distance d_i, and $p_R(d_i)$ is the probability of the rear observer detecting the same group, then under an assumption of full independence, the probability of both observers detecting the group should be $p_{FR}(d_i) = p_F(d_i)p_R(d_i)$. To allow for a lack of independence, Buckland et al. (2010) define $p_{FR}(d_i)$ to be:

$$p_{FR}(d_i) = \delta(d_i)p_F(d_i)p_R(d_i) \qquad (1)$$

where $\delta(d_i)$ is a measure of dependence, with $\delta(d_i) = 1$ for all distances implying full independence, and some form of dependence otherwise. Hence, the probability of the group being detected by at least one individual is:

$$p_\bullet(d_i) = p_F(d_i) + p_R(d_i) - \delta(d_i)p_F(d_i)p_R(d_i) \qquad (2)$$

However, with this parameterization there are limits on the possible values of $\delta(d_i)$ that depend upon the values of $p_F(d_i)$ and $p_R(d_i)$. It has been our experience in other situations using similar approaches (species co occurrence modelling; MacKenzie et al. 2004, 2006) that such a parameterisation can have convergence issues because of these limits. The simulation results of Buckland et al. (2010) also suggest they may have had similar issues with a very high degree of correlation between parameter estimates from some simulated datasets. The approach developed for this analysis uses an alternative parameterisation to define (1) and (2) based upon odds ratios and conditional probabilities.

Methods
Let:

$p_F(d_i)$ = the probability of the *i*th group at distance d_i being detected by the front observer.

$p_{R|F}(d_i)$ = the probability of the *i*th group at distance d_i being detected by the rear observer given the group was detected by the front observer.

$p_{R|NF}(d_i)$ = the probability of the *i*th group at distance d_i being detected by the rear observer given the group was *not* detected by the front observer (*NF* = not front).

$v(d_i) = \dfrac{p_{R|F}(d_i)\big/\big(1 - p_{R|F}(d_i)\big)}{p_{R|NF}(d_i)\big/\big(1 - p_{R|NF}(d_i)\big)}$ = the odds ratio for the odds of detection by the rear observer given the group was detected by the front observer compared to the odds of detection by the rear observer given the group was not detected by the front observer.

The odds ratio, $v(d_i)$, has a similar interpretation to $\delta(d_i)$ in that a value of 1 implies full independence, i.e., detection of the group by the front observer has no effect on the odds (and therefore the probability) of detection by the rear observer. Other values would imply some form of dependence in the detections from the front and rear positions. An advantage of this parameterisation is that there are no limits placed on the allowable values for $v(d_i)$ that depend upon other parameters (although given that it is an odds ratio, it must take a value between 0 and infinity). It also fits naturally into analyses where the effect of covariates on detection (including distance) are incorporated via the logit link (e.g., logistic regression). That is:

$$\ln(v(d_i)) = \ln\!\left(\frac{p_{R|F}(d_i)\big/\big(1 - p_{R|F}(d_i)\big)}{p_{R|NF}(d_i)\big/\big(1 - p_{R|NF}(d_i)\big)}\right)$$

$$= \ln\!\left(\frac{p_{R|F}(d_i)}{\big(1 - p_{R|F}(d_i)\big)}\right) - \ln\!\left(\frac{p_{R|NF}(d_i)}{\big(1 - p_{R|NF}(d_i)\big)}\right)$$

$$= \mathrm{logit}\big(p_{R|F}(d_i)\big) - \mathrm{logit}\big(p_{R|NF}(d_i)\big)$$

hence

$$\mathrm{logit}\big(p_{R|F}(d_i)\big) = \mathrm{logit}\big(p_{R|NF}(d_i)\big) + \ln(v(d_i)) \qquad (3)$$

That is, on the logit scale, the probability of the rear observer detecting a group is greater by an amount $\ln(v(d_i))$ when the front observer detects a group than when they did not.

Therefore we could express the probability of the rear observer detecting the ith group at distance d_i as:

$$\text{logit}(p_R(d_i)) = f(d_i) + g(d_i)X_F \qquad (4)$$

where $f(d_i)$ and $g(d_i)$ are some functions of distance, and X_F is an indicator variable for whether the group was detected from the front observer position or not. That is, dependence between detection can be accounted for by including the observations from the front position (detected or not) as covariate, along with potential interactions, for the detection probability for the rear observer.

Using $g(d_i) = \gamma_0 + \gamma_1 d_i$ enables a range of models to be fit to the data. Estimating both γ_0 and γ_1 allows for limiting independence, e.g., Buckland et al. (2010), with the detections of the observers deemed to be independent at a distance of $-\gamma_0/\gamma_1$. Point independence at $d = 0$ is achieved by setting $\gamma_0 = 0$ and full independence of observers is achieved when $\gamma_0 = \gamma_1 = 0$. A constant (with respect to distance) level of dependence between the observers occurs when $\gamma_1 = 0$.

Based on this parameterisation, (2) becomes:

$$p_\bullet(d_i) = p_F(d_i) + (1 - p_F(d_i))p_{R|NF}(d_i) \qquad (5)$$

and the unconditional probability of detection for the rear observer is:

$$p_R(d_i) = p_F(d_i)p_{R|F}(d_i) + (1 - p_F(d_i))p_{R|NF}(d_i). \qquad (6)$$

Following this, MRDS methods can be applied as usual by developing likelihood statements for the mark-recapture (MR) and distance sampling (DS) components and obtained parameter estimates by maximising the joint likelihood (e.g., Buckland et al. 2010).

The MR likelihood component is:

$$L_{MR} = \prod_{i=1}^{n} \frac{\Pr(\omega_i | d_i)}{p_\bullet(d_i)} \qquad (7)$$

where ω_i is the observed combination of detection from the observers; (1,1), (1,0) or (0,1), and:

$$\Pr(\omega_i = (1,1)|d_i) = p_F(d_i)p_{R|F}(d_i),$$
$$\Pr(\omega_i = (1,0)|d_i) = p_F(d_i)(1 - p_{R|F}(d_i)) \text{ and}$$
$$\Pr(\omega_i = (0,1)|d_i) = (1 - p_F(d_i))p_{R|NF}(d_i)$$

The DS likelihood component is:

$$L_{DS} = \prod_{i=1}^{n} \frac{p_\bullet(d_i)}{E(p_\bullet)} \qquad (8)$$

where $E(p_\bullet) = \int_o^w \pi(y)p_\bullet(y)dy$, w is the half width of the surveyed transect and $\pi(d_i)$ is the probability density function for distances of groups from the line, which is $1/w$ given the random placement of transects.

Following maximisation of $L_{MR} \times L_{DS}$ to gain the parameter estimates of the detection function, abundance estimates can be obtained in the usual manner. The methods detailed below also incorporate availability into the estimate of abundance, where availability estimates may be stratum-specific. The number of available dolphins within the area of stratum k covered by the surveys is estimated using a Horvitz-Thomson type estimator, i.e.,

$$\hat{N}_{ck} = \sum_{i=1}^{n_k} \frac{s_i}{E(p_\bullet(s_i))} \tag{9}$$

where n_k is the number of groups detected in the stratum, s_i is the size of the ith group and $E(p_\bullet(s_i))$ is the expected probability of the ith group being detected given its size, which is obtained from the detection function analysis.

The number of *available* dolphins (i.e., near the surface with a non-zero chance of detection by the observers in the plane) within the stratum is therefore

$$\hat{N}_{\alpha k} = \frac{A_k \hat{N}_{ck}}{a_k} \tag{10}$$

where, A_k is the total area of the stratum; $a_k = 2wL_k$ is the area covered by the survey transects with w being the truncated width (0.3 km) and L_k the total transect length flown. Accounting for availability, that total number of dolphins within a stratum is therefore:

$$\hat{N}_k = \frac{\hat{N}_{\alpha k}}{\hat{P}_{\alpha k}} \tag{11}$$

with total abundance being

$$\hat{N} = \sum_{k=1}^{K} \hat{N}_k \tag{12}$$

Following Buckland et al. (2010), the standard error for the stratum specific estimates was calculated as:

$$SE(\hat{N}_k) = \sqrt{\left(\frac{A_k}{\hat{P}_{\alpha k} a_k}\right)^2 \left\{ L_k \sum_{j=1}^{J_k} \frac{l_j \left(\hat{N}_{cj}/l_j - \hat{N}_{ck}/L_k\right)^2}{J_k - 1} + \hat{g}_k^T \hat{H}^{-1} g_k \right\} + \left(\frac{\hat{N}_k}{\hat{P}_{\alpha k}}\right)^2 SE(\hat{P}_{\alpha k})^2}$$

where l_j is the length of the jth transect line in stratum k, J_k is the number of lines in the stratum, $\hat{N}_{cj}$ is the estimated number of dolphins in the covered region along transect j, $\hat{g}_k$ is the vector of partial derivatives, $\partial \hat{N}_{ck}/\partial \theta_m$, for the θ_m parameters in the detection function and $\hat{H}$ is the Hessian matrix (i.e., matrix of second partial derivatives of the negative log-likelihood function). Note that the standard error consists of three components; one due to among line variation in abundance (involving the inner summation term), and one due to estimation uncertainty of the parameters in the detection function (associated with the Hessian matrix) and one due to uncertainty in the estimated availability.

Given that some strata share parameters (either through the detection function or availability estimates), the standard errors from the stratum-specific abundance estimates cannot be

simply combined to obtain the standard error for total dolphin abundance. The standard error for total abundance was calculated as:

$$SE(\hat{N}) = \sqrt{\sum_{k=1}^{K}\left(\frac{A_k}{\hat{P}_{\alpha k}a_k}\right)^2 \left\{ L_k \sum_{j=1}^{J_k} \frac{l_j\left(\hat{N}_{cj}/l_j - \hat{N}_{ck}/L_k\right)^2}{J_k - 1}\right\} + \hat{\mathbf{g}}^T \mathbf{H}^{-1}\hat{\mathbf{g}} + \hat{\mathbf{h}}^T \mathbf{V}\hat{\mathbf{h}}} \ ,$$

where $\hat{\mathbf{g}}$ is the vector of partial derivatives:

$$\frac{\partial \hat{N}}{\partial \theta_m} = \sum_{k=1}^{K} \frac{A_k}{\hat{P}_{\alpha k}a_k}\frac{\partial \hat{N}_{ck}}{\partial \theta_m} \ ,$$

$\hat{\mathbf{h}}$ is the $1 \times K$ vector of partial derivatives $\dfrac{\partial \hat{N}}{\partial \hat{P}_{\alpha k}}$ and $\mathbf{V}$ is variance covariance matrix of the stratum-specific availability estimates.

These standard error equations are extensions of the simpler form that are often used in distance sampling, e.g., $SE(\hat{N}) = \hat{N}\sqrt{\left(CV(\hat{N}_\alpha)\right)^2 + \left(CV(\hat{P}_\alpha)\right)^2}$, and arise through the application of the delta method (Williams et al. 2002).

All of the above can be generalised in the obvious manner if there are other covariates to include for the detection process.

References

Buckland, S.T.; Laake, J.L.; Borchers, D.L. (2010). Double-observer line transect methods: levels of independence. *Biometrics 66*: 169–177.

Laake, J.L.; Borchers, D.L. (2004). Methods for incomplete detection at distance zero. Pp. 108–189 in Advanced Distance Sampling, eds S.T. Buckland, D.R. Anderson, K.P. Burnham, J.L. Laake, D.L. Borchers and L. Thomas. Oxford University Press, Oxford.

MacKenzie, D.I.; Bailey, L.L.; Nichols, J.D. (2004). Investigating species co-occurrence patterns when species are detected imperfectly. *Journal of Animal Ecology 3*: 546–555.

MacKenzie, D.I.; Nichols, J.D.; Royle, J.A.; Pollock, K.H.; Bailey ,L.L.; Hines, J.E. (2006). Occupancy estimation and modeling : inferring patterns and dynamics of species occurrence. Elsevier, Amsterdam.

Williams, B.K.; Nichols, J.D.; Conroy, M.J. (2002). Analysis and management of animal populations. Academic Press, San Diego, CA, USA.

SECTION B

Simulation study on the performance of the detection function modelling.

A simulation study was performed to verify the performance of the detection function modelling to estimate the number of available groups within the area covered by the line transect surveys (see §A for details of the estimation methods).

Sighting data were simulated using four base detection functions (see Figure B.1). Each function involved a quadratic relationship between distance and detection (on the logistic scale). Function 1 is based upon the estimated relationship from the top-ranked model of the full, summer data analysis (see Table 5 of main report). Function 2, is the same as function 1 with an additional random error component to introduce unmodelled heterogeneity (which may be due to covariates not included in the estimating model). Note that both functions 1 and 2 are not monotonically decreasing with distance. Function 3 is monotonically decreasing with distance for both observer positions (with the same relationship), and function 4 is the same as 3 with additional random variation.

For each base detection function, four different levels of dependence were considered. Representing the form of dependence as $g(d_i) = \gamma_0 + \gamma_1 d_i$ (§A, Eqn 4), the levels were:

1. $\gamma_0 = \gamma_1 = 0$ (full independence)
2. $\gamma_0 = 1$ and $\gamma_1 = 0$ (constant dependence)
3. $\gamma_0 = 0$ and $\gamma_1 = 0.1$ (point independence)
4. $\gamma_0 = -1.4$ and $\gamma_1 = 0.1$ (limiting independence)

The effects of these forms of dependence are illustrated in Figures B.2–B.3 for base function 1. The size of the effects used here are similar to those observed in the analysis of the summer data.

A)

B)

C)

D)
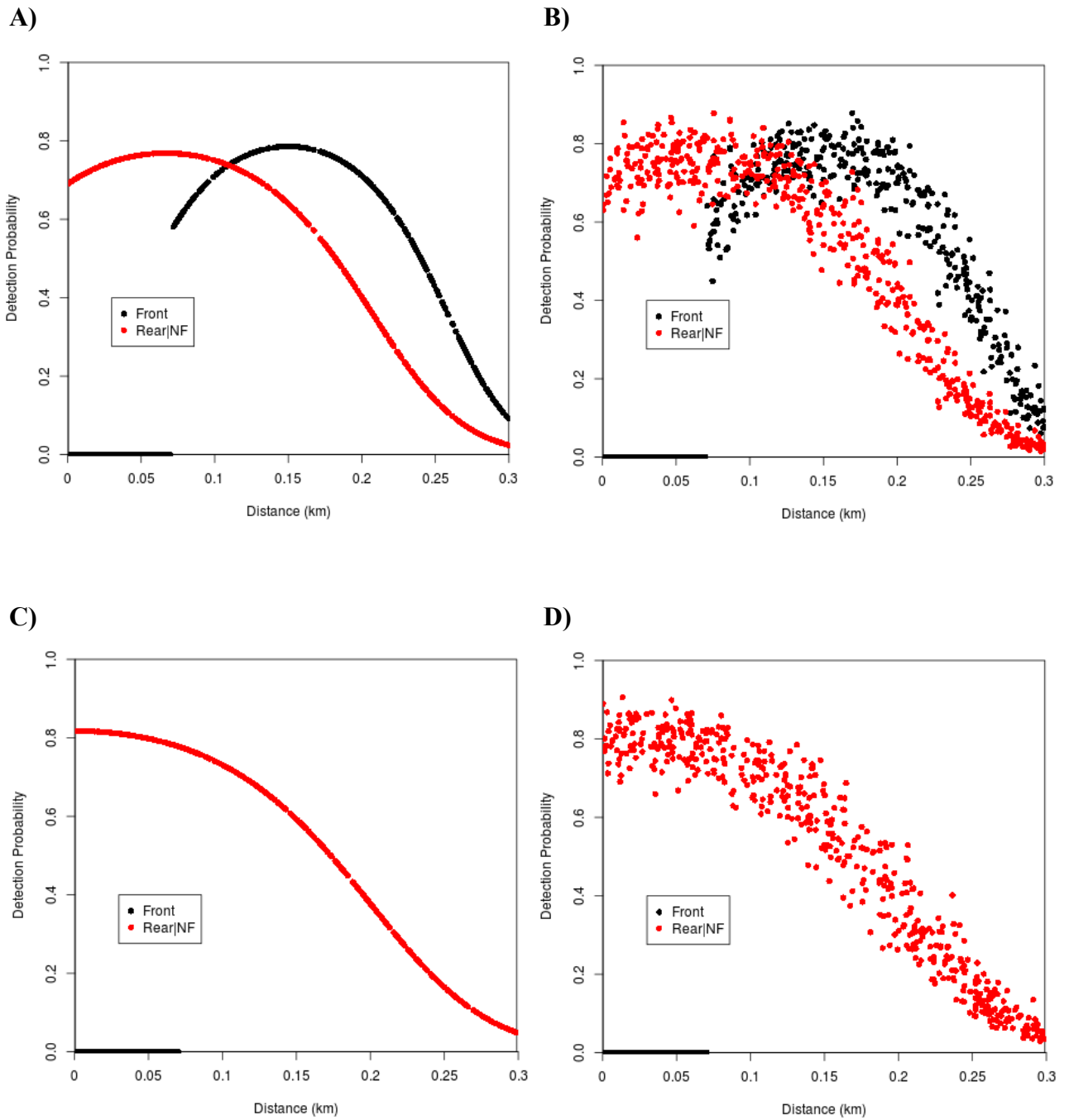
Figure B.1: Example of the first (A), second (B), third (C) and fourth (D) base detection functions used in the simulation study. Points represent the detection probability for 500 groups at a uniformly distributed, random distance from the transect line. Black points indicate the detection probability from the front observer position (Front), and red dots the probability of detection from the rear position, given not detected from the front position (Rear|NF).

.

A)

B)
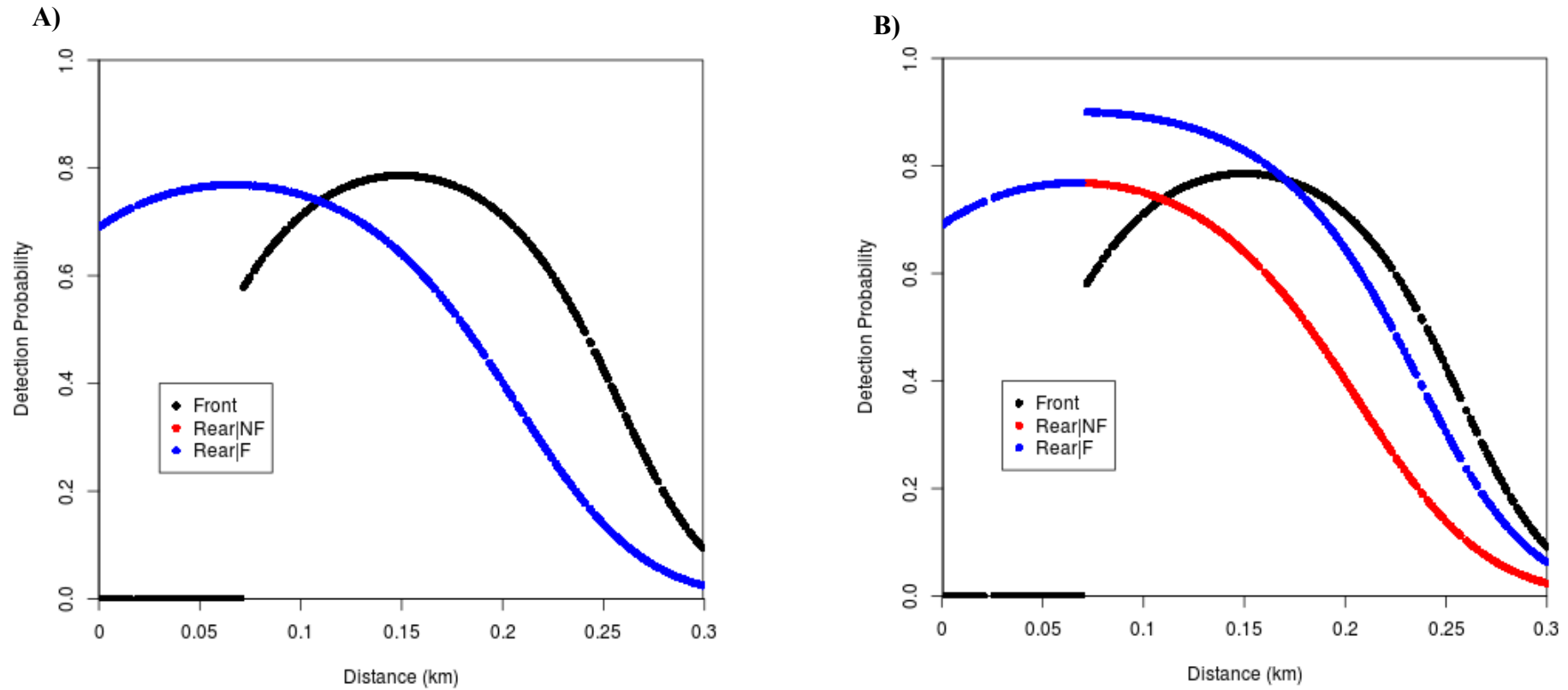
Figure B.2: **A) An example of the first level of dependence ($\gamma_0 = \gamma_1 = 0$; full independence) and B) an example of the second level of dependence ($\gamma_0 = 1$ and $\gamma_1 = 0$; constant dependence) with the first base detection function used in the simulation study. Points represent the detection probability for 500 groups at a uniformly distributed, random distance from the transect line. Black points indicate the detection probability from the front observer position (Front), red dots the probability of detection from the rear position, given not detected from the front position (Rear|NF), and blue dots the probability of detection from the rear position, given was detected from the front position (Rear|F). Note in example A that the blue dots overlap the red dots in this case.**
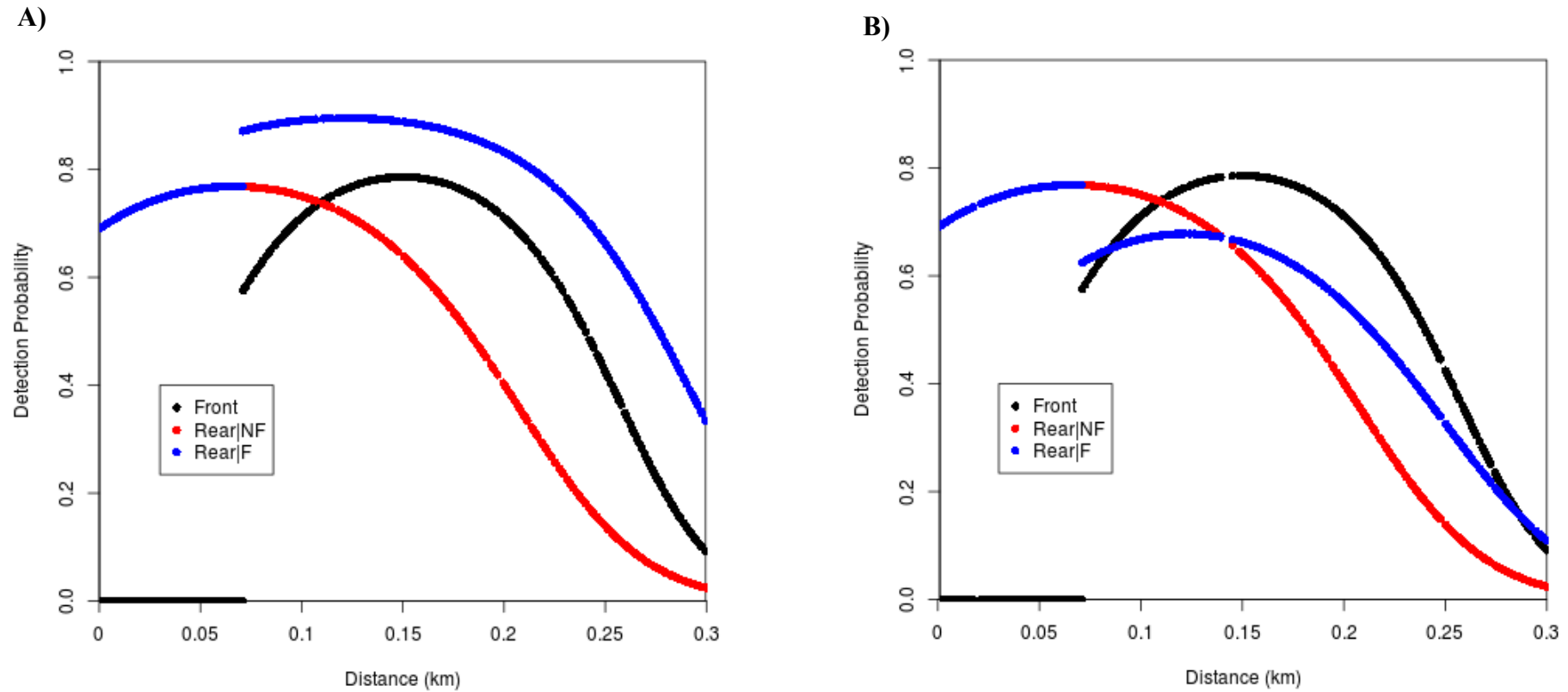
Figure B.3: **A) An example of the third level of dependence ($\gamma_0 = 0$ and $\gamma_1 = 0.1$; point independence) and B) an example of the fourth level of dependence ($\gamma_0 = -1.4$ and $\gamma_1 = 1$; limiting independence) with the first base detection function used in the simulation study. Points represent the detection probability for 500 groups at a uniformly distributed, random distance from the transect line. Black points indicate the detection probability from the front observer position (Front), red dots the probability of detection from the rear position, given not detected from the front position (Rear|NF), and blue dots the probability of detection from the rear position, given was detected from the front position (Rear|F).**

In total, 16 scenarios were considered with all combinations of base detection functions and levels of dependence. For each scenario, 1000 simulated data sets were created with 500 groups in the areas covered by the survey. For each simulated data set, distance from the trackline for each group was randomly selected from a uniform distribution with boundaries at 0 and 0.3 km. Each group could be detected from the front and/or rear observer position, with the probability of detection depending upon the group's distance and particular scenario being considered. To represent the field methods used, two data sets were created for analysis from each simulated set of data. The first involved the full data where the front observer could only make sightings between distances of 0.071–0.3 km while the rear observer could see between 0–0.3 km. The second data set excluded sightings from the rear observer position less than 0.071 km, and only used sightings for both observer positions between 0.071–0.3 km. In the latter case, distances were rescaled so that they took values between 0–0.229 km, and note that because of the truncation, the expected number of groups within the smaller surveyed area is 382, not 500.

Four models were fit to each simulated data set. All four models allowed a quadratic relationship between distance and detection that potential differed for each observer position (e.g., same general form as base function 1) and only differed in the form of dependence allowed; full independence, constant dependence, point independence or limiting independence. From the fitted detection function, the estimated abundance of groups within the covered region was estimated. The AIC values for each detection function model were used to obtain a model averaged estimate of abundance.

Buckland et al. (2010) explored the properties of an alternative parameterisation to account for limiting independence and noted that unrealistic estimates of abundance were obtained when the correlation between the estimated intercept term for the detection function model and the estimate intercept for the limiting independence term (i.e., $\hat{\gamma}_0$) approached -1. Similar results were obtained here for both the constant dependence and limiting independence estimation models (Figures B.4–B.5). This suggests that the correlation term can be a useful diagnostic to help identify whether a particular estimate could be unrealistically high. Interestingly, the issue of unrealistically high estimates was greater when the sighting data was truncated such that only detections between 0.071–0.3 km were used (Figure B.5), although a positive bias in estimated abundance is apparent for more moderate levels of negative correlation for the fuller data set where view-zones for each observer position only partially overlap (Figure B.4).

A)

B)
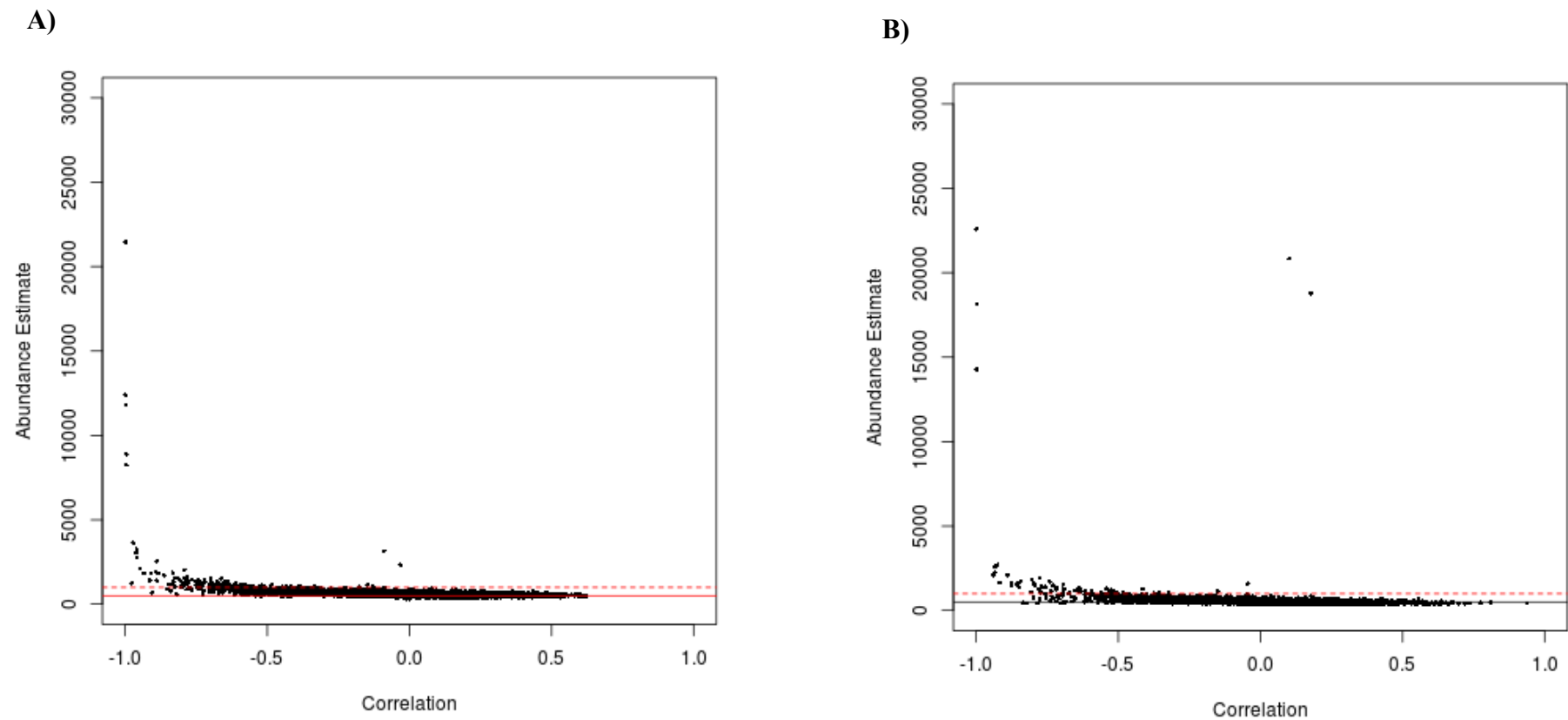
Figure B.4: Estimated group abundance within the area covered by the survey plotted against correlation between estimated intercept terms of detection and dependence functions; A) for the estimation model with constant dependence and B) for the estimation model with limiting independence. Results for all 16 scenarios where left truncation of 0.071 km and 0 km are used for the front and rear observer positions respectively, and right truncation of 0.3 km for both positions, are plotted. The solid red line indicates the true value of 500 groups, and dashed red line indicates 1000 groups.
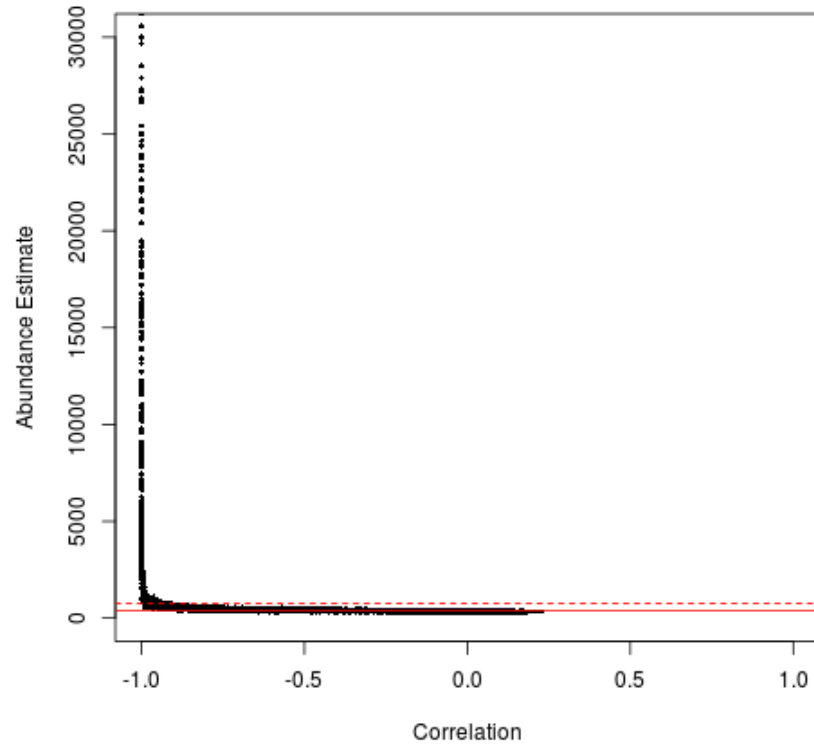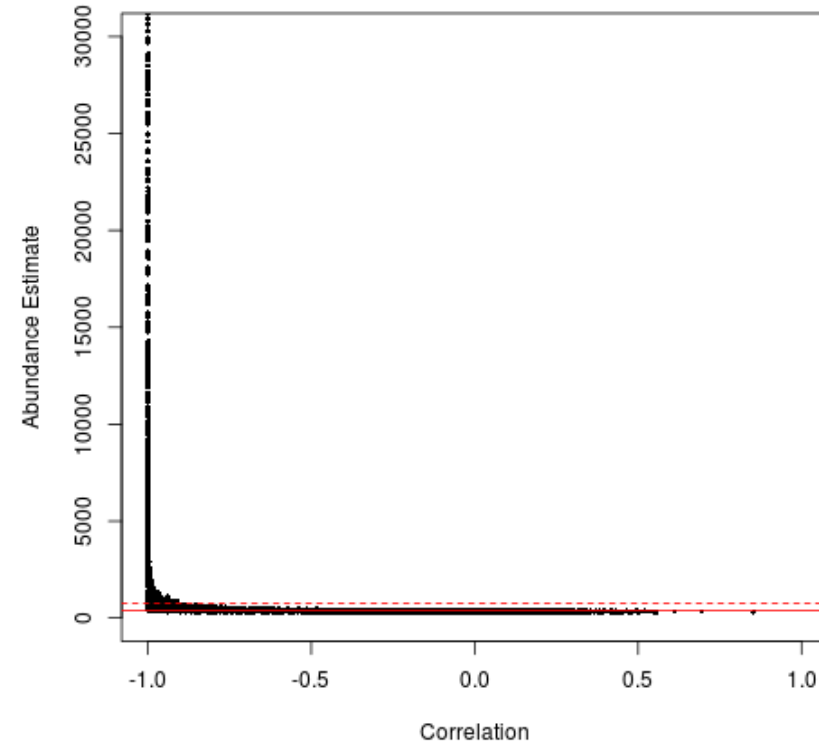
Figure B.5: Estimated group abundance within the area covered by the survey plotted against correlation between estimated intercept terms of detection and dependence functions; A) for the estimation model with constant dependence and B) for the estimation model with limiting independence. Results for all 16 scenarios where left truncation of 0.071 km and right truncation of 0.3 km was used for both positions are plotted. The solid red line indicates the true value of 382 groups, and dashed red line indicates 764 groups.

To reduce the effect of estimates that would be deemed unrealistic in a real data analysis, estimates that were greater than twice the true group abundance (500 and 382 for full and truncated data sets, respectively) were excluded from the results below. In addition, for some simulated data sets, the estimation procedure failed to produce valid standard errors (which also tended to be for unrealistically high abundance estimates); the associated estimates for these cases have also been excluded. The number of excluded results (out of 1000) are given in Tables B.1–B.2, with the average abundance estimate for each estimating model given in Tables B.3–B.4. A comparison of the average standard error with the standard deviation of the abundance estimates are given in Figure B.6, which theoretically, should be equal.

Table B.1: Number of cases excluded (out of 1000) for each scenario and estimation model for the fuller data sets where left truncation of 0.071 km and 0 km are used for the front and rear observer positions respectively, and right truncation of 0.3 km for both positions. Types of dependence are denoted as: FI = full independence, C = constant dependence, PI = point independence and LI = limiting independence.

Generating Model		Estimation Model			
Base	Dependence	FI	C	PI	LI
1	FI	0	1	0	8
	C	1	1	0	9
	PI	0	24	0	8
	LI	0	23	0	4
2	FI	0	2	0	7
	C	0	2	1	12
	PI	0	18	0	12
	LI	0	25	0	7
3	FI	0	0	0	3
	C	0	1	0	9
	PI	0	9	0	5
	LI	0	8	0	2
4	FI	0	0	0	4
	C	0	0	0	1
	PI	0	9	0	0
	LI	0	7	0	3

Table B.2: Number of cases excluded (out of 1000) for each scenario and estimation model for the reduced data sets where left truncation of 0.071 km and right truncation of 0.3 km was used for both positions. Types of dependence are denoted as: FI = full independence, C = constant dependence, PI = point independence and LI = limiting independence.

Generating Model		Estimation Model			
Base	Dependence	FI	C	PI	LI
1	FI	0	6	0	90
	C	0	7	0	86
	PI	0	169	2	53
	LI	0	193	0	83
2	FI	0	17	0	109
	C	0	15	0	103
	PI	0	201	2	59
	LI	0	213	0	68
3	FI	0	0	0	176
	C	0	1	0	195
	PI	0	299	0	155
	LI	0	262	0	179
4	FI	0	4	0	202
	C	0	8	0	199
	PI	0	330	0	134
	LI	0	281	0	168

Table B.3: Average of the included abundance estimates with percent bias indicated in brackets, for the fuller data sets where left truncation of 0.071 km and 0 km are used for the front and rear observer positions respectively, and right truncation of 0.3 km for both positions. Types of dependence are denoted as: FI = full independence, C = constant dependence, PI = point independence and LI = limiting independence. MA is the AIC-based model averaged abundance estimate.

Generating Model		Estimation Model				
Base	Dependence	FI	C	PI	LI	MA
1	FI	500 (0%)	512 (2%)	503 (1%)	516 (3%)	508 (2%)
	C	453 (-9%)	513 (3%)	478 (-4%)	517 (3%)	500 (0%)
	PI	426 (-15%)	588 (18%)	504 (1%)	514 (3%)	522 (4%)
	LI	491 (-2%)	594 (19%)	576 (15%)	515 (3%)	539 (8%)
2	FI	497 (-1%)	516 (3%)	504 (1%)	518 (4%)	510 (2%)
	C	450 (-10%)	516 (3%)	477 (-5%)	519 (4%)	503 (1%)
	PI	422 (-16%)	594 (19%)	501 (0%)	513 (3%)	522 (4%)
	LI	484 (-3%)	597 (19%)	575 (15%)	513 (3%)	537 (7%)
3	FI	503 (1%)	509 (2%)	504 (1%)	509 (2%)	506 (1%)
	C	441 (-12%)	507 (1%)	470 (-6%)	507 (1%)	492 (-2%)
	PI	416 (-17%)	581 (16%)	503 (1%)	503 (1%)	514 (3%)
	LI	503 (1%)	604 (21%)	590 (18%)	511 (2%)	542 (8%)
4	FI	496 (-1%)	513 (3%)	503 (1%)	508 (2%)	505 (1%)
	C	437 (-13%)	515 (3%)	470 (-6%)	513 (3%)	497 (-1%)
	PI	412 (-18%)	583 (17%)	501 (0%)	504 (1%)	514 (3%)
	LI	495 (-1%)	597 (19%)	583 (17%)	503 (1%)	532 (6%)

Table B.4: Average of the included abundance estimates with percent bias indicated in brackets, for the fuller data sets where left truncation of 0.071 km and right truncation of 0.3 km is used for both positions. Types of dependence are denoted as: FI = full independence, C = constant dependence, PI = point independence and LI = limiting independence. MA is the AIC-based model averaged abundance estimate.

Generating Model		Estimation Model				
Base	Dependence	FI	C	PI	LI	MA
1	FI	382 (0%)	394 (3%)	382 (0%)	413 (8%)	390 (2%)
	C	348 (-9%)	393 (3%)	366 (-4%)	405 (6%)	381 (0%)
	PI	322 (-16%)	477 (25%)	370 (-3%)	398 (4%)	408 (7%)
	LI	367 (-4%)	479 (25%)	406 (6%)	412 (8%)	420 (10%)
2	FI	379 (-1%)	397 (4%)	383 (0%)	409 (7%)	390 (2%)
	C	346 (-10%)	397 (4%)	365 (-4%)	406 (6%)	384 (0%)
	PI	318 (-17%)	483 (26%)	367 (-4%)	400 (5%)	406 (6%)
	LI	362 (-5%)	476 (25%)	404 (6%)	405 (6%)	414 (8%)
3	FI	383 (0%)	390 (2%)	382 (0%)	398 (4%)	386 (1%)
	C	335 (-12%)	389 (2%)	360 (-6%)	405 (6%)	375 (-2%)
	PI	304 (-20%)	493 (29%)	365 (-4%)	388 (1%)	404 (6%)
	LI	366 (-4%)	497 (30%)	410 (7%)	401 (5%)	424 (11%)
4	FI	377 (-1%)	391 (2%)	380 (0%)	401 (5%)	384 (1%)
	C	332 (-13%)	393 (3%)	360 (-6%)	402 (5%)	378 (-1%)
	PI	300 (-21%)	493 (29%)	363 (-5%)	396 (4%)	407 (6%)
	LI	359 (-6%)	494 (29%)	405 (6%)	393 (3%)	417 (9%)

Overall, there are no major causes for concern about the methods. While there tends to be a small positive bias for many scenarios, the degree of bias is small relative to the standard errors. Using a full independence estimation models tends to lead to a negative bias in estimated abundance when detections are not fully independent, and assuming constant dependence when there is actually point or limiting independence in detections leads to a severe positive bias. Interestingly, the results suggest that the estimation methods are robust to unmodelled heterogeneity in detection (i.e., results for base detection functions 1 and 3 are very similar to those of 2 and 4). That the standard error for the constant dependence and limiting independence estimation models (and consequently the model average estimates) tends to be too large in some scenarios for the reduced data set (Figure B.6b) is due to occasional, unrealistically large standard error values that would be clearly identifiable in an analysis of real data.

References

Buckland, S.T.; Laake, J.L.; Borchers, D.L. (2010). Double-observer line transect methods: levels of independence. *Biometrics 66*: 169–177.

A)
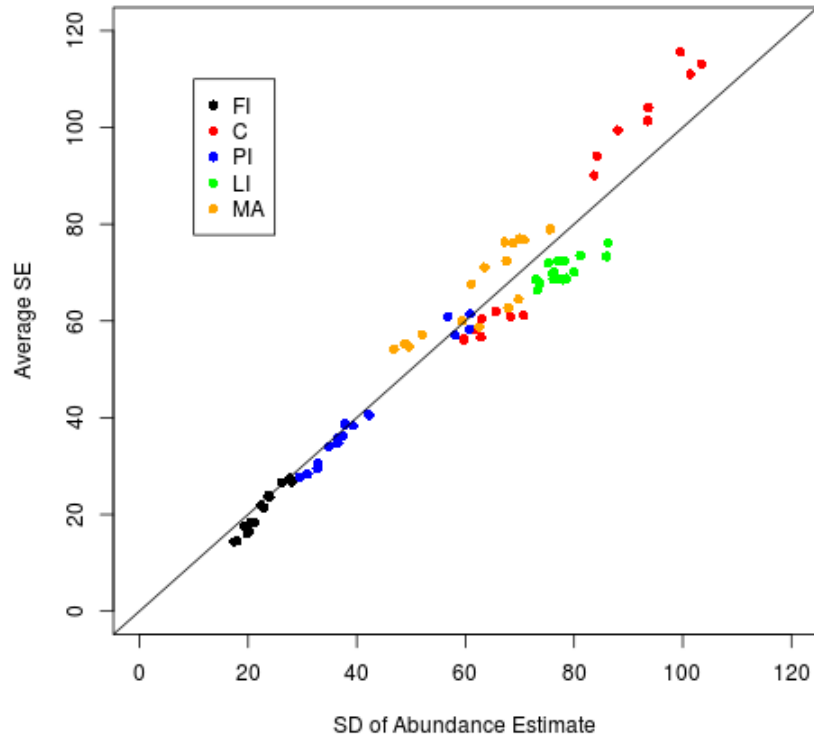
B)
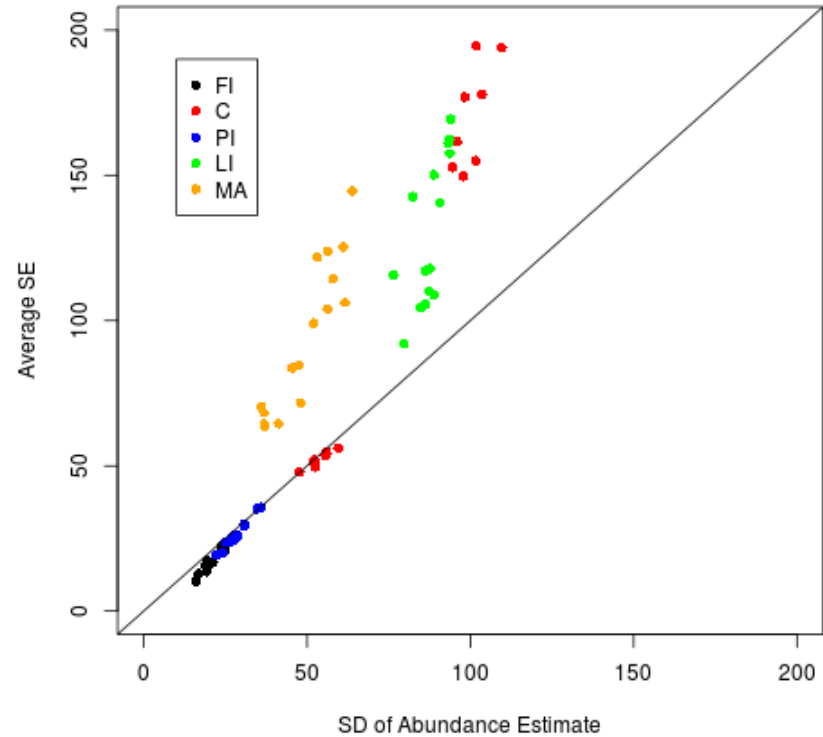
Figure B.6: Comparison of the average standard error with the standard deviation of the abundance estimates for the A) fuller data sets where left truncation of 0.071 km and 0 km are used for the front and rear observer positions respectively, and right truncation of 0.3 km for both positions and B) reduce data sets where left truncation of 0.071 km and right truncation of 0.3 km are used for both positions. Estimation models are denoted as: FI = full independence, C = constant dependence, PI = point independence, LI = limiting independence and MA = AIC-based model averaged estimate.

SECTION C

### Model Averaging

Model averaging is a technique to combine estimates and standard errors from a range of models and is often used when a number of different models all have substantial support from the data which leads to model selection uncertainty (Burnham & Anderson 2002, Anderson 2008).

Given a set of model weights, w, which sum to 1 and indicate the level of support for each of the M models being considered, a model averaged estimate of the quantity θ can be calculated as:

$$\hat{\theta}_A = \sum_{m=1}^{M} w_m \hat{\theta}_m$$

Extending the variance equation from Anderson (2008) in the obvious manner, the covariance for two model averaged quantities $\hat{\theta}_A$ and $\hat{\delta}_A$ can be calculated as

$$Cov\left(\hat{\theta}_A, \hat{\delta}_A\right) = \sum_{m=1}^{M} w_m \left\{ Cov\left(\hat{\theta}_m, \hat{\delta}_m | g_m\right) + \left(\hat{\theta}_m - \hat{\theta}_A\right)\left(\hat{\delta}_m - \hat{\delta}_A\right) \right\},$$

where $Cov\left(\hat{\theta}_m, \hat{\delta}_m | g_m\right)$ is the covariance for the two quantities under model g_m.

The standard error for a single quantity is then

$$SE\left(\hat{\theta}_A\right) = \sqrt{Cov\left(\hat{\theta}_A, \hat{\theta}_A\right)}.$$

References

Anderson, D.R. Model based inference in the life sciences. 2008. Springer. New York, USA.

Burnham, K.P.; Anderson, D.R. (2002). Model selection and multimodel inference. 2nd Ed., Springer-Verlag, New York, USA.

SECTION D

Sightings of other marine mammal species

Table D.1: Sighting summary of all other marine mammal and non-marine mammal species recorded by observers during both the summer and winter surveys.

Species	Summer # Sightings	Summer # Individuals	Winter # Sightings	Winter # Individuals
Bottlenose dolphin	3	44	1	1
Common dolphin	16	1072	4	62
Dusky dolphin	26	2825	78	4543
Killer whale	1	5	2	2
Pilot whales	1	2	0	0
Possible hourglass dolphin	0	0	1	1
Unidentified dolphin	16	358	45	194
Humpback whale	0	0	2	2
Blue whale	13	19	0	0
Sperm whale	1	1	4	4
Unidentified cetacean	2	3	1	1
Seal	10	11	4	9
Fish *	2	8	0	0
Shark *	8	8	0	0

* Non-marine mammal species were not always recorded
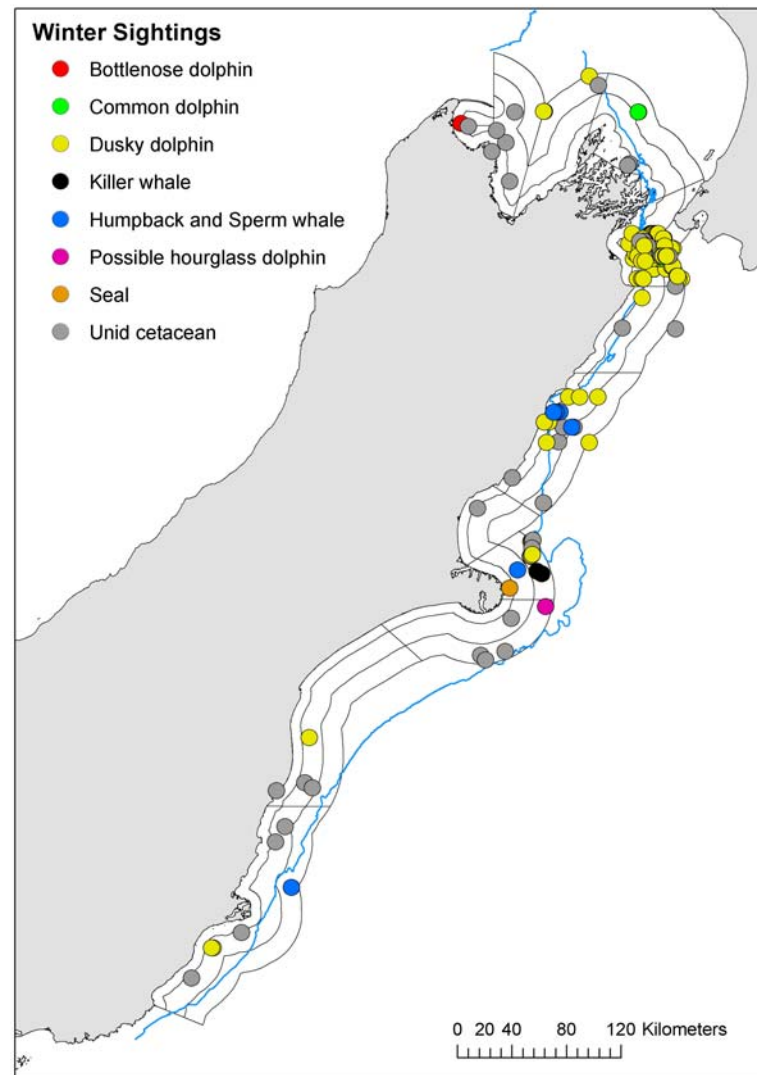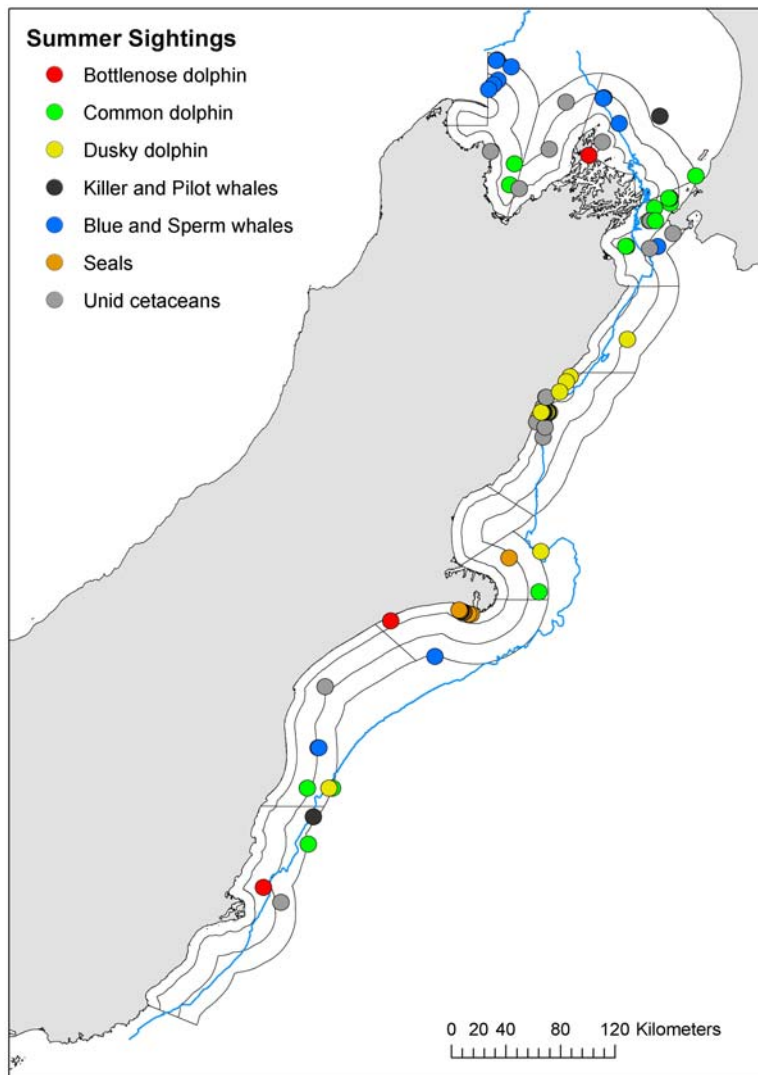
Figure D.1: Locations of other marine mammal sightings along the ECSI from the summer survey (left) and winter survey (right).

Ministry for Primary Industries

SECTION E

Number of dolphin sightings in each stratum in summer and winter surveys.

Table E.1: Survey effort and summary of summer line transect surveys of sightings between 0.071–0.300 km from front observer position and between 0–0.300 km from rear observer position (full data set). Given is the area of each stratum, number of survey lines flown, total length of transect flown, area covered by the line transect survey (length × 0.300 × 2), number of groups sighted (Sightings), number seen from front position (Front), number seen from rear position (Rear), number of groups sighted from both positions (i.e., duplicates; Both), number of individual dolphins seen (Individuals), average group size, and naïve estimate assuming 100% detection within survey width and 100% availability ($\widetilde{N}_k$). Note that the number of groups sighted only from the front position would be Front − Both, and similarly for the number of groups sighted only from the rear position.

Coastal Section	Offshore Stratum (nmi)	Area (km²)	Lines	Length Flown (km)	Covered (km²)	Sightings	Front	Rear	Both	Individuals	Av. Group Size	$\widetilde{N}_k$
Golden Bay North	0–4	291.3	4	32.0	19.2							
	4–12	190.8	2	17.8	10.7							
Golden Bay A	0–4	881.5	7	64.9	38.9							
	4–12	1 552.0	8	139.2	83.5							
	12–20	1 104.2	7	101.8	61.1							
Golden Bay B	0–4	708.2	9	59.5	35.7							
	4–12	1 226.2	8	109.7	65.8							
	12–20	1 083.3	9	95.2	57.1							
Marlborough Sounds	0–4	1 054.8	7	88.4	53.1							
	4–12	1 441.4	8	135.8	81.5							
	12–20	1 544.9	10	136.7	82.0							
Cloudy/Clifford Bay	0–4	697.6	36	365.7	219.4	29	17	22	10	63	2.17	200
	4–12	1 309.6	40	711.6	427.0	31	20	20	9	76	2.45	233
	12–20	924.7	11	138.4	83.0							
Kaikoura	0–4	887.9	23	233.2	139.9	8	3	7	2	28	3.50	178
	4–12	1 778.7	10	158.8	95.3							
	12–20	1 897.3	9	168.0	100.8							
Clarence	0–4	603.2	17	155.9	93.6	3	2	2	1	10	3.33	64
	4–12	1 135.8	5	89.3	53.6							
	12–20	1 085.8	5	86.4	51.8							

Table E.1 (cont): Survey effort and summary of summer line transect surveys of sightings between 0.071–0.300 km from front observer position and between 0-0.300 km from rear observer position (full data set). Given is the area of each stratum, number of survey lines flown, total length of transect flown, area covered by the line transect survey (length × 0.300 × 2), number of groups sighted (Sightings), number seen from front position (Front), number seen from rear position (Rear), number of groups sighted from both positions (i.e., duplicates; Both), number of individual dolphins seen (Individuals), average group size, and naïve estimate assuming 100% detection within survey width and 100% availability ($\widetilde{N}_k$). Note that the number of groups sighted only from the front position would be Front − Both, and similarly for the number of groups sighted only from the rear position.

Coastal Section	Offshore Stratum (nmi)	Area (km²)	Lines	Length Flown (km)	Covered (km²)	Sightings	Front	Rear	Both	Individuals	Av. Group Size	$\widetilde{N}_k$
Pegasus Bay	0–4	523.5	31	275.1	165.1	34	21	28	15	53	1.56	168
	4–12	860.2	12	229.1	137.5	8	6	8	6	19	2.38	119
	12–20	570.9	4	78.2	46.9	5	3	3	1	10	2.00	122
Banks Pen. North	0–4	327.0	23	173.7	104.2	53	32	46	25	118	2.23	370
	4–12	726.5	14	196.7	118.0	33	23	28	18	59	1.79	363
	12–20	828.5	8	114.5	68.7	8	7	7	6	15	1.88	181
Banks Pen. South	0–4	749.0	44	397.2	238.3	87	49	75	37	199	2.29	625
	4–12	1 605.8	25	438.3	263.0	20	14	17	11	60	3.00	366
	12–20	1 753.0	14	236.9	142.1							
Timaru	0–4	1 256.5	36	338.1	202.9	19	12	16	9	38	2.00	235
	4–12	2 347.0	35	630.9	378.6	16	11	12	7	67	4.19	415
	12–20	2 160.3	16	284.3	170.6							
Otago	0–4	1 601.6	14	130.5	78.3							
	4–12	2 987.9	14	277.1	166.3							
	12–20	2 980.3	15	266.8	160.1							
Total		42 677.1	540	7 155.8	4 293.5	354	220	291	157	815	2.30	3641

Table E.2: Survey effort and summary of summer line transect surveys of sightings between 0.071–0.300 km from both observer positions (reduced data set). Given is the area of each stratum, number of survey lines flown, total length of transect flown, area covered by the line transect survey (length × 0.300 × 2), number of groups sighted (Sightings), number seen from front position (Front), number seen from rear position (Rear), number of groups sighted from both positions (i.e., duplicates; Both), number of individual dolphins seen (Individuals), average group size, and naïve estimate assuming 100% detection within survey width and 100% availability ($\widetilde{N}_k$). Note that the number of groups sighted only from the front position would be Front − Both, and similarly for the number of groups sighted only from the rear position.

Coastal Section	Offshore Stratum (nmi)	Area (km²)	Lines	Length Flown (km)	Covered (km²)	Sightings	Front	Rear	Both	Individuals	Av. Group Size	$\widetilde{N}_k$
Golden Bay North	0–4	291.3	4	32.0	14.7							
	4–12	190.8	2	17.8	8.2							
Golden Bay A	0-4	881.5	7	64.9	29.7							
	4–12	1 552.0	8	139.2	63.8							
	12–20	1 104.2	7	101.8	46.6							
Golden Bay B	0–4	708.2	9	59.5	27.3							
	4–12	1 226.2	8	109.7	50.2							
	12–20	1 083.3	9	95.2	43.6							
Marlborough Sounds	0–4	1 054.8	7	88.4	40.5							
	4–12	1 441.4	8	135.8	62.2							
	12–20	1 544.9	10	136.7	62.6							
Cloudy/Clifford Bay	0–4	697.6	36	365.7	167.5	21	17	14	10	49	2.33	204
	4–12	1 309.6	40	711.6	325.9	23	20	12	9	53	2.30	213
	12–20	924.7	11	138.4	63.4							
Kaikoura	0–4	887.9	23	233.2	106.8	4	3	3	2	20	5.00	166
	4–12	1 778.7	10	158.8	72.7							
	12–20	1 897.3	9	168.0	76.9							
Clarence	0–4	603.2	17	155.9	71.4	3	2	2	1	10	3.33	84
	4–12	1 135.8	5	89.3	40.9							
	12–20	1 085.8	5	86.4	39.6							

Table E.2 (cont): Survey effort and summary of summer line transect surveys of sightings between 0.071–0.300 km from both observer positions (reduced data set). Given is the area of each stratum, number of survey lines flown, total length of transect flown, area covered by the line transect survey (length × 0.300 × 2), number of groups sighted (Sightings), number seen from front position (Front), number seen from rear position (Rear), number of groups sighted from both positions (i.e., duplicates; Both), number of individual dolphins seen (Individuals), average group size, and naïve estimate assuming 100% detection within survey width and 100% availability ($\widetilde{N}_k$). Note that the number of groups sighted only from the front position would be Front − Both, and similarly for the number of groups sighted only from the rear position.

Coastal Section	Offshore Stratum (nmi)	Area (km^2)	Lines	Length Flown (km)	Covered (km^2)	Sightings	Front	Rear	Both	Individuals	Av. Group Size	$\widetilde{N}_k$
Pegasus Bay	0–4	523.5	31	275.1	126.0	26	21	20	15	41	1.58	170
	4–12	860.2	12	229.1	104.9	6	6	6	6	17	2.83	139
	12–20	570.9	4	78.2	35.8	3	3	1	1	6	2.00	96
Banks Pen. North	0–4	327.0	23	173.7	79.5	39	32	32	25	90	2.31	370
	4–12	726.5	14	196.7	90.1	26	23	21	18	47	1.81	379
	12–20	828.5	8	114.5	52.5	7	7	6	6	14	2.00	221
Banks Pen. South	0–4	749.0	44	397.2	181.9	70	49	58	37	157	2.24	646
	4–12	1 605.8	25	438.3	200.7	17	14	14	11	53	3.12	424
	12–20	1 753.0	14	236.9	108.5							
Timaru	0–4	1 256.5	36	338.1	154.8	14	12	11	9	30	2.14	243
	4–12	2 347.0	35	630.9	289.0	12	11	8	7	48	4.00	390
	12–20	2 160.3	16	284.3	130.2							
Otago	0–4	1 601.6	14	130.5	59.8							
	4–12	2 987.9	14	277.1	126.9							
	12–20	2 980.3	15	266.8	122.2							
Total		42 677.1	540	7 155.8	3 277.4	271	220	208	157	635	2.34	3747

Table E.3: Survey effort and summary of winter line transect surveys of sightings between 0.071–0.300 km from front observer position and between 0–0.300 km from rear observer position (full data set). Given is the area of each stratum, number of survey lines flown, total length of transect flown, area covered by the line transect survey (length × 0.300 × 2), number of groups sighted (Sightings), number seen from front position (Front), number seen from rear position (Rear), number of groups sighted from both positions (i.e., duplicates; Both), number of individual dolphins seen (Individuals), average group size, and naïve estimate assuming 100% detection within survey width and 100% availability ($\widetilde{N}_k$). Note that the number of groups sighted only from the front position would be Front − Both, and similarly for the number of groups sighted only from the rear position.

Coastal Section	Offshore Stratum (nmi)	Area (km^2)	Lines	Length Flown (km)	Covered (km^2)	Sightings	Front	Rear	Both	Individuals	Av. Group Size	$\widetilde{N}_k$
Golden Bay North	0–4	291.3	3	24.3	14.6							
	4–12	190.8	2	17.8	10.7							
Golden Bay A	0–4	881.5	8	74.5	44.7							
	4–12	1 552.0	8	139.1	83.5	1	1	1	1	3	3	56
	12–20	1 104.2	7	101.6	61.0							
Golden Bay B	0–4	708.2	9	61.0	36.6							
	4–12	1 226.2	9	109.8	65.9							
	12–20	1 083.3	9	95.0	57.0							
Marlborough Sounds	0–4	1 054.8	7	88.1	52.9							
	4–12	1 441.4	8	135.9	81.5							
	12–20	1 544.9	10	137.4	82.5							
Cloudy/Clifford Bay	0–4	697.6	18	182.1	109.3	3		3		6	2.00	38
	4–12	1 309.6	20	352.2	211.3	12	5	9	2	20	1.67	124
	12-20	924.7	9	119.1	71.5	4	1	4	1	5	1.25	65
Kaikoura	0–4	887.9	25	234.0	140.4	7	2	5		8	1.14	51
	4–12	1 778.7	10	159.3	95.6							
	12–20	1 897.3	9	167.9	100.7							
Clarence	0–4	603.2	17	155.6	93.3	7	2	6	1	16	2.29	103
	4–12	1 135.8	5	89.2	53.5							
	12–20	1 085.8	5	86.1	51.7							

Table E.3 (cont): Survey effort and summary of winter line transect surveys of sightings between 0.071–0.300 km from front observer position and between 0–0.300 km from rear observer position (full data set). Given is the area of each stratum, number of survey lines flown, total length of transect flown, area covered by the line transect survey (length × 0.300 × 2), number of groups sighted (Sightings), number seen from front position (Front), number seen from rear position (Rear), number of groups sighted from both positions (i.e., duplicates; Both), number of individual dolphins seen (Individuals), average group size, and naïve estimate assuming 100% detection within survey width and 100% availability ($\widetilde{N}_k$). Note that the number of groups sighted only from the front position would be Front − Both, and similarly for the number of groups sighted only from the rear position.

Coastal Section	Offshore Stratum (nmi)	Area (km^2)	Lines	Length Flown (km)	Covered (km^2)	Sightings	Front	Rear	Both	Individuals	Av. Group Size	$\widetilde{N}_k$
Pegasus Bay	0–4	523.5	16	143.1	85.9	2		2		3	1.50	18
	4–12	860.2	12	230.2	138.1	26	16	20	10	34	1.31	212
	12–20	570.9	8	153.0	91.8	19	10	15	6	29	1.53	180
Banks Pen. North	0–4	327.0	23	174.9	104.9	23	10	17	4	41	1.78	128
	4–12	726.5	27	391.9	235.1	49	29	36	16	65	1.33	201
	12–20	828.5	16	223.5	134.1	21	8	17	4	35	1.67	216
Banks Pen. South	0–4	749.0	43	395.3	237.2	37	17	24	4	61	1.65	193
	4–12	1 605.8	49	867.4	520.4	21	13	19	11	33	1.57	102
	12–20	1 753.0	14	235.9	141.5	3		3		4	1.33	50
Timaru	0–4	1 256.5	36	340.8	204.5	11	4	10	3	17	1.55	104
	4–12	2 347.0	35	630.8	378.5	62	38	54	30	124	2.00	769
	12–20	2 160.3	16	283.1	169.8	20	13	17	10	33	1.65	420
Otago	0–4	1 601.6	14	130.9	78.5							
	4–12	2 987.9	14	277.1	166.2							
	12–20	2 980.3	15	268.4	161.0							
Total		42 677.1	536	7 276.2	4 365.7	328	169	262	103	537	1.64	3029

Table E.4: Survey effort and summary of winter line transect surveys of sightings between 0.071–0.300 km from both observer positions (reduced data set). Given is the area of each stratum, number of survey lines flown, total length of transect flown, area covered by the line transect survey (length × 0.300 × 2), number of groups sighted (Sightings), number seen from front position (Front), number seen from rear position (Rear), number of groups sighted from both positions (i.e., duplicates; Both), number of individual dolphins seen (Individuals), average group size, and naïve estimate assuming 100% detection within survey width and 100% availability ($\widetilde{N}_k$). Note that the number of groups sighted only from the front position would be Front − Both, and similarly for the number of groups sighted only from the rear position.

Coastal Section	Offshore Stratum (nmi)	Area (km²)	Lines	Length Flown (km)	Covered (km²)	Sightings	Front	Rear	Both	Individuals	Av. Group Size	$\widetilde{N}_k$
Golden Bay North	0–4	291.3	3	24.3	11.1							
	4–12	190.8	2	17.8	8.1							
Golden Bay A	0–4	881.5	8	74.5	34.1							
	4–12	1 552.0	8	139.1	63.7	1	1	1	1	3	3	73
	12–20	1 104.2	7	101.6	46.5							
Golden Bay B	0–4	708.2	9	61.0	28.0							
	4–12	1 226.2	9	109.8	50.3							
	12–20	1 083.3	9	95.0	43.5							
Marlborough Sounds	0–4	1 054.8	7	88.1	40.4							
	4–12	1 441.4	8	135.9	62.2							
	12–20	1 544.9	10	137.4	62.9							
Cloudy/Clifford Bay	0–4	697.6	18	182.1	83.4	1		1		2	2.00	17
	4–12	1 309.6	20	352.2	161.3	6	5	3	2	10	1.67	81
	12–20	924.7	9	119.1	54.6	2	1	2	1	3	1.50	51
Kaikoura	0–4	887.9	25	234.0	107.2	3	2	1		4	1.33	33
	4–12	1 778.7	10	159.3	73.0							
	12–20	1 897.3	9	167.9	76.9							
Clarence	0–4	603.2	17	155.6	71.2	3	2	2	1	9	3.00	76
	4–12	1 135.8	5	89.2	40.9							
	12–20	1 085.8	5	86.1	39.4							

Table E.4 (cont): Survey effort and summary of winter line transect surveys of sightings between 0.071–0.300 km from both observer positions (reduced data set). Given is the area of each stratum, number of survey lines flown, total length of transect flown, area covered by the line transect survey (length × 0.300 × 2), number of groups sighted (Sightings), number seen from front position (Front), number seen from rear position (Rear), number of groups sighted from both positions (i.e., duplicates; Both), number of individual dolphins seen (Individuals), average group size, and naïve estimate assuming 100% detection within survey width and 100% availability ($\widetilde{N}_k$). Note that the number of groups sighted only from the front position would be Front − Both, and similarly for the number of groups sighted only from the rear position.

Coastal Section	Offshore Stratum (nmi)	Area (km²)	Lines	Length Flown (km)	Covered (km²)	Sightings	Front	Rear	Both	Individuals	Av. Group Size	$\widetilde{N}_k$
Pegasus Bay	0–4	523.5	16	143.1	65.6	2		2		3	1.50	24
	4–12	860.2	12	230.2	105.4	19	16	13	10	26	1.37	212
	12–20	570.9	8	153.0	70.1	11	10	7	6	16	1.45	130
Banks Pen. North	0–4	327.0	23	174.9	80.1	19	10	13	4	28	1.47	114
	4–12	726.5	27	391.9	179.5	33	29	20	16	45	1.36	182
	12–20	828.5	16	223.5	102.4	13	8	9	4	25	1.92	202
Banks Pen. South	0–4	749.0	43	395.3	181.1	24	17	11	4	41	1.71	170
	4–12	1 605.8	49	867.4	397.3	15	13	13	11	24	1.60	97
	12–20	1 753.0	14	235.9	108.0	1		1		1	1.00	16
Timaru	0–4	1 256.5	36	340.8	156.1	6	4	5	3	8	1.33	64
	4–12	2 347.0	35	630.8	288.9	46	38	38	30	90	1.96	731
	12–20	2 160.3	16	283.1	129.6	14	13	11	10	27	1.93	450
Otago	0–4	1 601.6	14	130.9	60.0							
	4–12	2 987.9	14	277.1	126.9							
	12–20	2 980.3	15	268.4	122.9							
Total		42 677.1	536	7 276.2	3 332.5	219	169	153	103	365	1.67	2725

SECTION F

Diagnostic plots of top-ranked detection function models fitted to full, summer line transect data set

Figure F.1: Fitted detection functions and histograms of empirical detection probabilities from the top ranked model in Table 4. Left is $p_{\bullet}(d_i, s_i)$**, centre is** $p_F(d_i, s_i)$**, and right is** $p_{R|NF}(d_i, s_i)$**.**
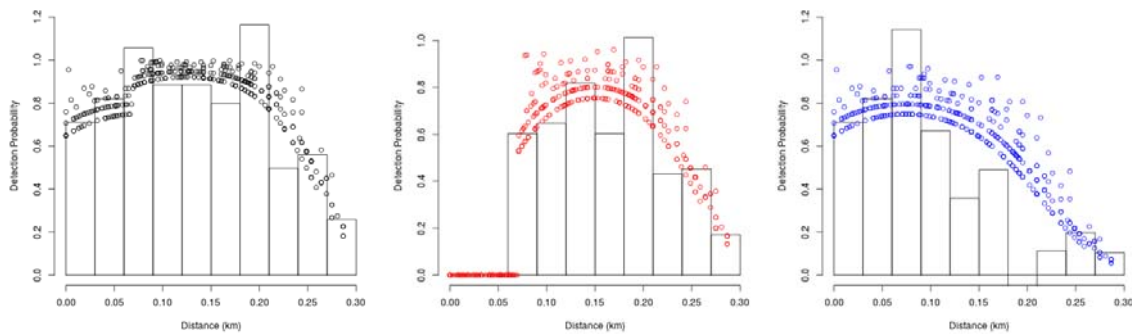
Figure F.2: Fitted detection functions and histograms of empirical detection probabilities from the second ranked model in Table 4. Left is $p_{\bullet}(d_i, s_i)$**, centre is** $p_F(d_i, s_i)$**, and right is** $p_{R|NF}(d_i, s_i)$**.**
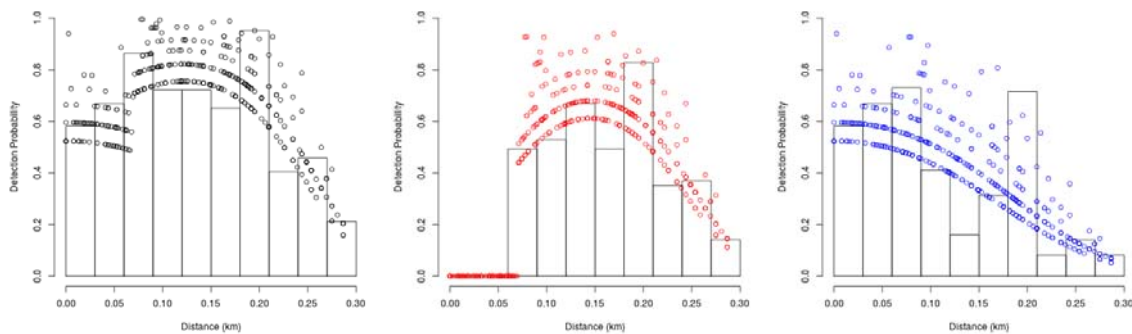
Figure F.3: Fitted detection functions and histograms of empirical detection probabilities from the third ranked model in Table 4. Left is $p_{\bullet}(d_i, s_i)$**, centre is** $p_F(d_i, s_i)$**, and right is** $p_{R|NF}(d_i, s_i)$**.**
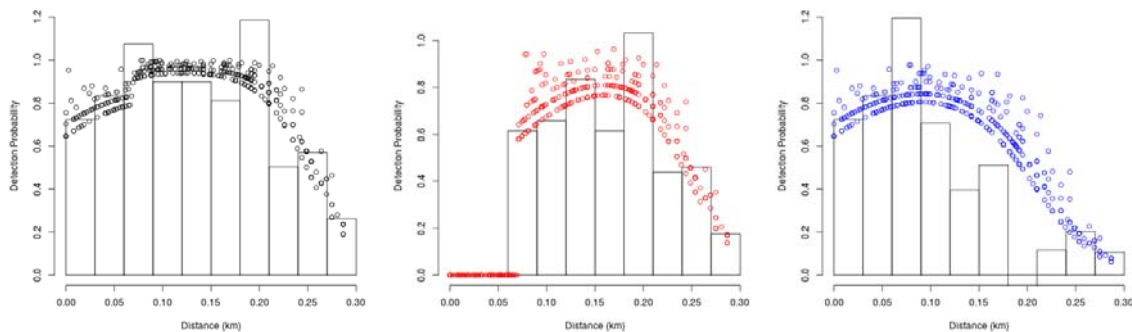
Figure F.4: Fitted detection functions and histograms of empirical detection probabilities from the fourth ranked model in Table 4. Left is $p_\bullet(d_i, s_i)$**, centre is** $p_F(d_i, s_i)$**, and right is** $p_{R|NF}(d_i, s_i)$**.**
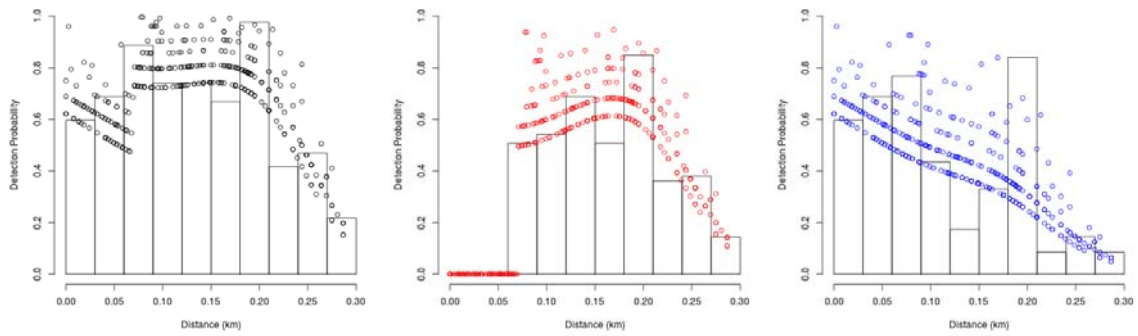
Figure F.5: Fitted detection functions and histograms of empirical detection probabilities from the fifth ranked model in Table 4. Left is $p_\bullet(d_i, s_i)$**, centre is** $p_F(d_i, s_i)$**, and right is** $p_{R|NF}(d_i, s_i)$**.**
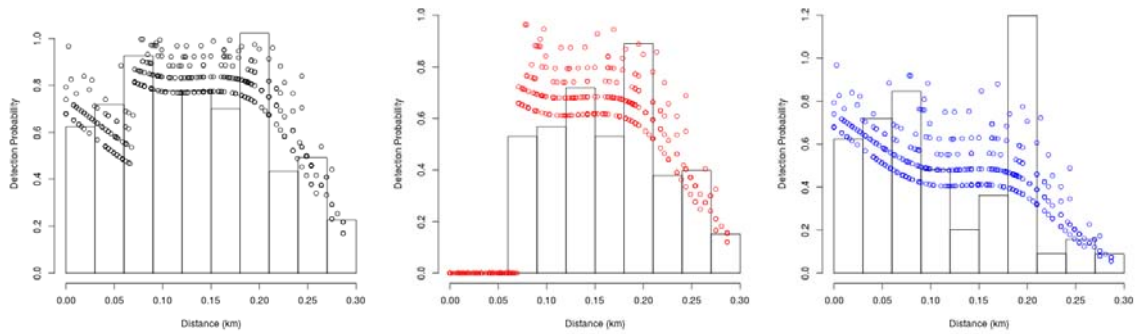
Figure F.6: Fitted detection functions and histograms of empirical detection probabilities from the sixth ranked model in Table 4. Left is $p_\bullet(d_i, s_i)$**, centre is** $p_F(d_i, s_i)$**, and right is** $p_{R|NF}(d_i, s_i)$**.**
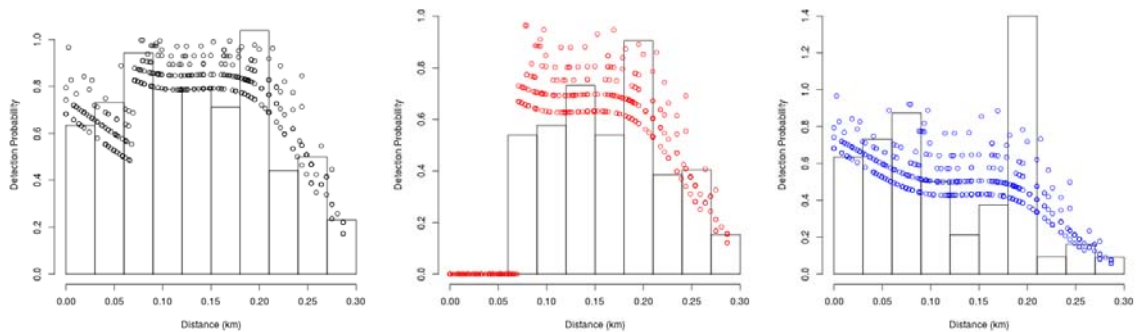
Figure F.7: Q-Q plot of the fitted and empirical cumulative density functions (CDF) for the top ranked model of the detection function analysis of the full summer data. Results of the Cramer-von Mises (CvM) and Kolmogorov-Smirnov (KS) tests with associated p-values are also presented.
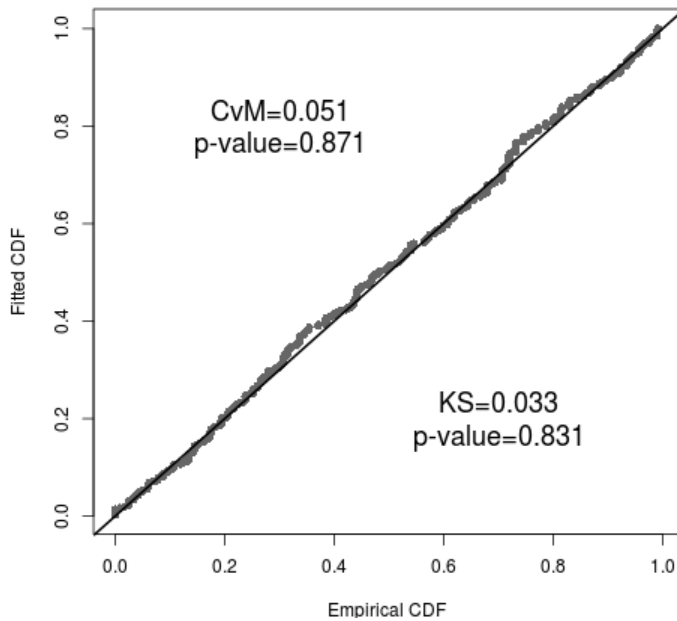
Figure F.8: Q-Q plot of the fitted and empirical cumulative density functions (CDF) for the second ranked model of the detection function analysis of the full summer data. Results of the Cramer-von Mises (CvM) and Kolmogorov-Smirnov (KS) tests with associated p-values are also presented.
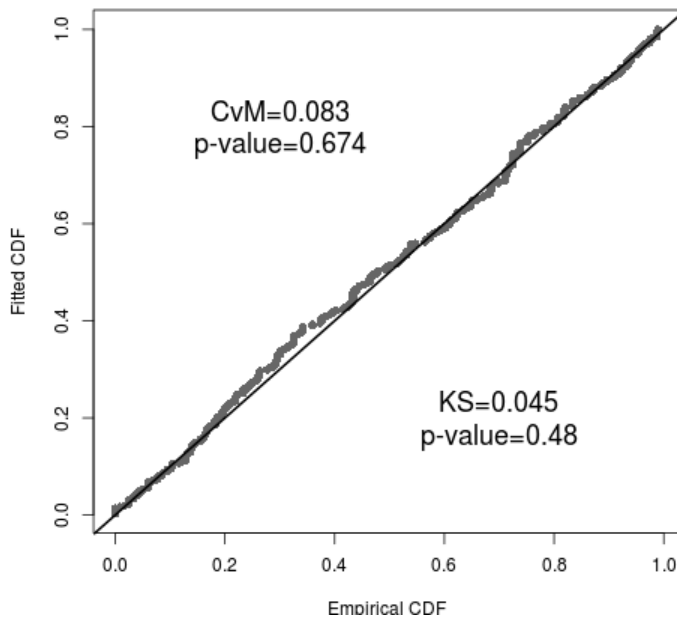
Figure F.9: Q-Q plot of the fitted and empirical cumulative density functions (CDF) for the third ranked model of the detection function analysis of the full summer data. Results of the Cramer-von Mises (CvM) and Kolmogorov-Smirnov (KS) tests with associated p-values are also presented.
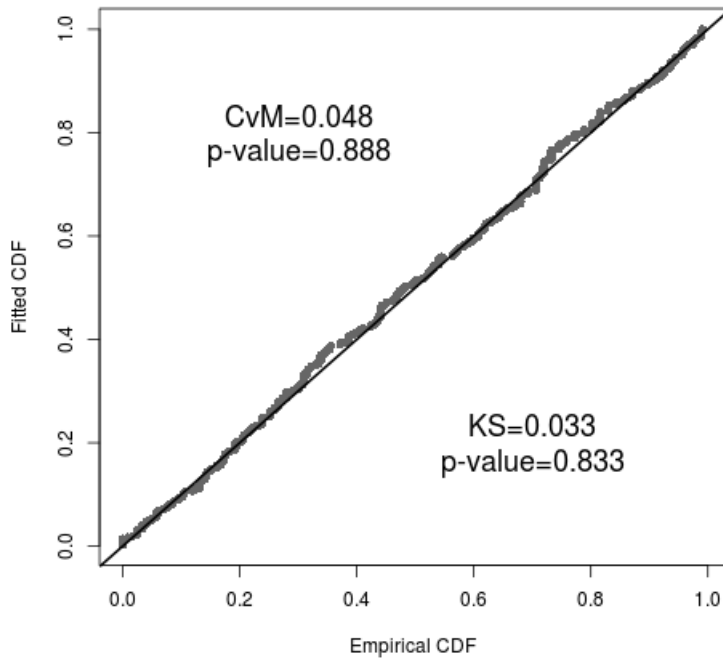
Figure F.10: Q-Q plot of the fitted and empirical cumulative density functions (CDF) for the fourth ranked model of the detection function analysis of the full summer data. Results of the Cramer-von Mises (CvM) and Kolmogorov-Smirnov (KS) tests with associated p-values are also presented.
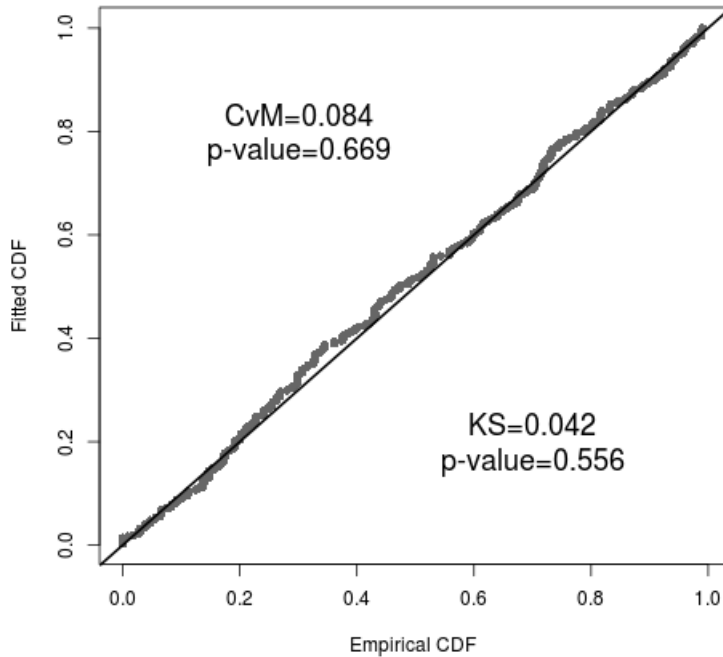
Figure F.11: Q-Q plot of the fitted and empirical cumulative density functions (CDF) for the fifth ranked model of the detection function analysis of the full summer data. Results of the Cramer-von Mises (CvM) and Kolmogorov-Smirnov (KS) tests with associated p-values are also presented.
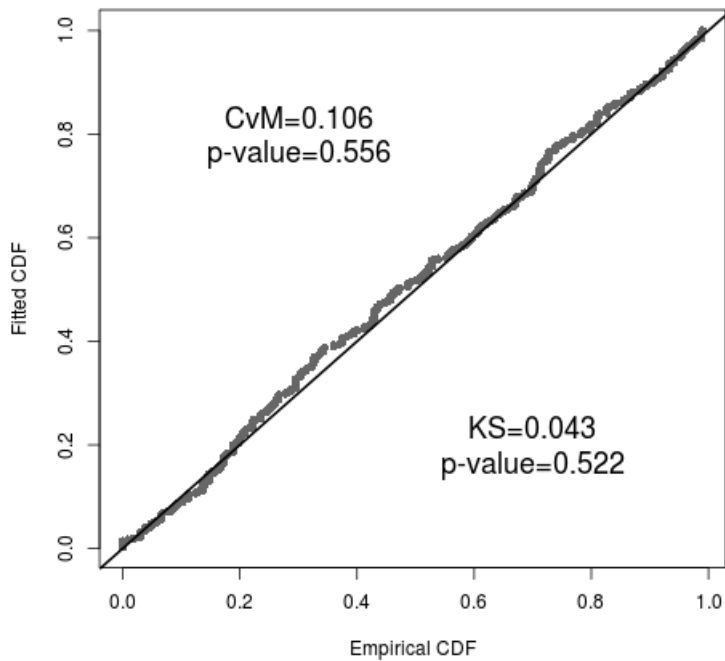
Figure F.12: Q-Q plot of the fitted and empirical cumulative density functions (CDF) for the sixth ranked model of the detection function analysis of the full summer data. Results of the Cramer-von Mises (CvM) and Kolmogorov-Smirnov (KS) tests with associated p-values are also presented.
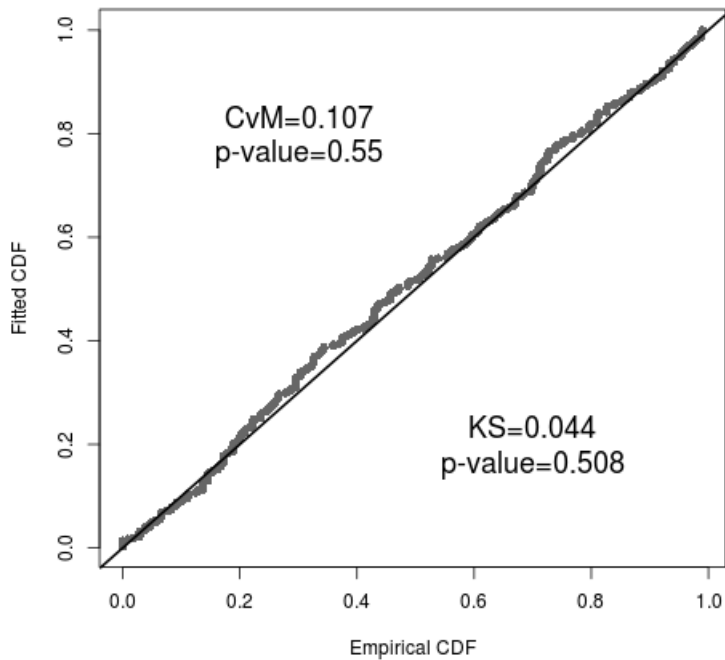
SECTION G

## Diagnostic plots of top-ranked detection function models fitted to reduced, summer line transect data set

Figure G.1: Fitted detection functions and histograms of empirical detection probabilities from the top ranked model in Table 6. Left is $p_\bullet(d_i, s_i)$**, centre is** $p_F(d_i, s_i)$**, and right is** $p_{R|NF}(d_i, s_i)$**.**
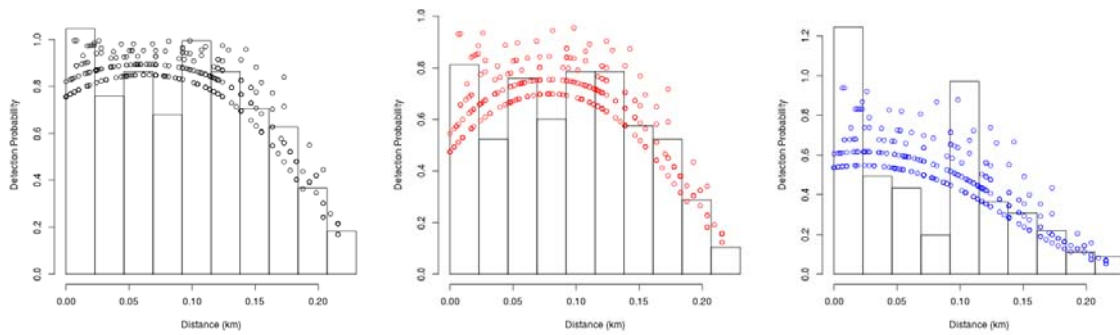

Figure G.2: Fitted detection functions and histograms of empirical detection probabilities from the second ranked model in Table 6. Left is $p_\bullet(d_i, s_i)$**, centre is** $p_F(d_i, s_i)$**, and right is** $p_{R|NF}(d_i, s_i)$**.**
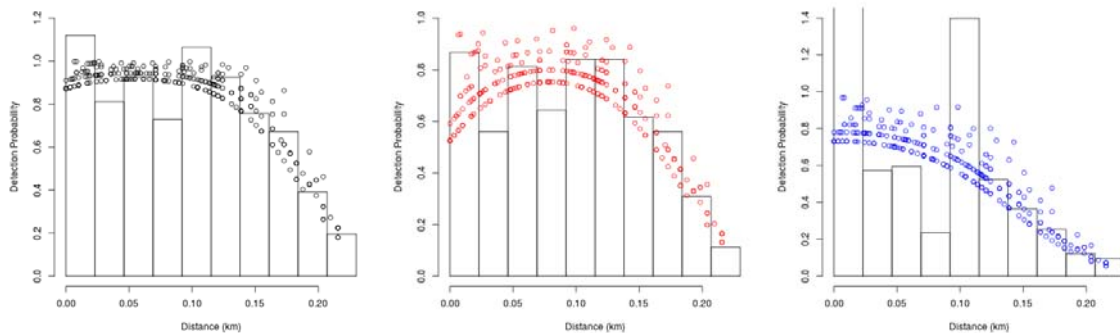
Figure G.3: Fitted detection functions and histograms of empirical detection probabilities from the third ranked model in Table 6. Left is $p_\bullet(d_i, s_i)$**, centre is** $p_F(d_i, s_i)$**, and right is** $p_{R|NF}(d_i, s_i)$**.**
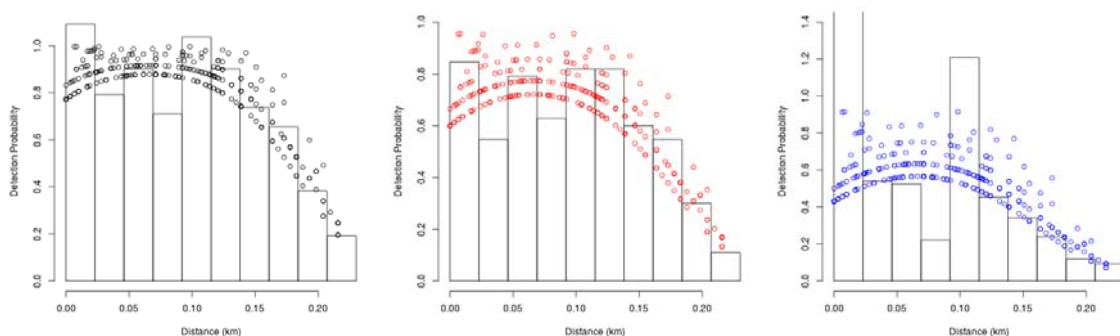
Figure G.4: Fitted detection functions and histograms of empirical detection probabilities from the fifth ranked model in Table 6. Left is $p_\bullet(d_i, s_i)$, centre is $p_F(d_i, s_i)$, and right is $p_{R|NF}(d_i, s_i)$.
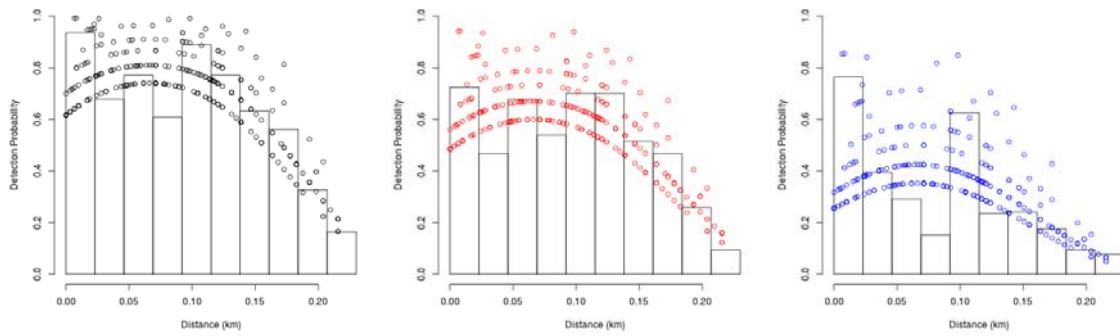
Figure G.5: Fitted detection functions and histograms of empirical detection probabilities from the sixth ranked model in Table 6. Left is $p_\bullet(d_i, s_i)$, centre is $p_F(d_i, s_i)$, and right is $p_{R|NF}(d_i, s_i)$.
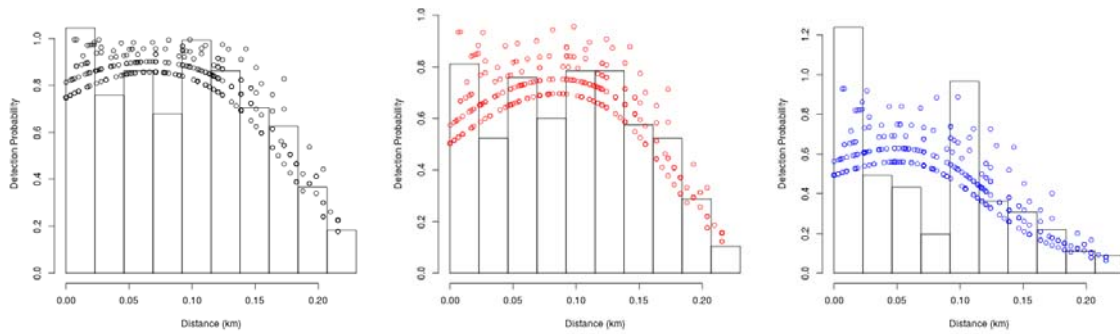

Figure G.6: Fitted detection functions and histograms of empirical detection probabilities from the seventh ranked model in Table 6. Left is $p_\bullet(d_i, s_i)$, centre is $p_F(d_i, s_i)$, and right is $p_{R|NF}(d_i, s_i)$.
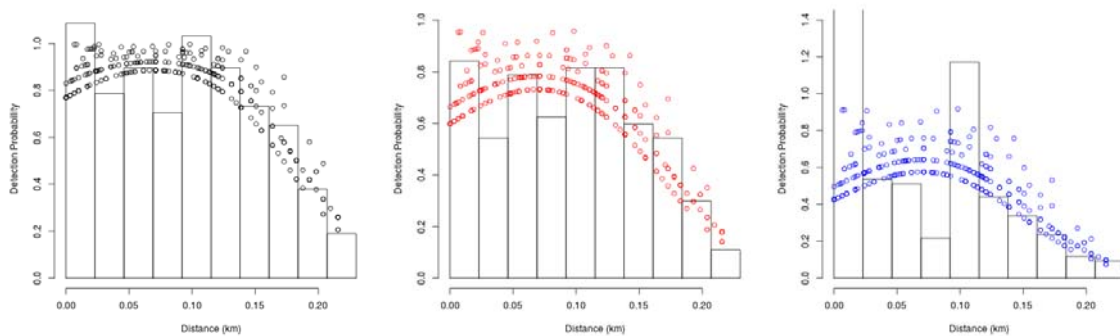
Figure G.7: Fitted detection functions and histograms of empirical detection probabilities from the eight ranked model in Table 6. Left is $p_\bullet(d_i, s_i)$, **centre is** $p_F(d_i, s_i)$, **and right is** $p_{R|NF}(d_i, s_i)$.
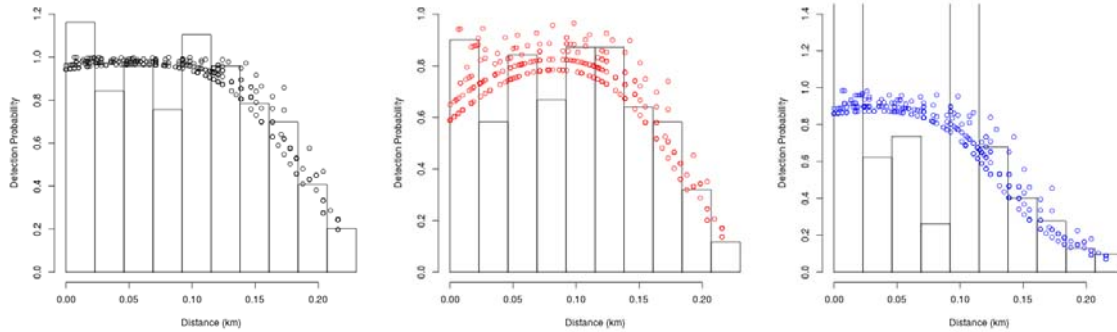

Figure G.8: Q-Q plot of the fitted and empirical cumulative density functions (CDF) for the top ranked model of the detection function analysis of the reduced summer data. Results of the Cramer-von Mises (CvM) and Kolmogorov-Smirnov (KS) tests with associated p-values are also presented.
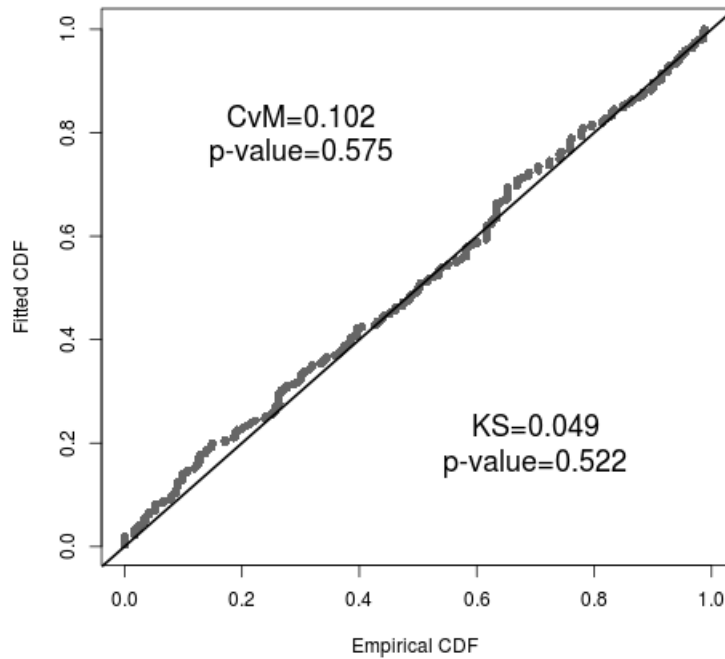
Figure G.9: Q-Q plot of the fitted and empirical cumulative density functions (CDF) for the second ranked model of the detection function analysis of the reduced summer data. Results of the Cramer-von Mises (CvM) and Kolmogorov-Smirnov (KS) tests with associated p-values are also presented.
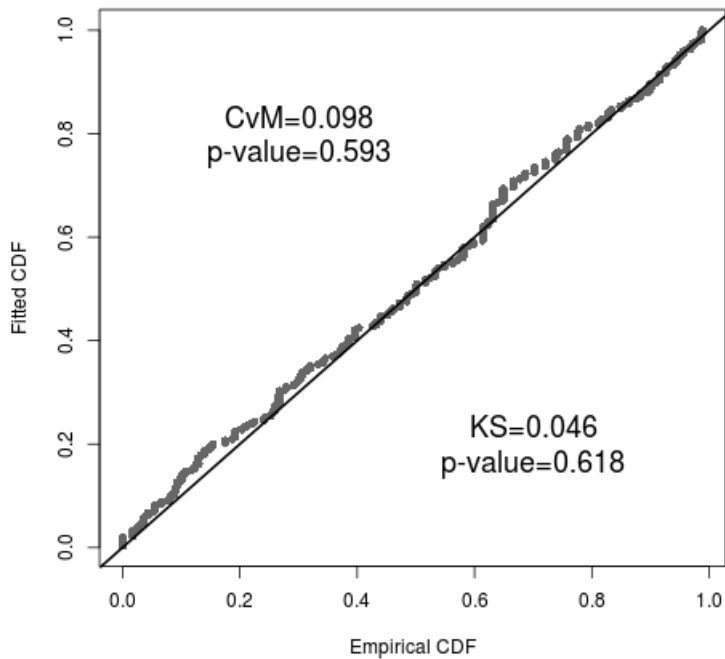
Figure G.10: Q-Q plot of the fitted and empirical cumulative density functions (CDF) for the third ranked model of the detection function analysis of the reduced summer data. Results of the Cramer-von Mises (CvM) and Kolmogorov-Smirnov (KS) tests with associated p-values are also presented.
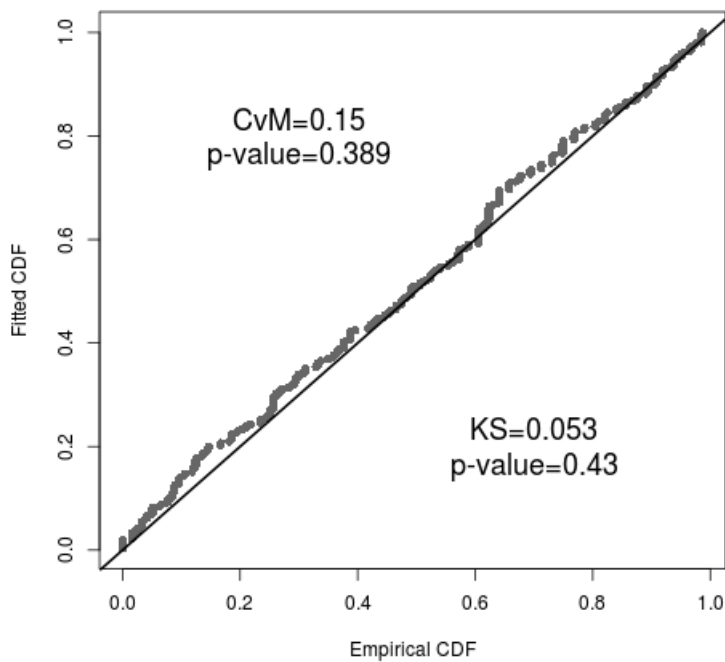
Figure G.11: Q-Q plot of the fitted and empirical cumulative density functions (CDF) for the fifth ranked model of the detection function analysis of the reduced summer data. Results of the Cramer-von Mises (CvM) and Kolmogorov-Smirnov (KS) tests with associated p-values are also presented.
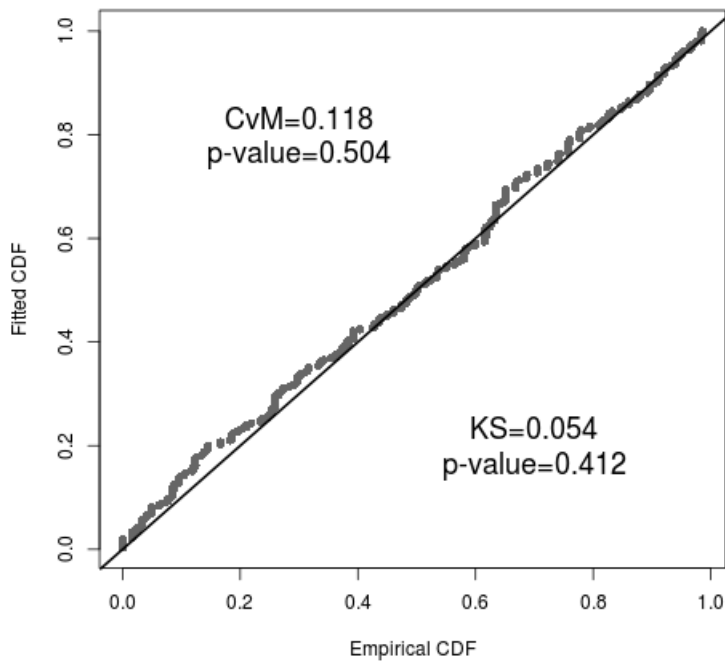
Figure G.12: Q-Q plot of the fitted and empirical cumulative density functions (CDF) for the sixth ranked model of the detection function analysis of the reduced summer data. Results of the Cramer-von Mises (CvM) and Kolmogorov-Smirnov (KS) tests with associated p-values are also presented.
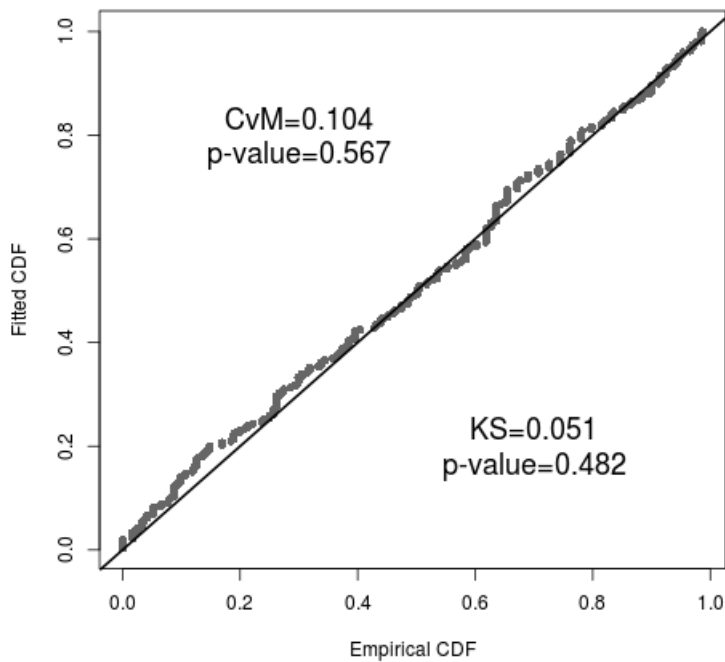
Figure G.13: Q-Q plot of the fitted and empirical cumulative density functions (CDF) for the seventh ranked model of the detection function analysis of the reduced summer data. Results of the Cramer-von Mises (CvM) and Kolmogorov-Smirnov (KS) tests with associated p-values are also presented.
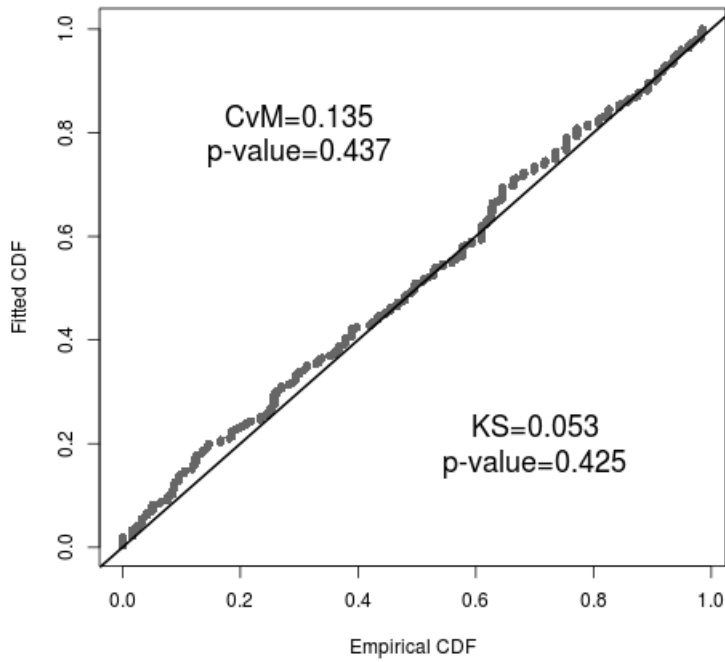
Figure G.14: Q-Q plot of the fitted and empirical cumulative density functions (CDF) for the eight ranked model of the detection function analysis of the reduced summer data. Results of the Cramer-von Mises (CvM) and Kolmogorov-Smirnov (KS) tests with associated p-values are also presented.
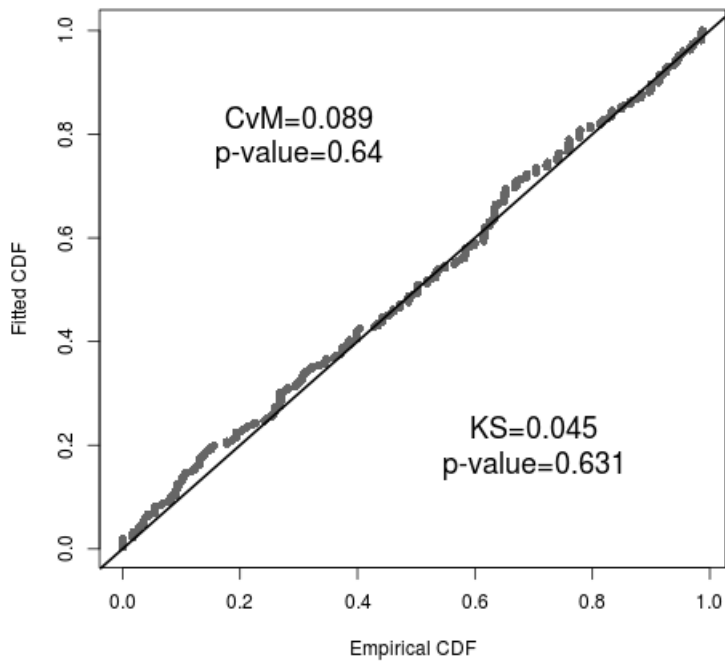
SECTION H

Diagnostic plots of top-ranked detection function models fitted to full, winter line transect data set

Figure H.1: Fitted detection functions and histograms of empirical detection probabilities from the top ranked model in Table 9. Left is $p_\bullet(d_i, s_i)$, centre is $p_F(d_i, s_i)$, and right is $p_{R|NF}(d_i, s_i)$.
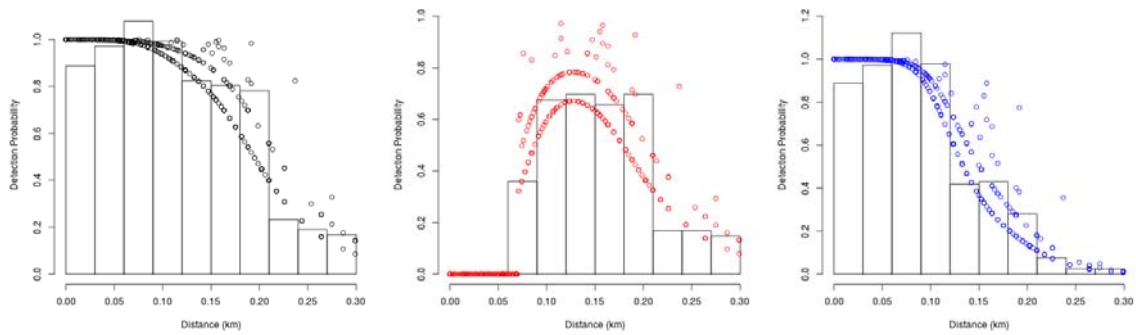
Figure H.2: Fitted detection functions and histograms of empirical detection probabilities from the second ranked model in Table 9. Left is $p_\bullet(d_i, s_i)$, centre is $p_F(d_i, s_i)$, and right is $p_{R|NF}(d_i, s_i)$.
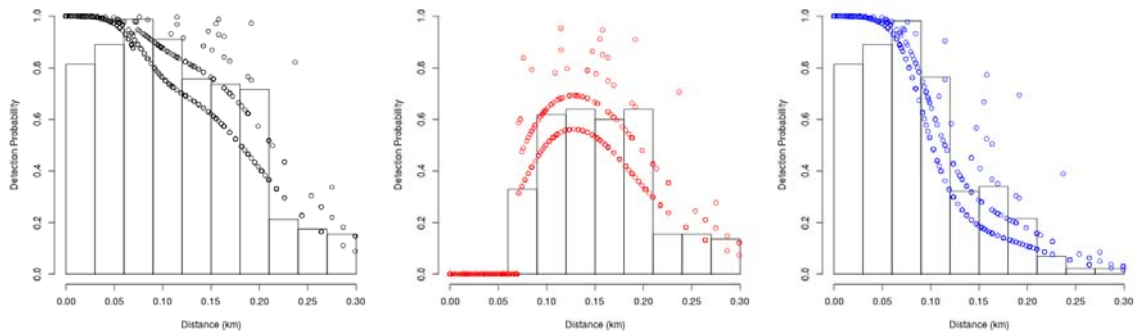
Figure H.3: Fitted detection functions and histograms of empirical detection probabilities from the third ranked model in Table 9. Left is $p_\bullet(d_i, s_i)$, centre is $p_F(d_i, s_i)$, and right is $p_{R|NF}(d_i, s_i)$.
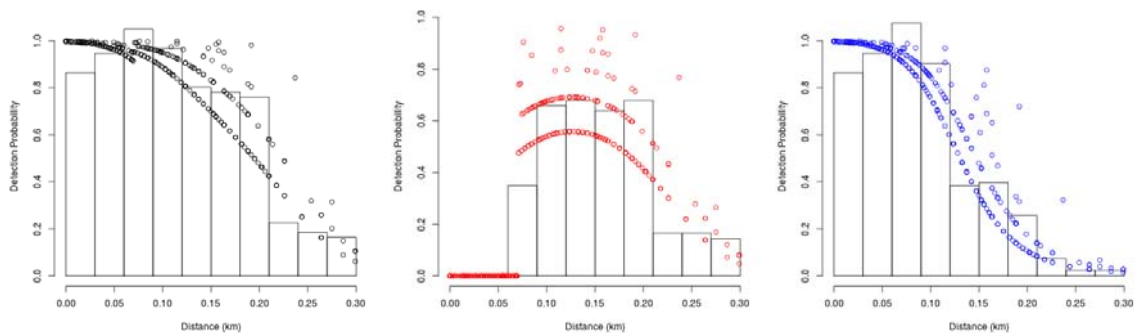
Figure H.4: Fitted detection functions and histograms of empirical detection probabilities from the fourth ranked model in Table 9. Left is $p_{\bullet}(d_i, s_i)$**, centre is** $p_F(d_i, s_i)$**, and right is** $p_{R|NF}(d_i, s_i)$**.**
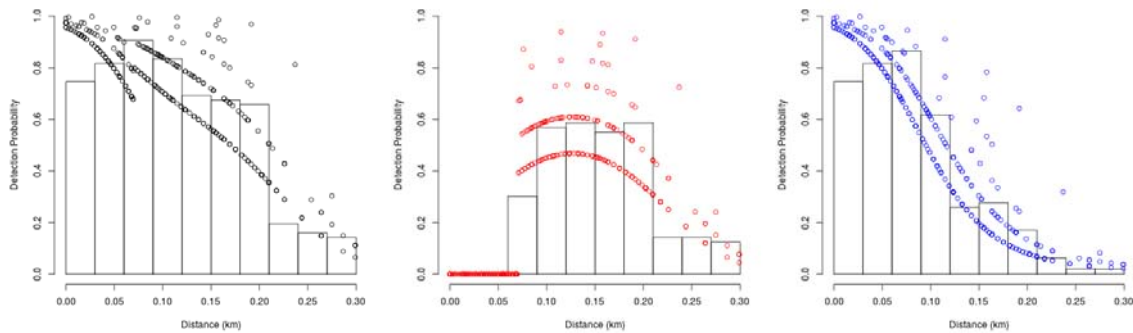
**Figure H.5: Q-Q plot of the fitted and empirical cumulative density functions (CDF) for the top ranked model of the detection function analysis of the full winter data. Results of the Cramer-von Mises (CvM) and Kolmogorov-Smirnov (KS) tests with associated p-values are also presented.**
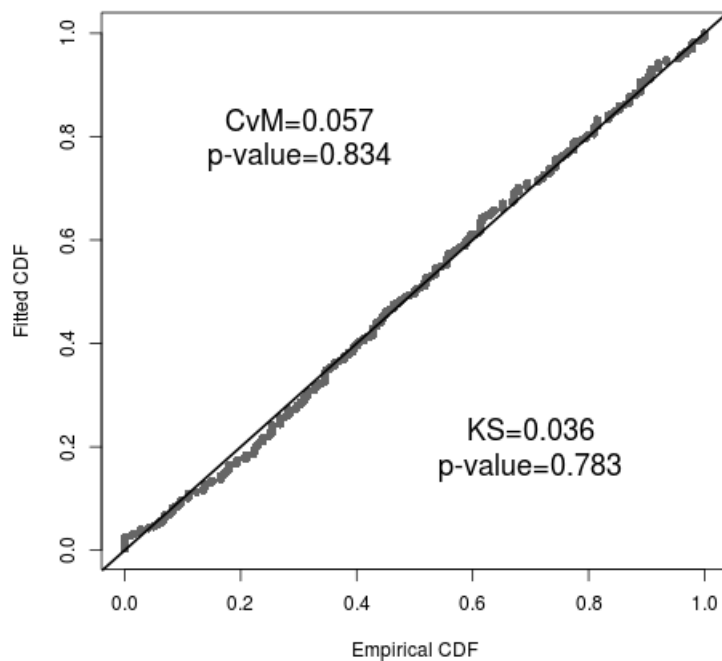
Figure H.6: Q-Q plot of the fitted and empirical cumulative density functions (CDF) for the second ranked model of the detection function analysis of the full winter data. Results of the Cramer-von Mises (CvM) and Kolmogorov-Smirnov (KS) tests with associated p-values are also presented.
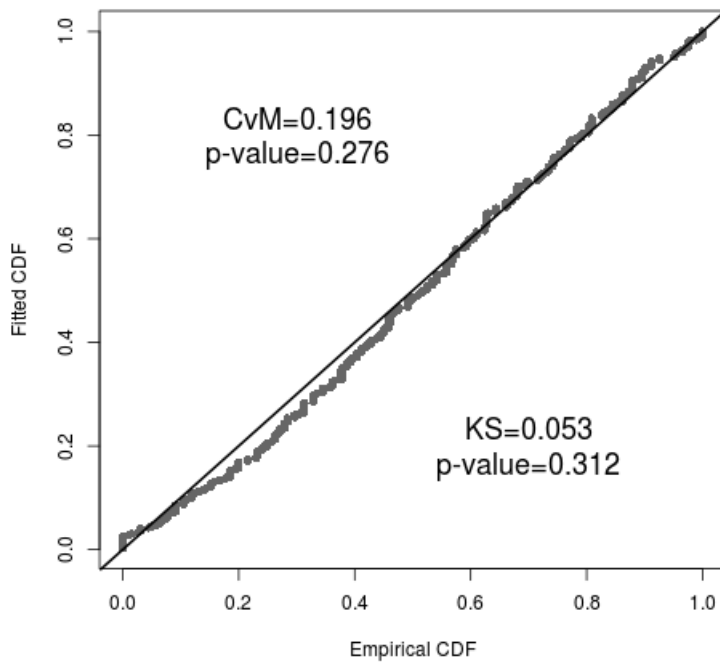
Figure H.7: Q-Q plot of the fitted and empirical cumulative density functions (CDF) for the third ranked model of the detection function analysis of the full winter data. Results of the Cramer-von Mises (CvM) and Kolmogorov-Smirnov (KS) tests with associated p-values are also presented.
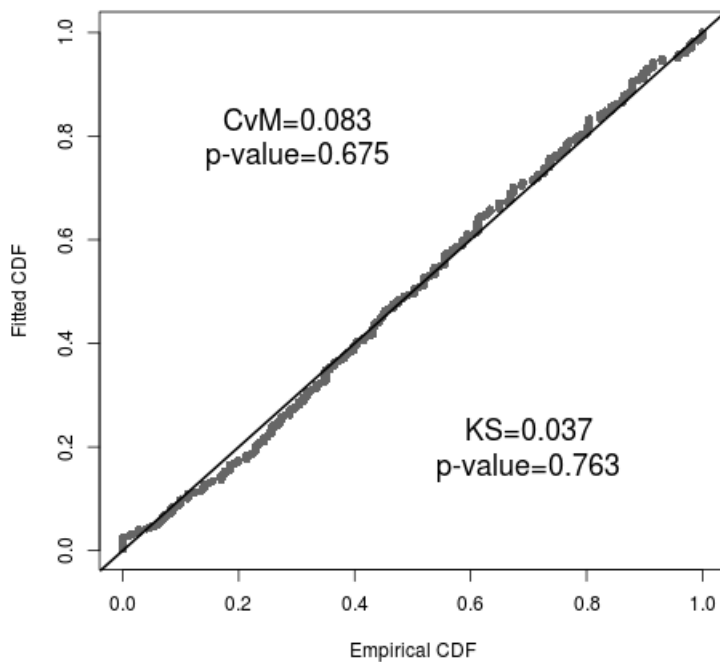
Figure H.8: Q-Q plot of the fitted and empirical cumulative density functions (CDF) for the fourth ranked model of the detection function analysis of the full winter data. Results of the Cramer-von Mises (CvM) and Kolmogorov-Smirnov (KS) tests with associated p-values are also presented.
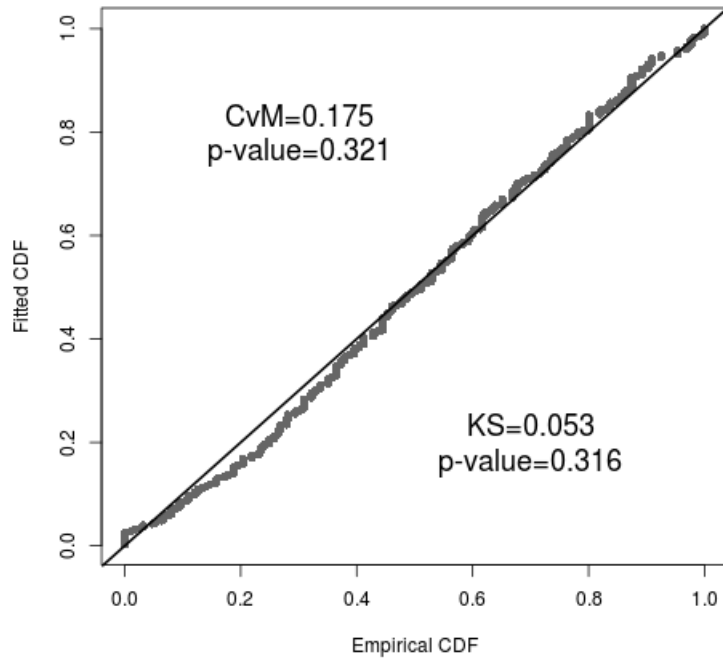
SECTION I

Diagnostic plots of top-ranked detection function models fitted to reduced, winter line transect data set

Figure I.1: Fitted detection functions and histograms of empirical detection probabilities from the top ranked model in Table 11. Left is $p_\bullet(d_i, s_i)$, centre is $p_F(d_i, s_i)$, and right is $p_{R|NF}(d_i, s_i)$.
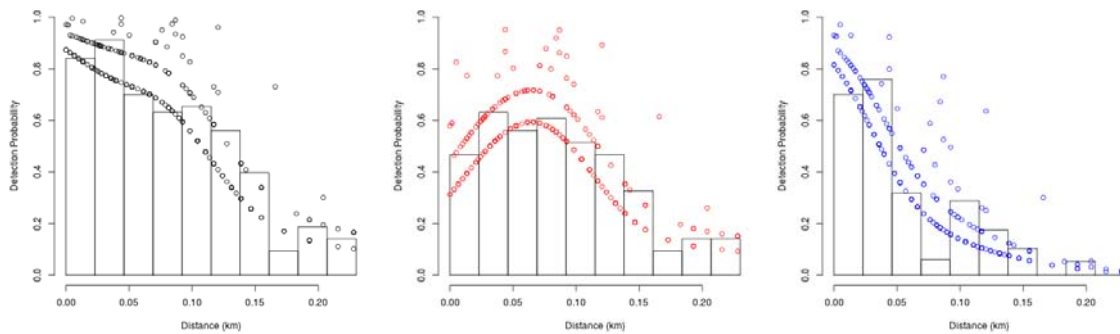

Figure I.2: Fitted detection functions and histograms of empirical detection probabilities from the second ranked model in Table 11. Left is $p_\bullet(d_i, s_i)$, centre is $p_F(d_i, s_i)$, and right is $p_{R|NF}(d_i, s_i)$.
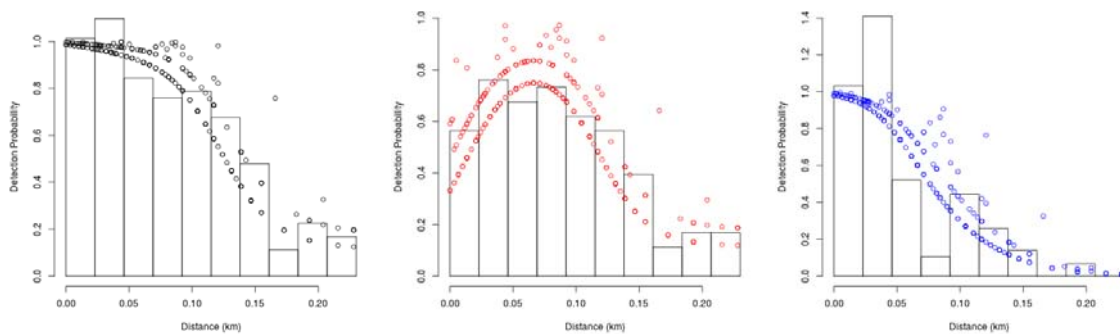
Figure I.3: Fitted detection functions and histograms of empirical detection probabilities from the third ranked model in Table 11. Left is $p_\bullet(d_i, s_i)$, centre is $p_F(d_i, s_i)$, and right is $p_{R|NF}(d_i, s_i)$.
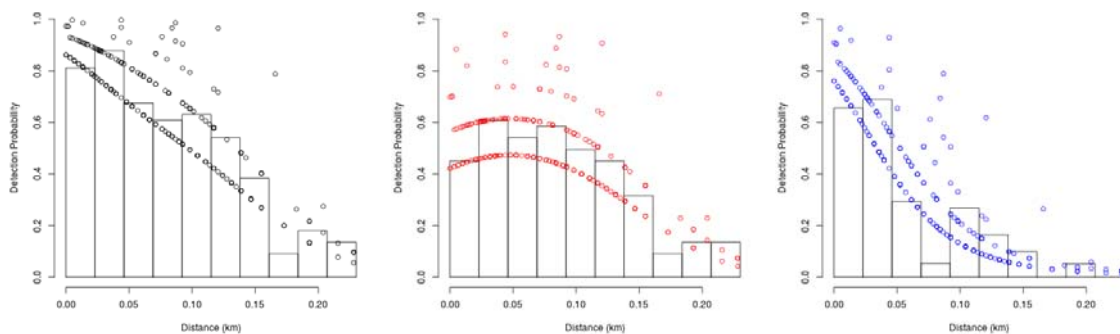
Figure I.4: Q-Q plot of the fitted and empirical cumulative density functions (CDF) for the top ranked model of the detection function analysis of the reduced winter data. Results of the Cramer-von Mises (CvM) and Kolmogorov-Smirnov (KS) tests with associated p-values are also presented.
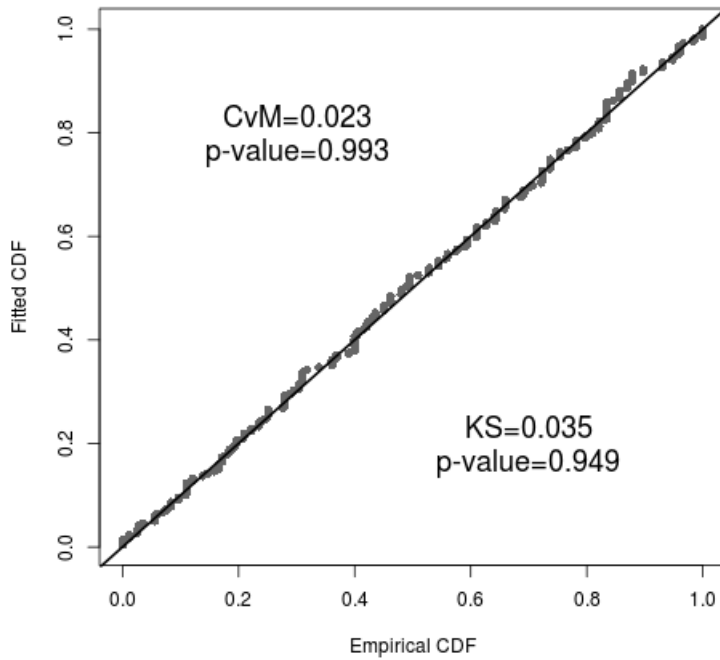
Figure I.5: Q-Q plot of the fitted and empirical cumulative density functions (CDF) for the second ranked model of the detection function analysis of the reduced winter data. Results of the Cramer-von Mises (CvM) and Kolmogorov-Smirnov (KS) tests with associated p-values are also presented.
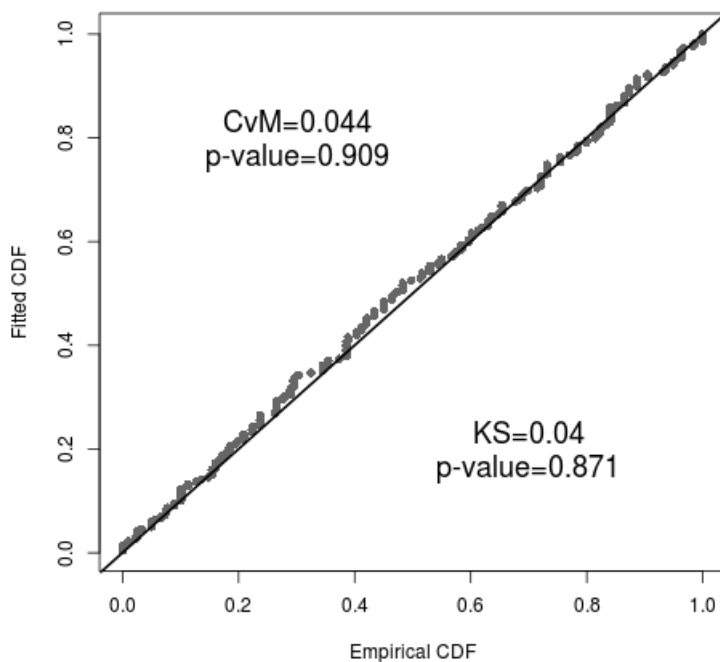
Figure I.6: Q-Q plot of the fitted and empirical cumulative density functions (CDF) for the third ranked model of the detection function analysis of the reduced winter data. Results of the Cramer-von Mises (CvM) and Kolmogorov-Smirnov (KS) tests with associated p-values are also presented.
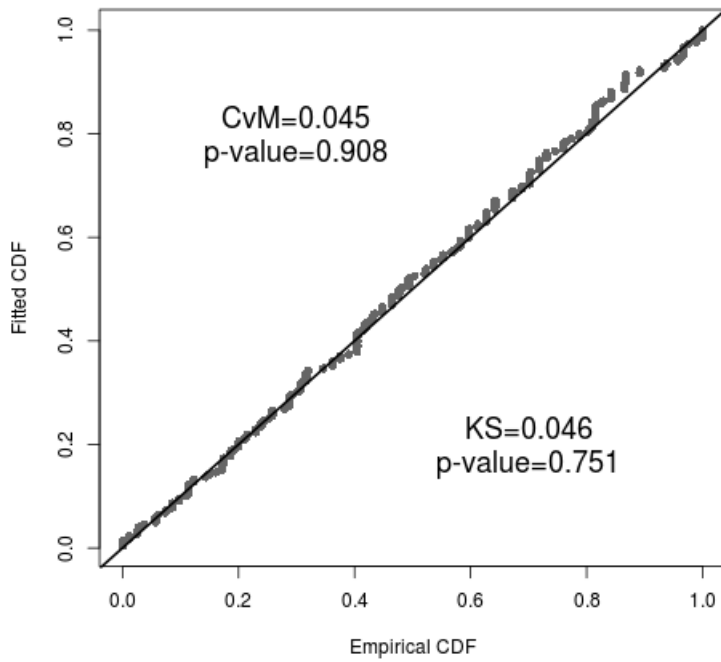
Model fitting summaries for analysis of circle-back availability data using the top-ranked detection function models for each data set

Full, summer data

Table J.1: Model selection summary for factors affecting summer availability as assessed from circle-back protocol, using the detection function from the top-ranked model in Table 4. Given is the relative difference in AIC values (ΔAIC), AIC model weights (*w*), adjusted weights for the four models used to obtain model averaged availability estimates (*w**), twice the negative log-likelihood (-2*l*) and the number of parameters in the model (*NPar*). The '.' model indicates availability is equal across all factors.

Model	ΔAIC	*w*	*w**	-2*l*	*NPar*
.	0.00	0.60	0.65	175.58	1
offshore	1.80	0.24	0.27	175.38	2
region	4.81	0.05	0.06	174.39	4
colour	4.85	0.05		174.42	4
offshore+colour	6.61	0.02		174.19	5
region+offshore	6.80	0.02	0.02	174.37	5
region+colour	9.93	0.00		173.51	7
region+offshore+colour	11.85	0.00		173.43	8

Table J.2: Model selection summary for factors affecting summer availability as assessed from circle-back protocol, using the detection function from the second-ranked model in Table 4. Given is the relative difference in AIC values (ΔAIC), AIC model weights (*w*), adjusted weights for the four models used to obtain model averaged availability estimates (*w**), twice the negative log-likelihood (-2*l*) and the number of parameters in the model (*NPar*). The '.' model indicates availability is equal across all factors.

Model	ΔAIC	*w*	*w**	-2*l*	*NPar*
.	0.00	0.60	0.66	174.42	1
offshore	1.81	0.24	0.27	174.23	2
colour	4.67	0.06		173.09	4
region	4.92	0.05	0.06	173.35	4
offshore+colour	6.50	0.02		172.92	5
region+offshore	6.92	0.02	0.02	173.34	5
region+colour	9.60	0.00		172.03	7
region+offshore+colour	11.60	0.00		172.02	8

Table J.3: Model selection summary for factors affecting summer availability as assessed from circle-back protocol, using the detection function from the third-ranked model in Table 4. Given is the relative difference in AIC values (ΔAIC), AIC model weights (*w*), adjusted weights for the four models used to obtain model averaged availability estimates (*w**), twice the negative log-likelihood (*-2l*) and the number of parameters in the model (*NPar*). The '.' model indicates availability is equal across all factors.

Model	ΔAIC	*w*	*w**	*-2l*	*NPar*
.	0.00	0.60	0.65	175.77	1
offshore	1.80	0.24	0.27	175.58	2
region	4.80	0.05	0.06	174.57	4
colour	4.86	0.05		174.63	4
offshore+colour	6.62	0.02		174.39	5
region+offshore	6.78	0.02	0.02	174.56	5
region+colour	9.94	0.00		173.71	7
region+offshore+colour	11.86	0.00		173.63	8

Table J.4: Model selection summary for factors affecting summer availability as assessed from circle-back protocol, using the detection function from the fourth-ranked model in Table 4. Given is the relative difference in AIC values (ΔAIC), AIC model weights (*w*), adjusted weights for the four models used to obtain model averaged availability estimates (*w**), twice the negative log-likelihood (*-2l*) and the number of parameters in the model (*NPar*). The '.' model indicates availability is equal across all factors.

Model	ΔAIC	*w*	*w**	*-2l*	*NPar*
.	0.00	0.60	0.66	174.54	1
offshore	1.80	0.24	0.27	174.35	2
colour	4.68	0.06		173.23	4
region	4.92	0.05	0.06	173.46	4
offshore+colour	6.50	0.02		173.05	5
region+offshore	6.91	0.02	0.02	173.46	5
region+colour	9.71	0.00		172.25	7
region+offshore+colour	11.69	0.00		172.24	8

Table J.5: Model selection summary for factors affecting summer availability as assessed from circle-back protocol, using the detection function from the fifth-ranked model in Table 4. Given is the relative difference in AIC values (ΔAIC), AIC model weights (*w*), adjusted weights for the four models used to obtain model averaged availability estimates (*w**), twice the negative log-likelihood (*-2l*) and the number of parameters in the model (*NPar*). The '.' model indicates availability is equal across all factors.

Model	ΔAIC	*w*	*w**	*-2l*	*NPar*
.	0.00	0.60	0.66	174.73	1
offshore	1.80	0.24	0.27	174.53	2
colour	4.73	0.06		173.46	4
region	4.89	0.05	0.06	173.62	4
offshore+colour	6.53	0.02		173.26	5
region+offshore	6.88	0.02	0.02	173.61	5
region+colour	9.80	0.00		172.53	7
region+offshore+colour	11.77	0.00		172.50	8

Table J.6: Model selection summary for factors affecting summer availability as assessed from circle-back protocol, using the detection function from the sixth-ranked model in Table 4. Given is the relative difference in AIC values (ΔAIC), AIC model weights (*w*), adjusted weights for the four models used to obtain model averaged availability estimates (*w**), twice the negative log-likelihood (*-2l*) and the number of parameters in the model (*NPar*). The '.' model indicates availability is equal across all factors.

Model	ΔAIC	*w*	*w**	*-2l*	*NPar*
.	0.00	0.60	0.66	174.81	1
offshore	1.80	0.24	0.27	174.61	2
colour	4.74	0.06		173.55	4
region	4.88	0.05	0.06	173.69	4
offshore+colour	6.54	0.02		173.35	5
region+offshore	6.87	0.02	0.02	173.68	5
region+colour	9.83	0.00		172.63	7
region+offshore+colour	11.79	0.00		172.59	8

Reduced, summer data

Table J.7: Model selection summary for factors affecting summer availability as assessed from circle-back protocol, using the detection function from the top-ranked model in Table 6. Given is the relative difference in AIC values (ΔAIC), AIC model weights (*w*), adjusted weights for the four models used to obtain model averaged availability estimates (*w**), twice the negative log-likelihood (*-2l*) and the number of parameters in the model (*NPar*). The '.' model indicates availability is equal across all factors.

Model	ΔAIC	*w*	*w**	*-2l*	*NPar*
.	0.00	0.50	0.55	143.89	1
offshore	1.58	0.23	0.25	143.47	2
region	2.61	0.14	0.15	140.50	4
region+offshore	4.51	0.05	0.06	140.40	5
colour	5.11	0.04		143.00	4
offshore+colour	6.60	0.02		142.49	5
region+colour	6.85	0.02		138.74	7
region+offshore+colour	8.81	0.01		138.70	8

Table J.8: Model selection summary for factors affecting summer availability as assessed from circle-back protocol, using the detection function from the second-ranked model in Table 6. Given is the relative difference in AIC values (ΔAIC), AIC model weights (*w*), adjusted weights for the four models used to obtain model averaged availability estimates (*w**), twice the negative log-likelihood (-2*l*) and the number of parameters in the model (*NPar*). The '.' model indicates availability is equal across all factors.

Model	ΔAIC	*w*	*w**	-2*l*	*NPar*
.	0.00	0.50	0.54	144.29	1
offshore	1.58	0.23	0.24	143.86	2
region	2.48	0.14	0.16	140.77	4
region+offshore	4.38	0.06	0.06	140.66	5
colour	5.21	0.04		143.50	4
offshore+colour	6.68	0.02		142.97	5
region+colour	7.30	0.01		139.58	7
region+offshore+colour	9.20	0.01		139.49	8

Table J.9: Model selection summary for factors affecting summer availability as assessed from circle-back protocol, using the detection function from the third-ranked model in Table 6. Given is the relative difference in AIC values (ΔAIC), AIC model weights (*w*), adjusted weights for the four models used to obtain model averaged availability estimates (*w**), twice the negative log-likelihood (-2*l*) and the number of parameters in the model (*NPar*). The '.' model indicates availability is equal across all factors.

Model	ΔAIC	*w*	*w**	-2*l*	*NPar*
.	0.00	0.50	0.54	144.07	1
offshore	1.57	0.23	0.25	143.65	2
region	2.56	0.14	0.15	140.63	4
region+offshore	4.46	0.05	0.06	140.53	5
colour	5.15	0.04		143.22	4
offshore+colour	6.63	0.02		142.70	5
region+colour	7.16	0.01		139.24	7
region+offshore+colour	9.09	0.01		139.16	8

Table J.10: Model selection summary for factors affecting summer availability as assessed from circle-back protocol, using the detection function from the fifth-ranked model in Table 6. Given is the relative difference in AIC values (ΔAIC), AIC model weights (*w*), adjusted weights for the four models used to obtain model averaged availability estimates (*w**), twice the negative log-likelihood (-2*l*) and the number of parameters in the model (*NPar*). The '.' model indicates availability is equal across all factors.

Model	ΔAIC	*w*	*w**	-2*l*	*NPar*
.	0.00	0.50	0.56	143.57	1
offshore	1.60	0.23	0.25	143.17	2
region	2.81	0.12	0.14	140.38	4
region+offshore	4.73	0.05	0.05	140.29	5
colour	4.91	0.04		142.47	4
region+colour	5.99	0.03		137.56	7
offshore+colour	6.46	0.02		142.03	5
region+offshore+colour	7.99	0.01		137.55	8

Table J.11: Model selection summary for factors affecting summer availability as assessed from circle-back protocol, using the detection function from the sixth-ranked model in Table 6. Given is the relative difference in AIC values (ΔAIC), AIC model weights (*w*), adjusted weights for the four models used to obtain model averaged availability estimates (*w**), twice the negative log-likelihood (-2*l*) and the number of parameters in the model (*NPar*). The '.' model indicates availability is equal across all factors.

Model	ΔAIC	*w*	*w**	-2*l*	*NPar*
.	0.00	0.50	0.55	143.97	1
offshore	1.58	0.23	0.25	143.55	2
region	2.61	0.14	0.15	140.58	4
region+offshore	4.50	0.05	0.06	140.47	5
colour	5.11	0.04		143.08	4
offshore+colour	6.61	0.02		142.58	5
region+colour	7.06	0.01		139.03	7
region+offshore+colour	9.00	0.01		138.97	8

Table J.12: Model selection summary for factors affecting summer availability as assessed from circle-back protocol, using the detection function from the seventh-ranked model in Table 6. Given is the relative difference in AIC values (ΔAIC), AIC model weights (*w*), adjusted weights for the four models used to obtain model averaged availability estimates (*w**), twice the negative log-likelihood (-2*l*) and the number of parameters in the model (*NPar*). The '.' model indicates availability is equal across all factors.

Model	ΔAIC	*w*	*w**	-2*l*	*NPar*
.	0.00	0.50	0.54	144.14	1
offshore	1.57	0.23	0.25	143.71	2
region	2.57	0.14	0.15	140.70	4
region+offshore	4.46	0.05	0.06	140.60	5
colour	5.15	0.04		143.28	4
offshore+colour	6.63	0.02		142.77	5
region+colour	7.29	0.01		139.42	7
region+offshore+colour	9.20	0.01		139.33	8

Table J.13: Model selection summary for factors affecting summer availability as assessed from circle-back protocol, using the detection function from the eighth-ranked model in Table 6. Given is the relative difference in AIC values (ΔAIC), AIC model weights (*w*), adjusted weights for the four models used to obtain model averaged availability estimates (*w**), twice the negative log-likelihood (-2*l*) and the number of parameters in the model (*NPar*). The '.' model indicates availability is equal across all factors.

Model	ΔAIC	*w*	*w**	-2*l*	*NPar*
.	0.00	0.50	0.53	144.70	1
offshore	1.58	0.23	0.24	144.28	2
region	2.40	0.15	0.16	141.10	4
region+offshore	4.29	0.06	0.06	140.99	5
colour	5.28	0.04		143.98	4
offshore+colour	6.73	0.02		143.43	5
region+colour	7.53	0.01		140.23	7
region+offshore+colour	9.40	0.00		140.10	8

Full, winter data

Table J.14: Model selection summary for factors affecting winter availability as assessed from circle-back protocol, using the detection function from the top-ranked model in Table 9. Given is the relative difference in AIC values (ΔAIC), AIC model weights (*w*), adjusted weights for the four models used to obtain model averaged availability estimates (*w**), twice the negative log-likelihood (-2*l*) and the number of parameters in the model (*NPar*). The '.' model indicates availability is equal across all factors.

Model	ΔAIC	*w*	*w**	-2*l*	*NPar*
region	0.00	0.45	0.57	144.53	4
region+offshore	1.92	0.17	0.22	144.45	5
region+colour	2.50	0.13		141.03	7
.	2.69	0.12	0.15	153.22	1
region+offshore+colour	4.47	0.05		141.00	8
offshore	4.48	0.05	0.06	153.01	2
colour	5.95	0.02		150.48	4
offshore+colour	7.92	0.01		150.45	5

Table J.15: Model selection summary for factors affecting winter availability as assessed from circle-back protocol, using the detection function from the second-ranked model in Table 9. Given is the relative difference in AIC values (ΔAIC), AIC model weights (*w*), adjusted weights for the four models used to obtain model averaged availability estimates (*w**), twice the negative log-likelihood (-2*l*) and the number of parameters in the model (*NPar*). The '.' model indicates availability is equal across all factors.

Model	ΔAIC	*w*	*w**	-2*l*	*NPar*
region	0.00	0.47	0.58	144.95	4
region+offshore	1.86	0.19	0.23	144.81	5
region+colour	2.72	0.12		141.67	7
.	3.00	0.11	0.13	153.95	1
region+offshore+colour	4.63	0.05		141.58	8
offshore	4.73	0.04	0.05	153.68	2
colour	6.43	0.02		151.38	4
offshore+colour	8.37	0.01		151.32	5

Table J.16: Model selection summary for factors affecting winter availability as assessed from circle-back protocol, using the detection function from the third-ranked model in Table 9. Given is the relative difference in AIC values (ΔAIC), AIC model weights (*w*), adjusted weights for the four models used to obtain model averaged availability estimates (*w**), twice the negative log-likelihood (-2*l*) and the number of parameters in the model (*NPar*). The '.' model indicates availability is equal across all factors.

Model	ΔAIC	*w*	*w**	-2*l*	*NPar*
region	0.00	0.46	0.58	144.71	4
region+offshore	1.90	0.18	0.22	144.61	5
region+colour	2.56	0.13		141.27	7
.	2.83	0.11	0.14	153.53	1
region+offshore+colour	4.51	0.05		141.22	8
offshore	4.60	0.05	0.06	153.31	2
colour	6.13	0.02		150.83	4
offshore+colour	8.09	0.01		150.79	5

Table J.17: Model selection summary for factors affecting winter availability as assessed from circle-back protocol, using the detection function from the fourth-ranked model in Table 9. Given is the relative difference in AIC values (ΔAIC), AIC model weights (*w*), adjusted weights for the four models used to obtain model averaged availability estimates (*w**), twice the negative log-likelihood (*-2l*) and the number of parameters in the model (*NPar*). The '.' model indicates availability is equal across all factors.

Model	ΔAIC	*w*	*w**	*-2l*	*NPar*
region	0.00	0.49	0.59	145.66	4
region+offshore	1.71	0.21	0.25	145.37	5
region+colour	3.01	0.11		142.67	7
.	3.32	0.09	0.11	154.98	1
region+offshore+colour	4.79	0.04		142.45	8
offshore	4.97	0.04	0.05	154.63	2
colour	6.98	0.01		152.64	4
offshore+colour	8.89	0.01		152.55	5

Reduced, winter data

Table J.18: Model selection summary for factors affecting winter availability as assessed from circle-back protocol, using the detection function from the top-ranked model in Table 11. Given is the relative difference in AIC values (ΔAIC), AIC model weights (*w*), adjusted weights for the four models used to obtain model averaged availability estimates (*w**), twice the negative log-likelihood (*-2l*) and the number of parameters in the model (*NPar*). The '.' model indicates availability is equal across all factors.

Model	ΔAIC	*w*	*w**	*-2l*	*NPar*
region	0.00	0.47	0.52	115.06	4
region+offshore	1.75	0.20	0.22	114.81	5
.	2.02	0.17	0.19	123.08	1
offshore	4.00	0.06	0.07	123.06	2
region+colour	4.24	0.06		113.30	7
region+offshore+colour	5.88	0.02		112.95	8
colour	7.33	0.01		122.39	4
offshore+colour	9.32	0.00		122.39	5

Table J.19: Model selection summary for factors affecting winter availability as assessed from circle-back protocol, using the detection function from the second-ranked model in Table 11. Given is the relative difference in AIC values (ΔAIC), AIC model weights (*w*), adjusted weights for the four models used to obtain model averaged availability estimates (*w**), twice the negative log-likelihood (*-2l*) and the number of parameters in the model (*NPar*). The '.' model indicates availability is equal across all factors.

Model	ΔAIC	*w*	*w**	*-2l*	*NPar*
region	0.00	0.43	0.49	114.34	4
.	1.47	0.21	0.24	121.82	1
region+offshore	2.00	0.16	0.18	114.34	5
offshore	3.47	0.08	0.09	121.82	2
region+colour	3.56	0.07		111.90	7
region+offshore+colour	5.56	0.03		111.90	8
colour	6.42	0.02		120.76	4
offshore+colour	8.40	0.01		120.74	5

Table J.20: Model selection summary for factors affecting winter availability as assessed from circle-back protocol, using the detection function from the third-ranked model in Table 11. Given is the relative difference in AIC values (ΔAIC), AIC model weights (*w*), adjusted weights for the four models used to obtain model averaged availability estimates (*w**), twice the negative log-likelihood (*-2l*) and the number of parameters in the model (*NPar*). The '.' model indicates availability is equal across all factors.

Model	ΔAIC	*w*	*w**	*-2l*	*NPar*
region	0.00	0.48	0.53	115.55	4
region+offshore	1.70	0.20	0.23	115.25	5
.	2.17	0.16	0.18	123.72	1
offshore	4.13	0.06	0.07	123.68	2
region+colour	4.35	0.05		113.91	7
region+offshore+colour	5.94	0.02		113.49	8
colour	7.52	0.01		123.08	4
offshore+colour	9.52	0.00		123.08	5

Stratum-specific estimates of summer abundance for the top-ranked detection function models using the full data set.

Table K.1: Estimated summer abundance of Hector's dolphins in each stratum ($\hat{N}_k$) and overall obtained from the top-ranked detection function models for the full data set, and using the dive-cycle based estimates of availability. Given is the estimate of availability ($\hat{P}_{ak}$) and the estimated abundance ($\hat{N}_k$) from each detection function model. Column labels indicate the order of the detection function models in Table 4 with the values in parentheses indicating the corresponding adjusted AIC model weight for each detection function model.

Coastal Section	Offshore Stratum (nmi)	All $\hat{P}_{ak}$	SE	1 (0.50) $\hat{N}_k$	SE	2 (0.27) $\hat{N}_k$	SE	3 (0.08) $\hat{N}_k$	SE
Golden Bay North	0–4	0.63	0.12						
	4–12	0.63	0.12						
Golden Bay A	0–4	0.63	0.12						
	4–12	0.63	0.12						
	12–20	0.63	0.12						
Golden Bay B	0–4	0.63	0.12						
	4–12	0.63	0.12						
	12–20	0.63	0.12						
Marlborough Sounds	0–4	0.63	0.12						
	4–12	0.63	0.12						
	12–20	0.63	0.12						
Cloudy/Clifford Bay	0–4	0.63	0.12	403	152	477	178	397	150
	4–12	0.63	0.12	468	168	552	198	462	166
	12–20	0.63	0.12						
Kaikoura	0–4	0.57	0.05	371	198	416	217	368	197
	4–12	0.57	0.05						
	12–20	0.57	0.05						
Clarence	0–4	0.57	0.05	137	115	155	129	135	114
	4–12	0.57	0.05						
	12–20	0.57	0.05						
Pegasus Bay	0–4	0.53	0.05	418	123	518	152	411	120
	4–12	0.53	0.05	277	160	323	185	273	158
	12–20	0.53	0.05	297	280	361	342	292	275
Banks Pen. North	0–4	0.53	0.05	878	191	1 041	230	865	188
	4–12	0.53	0.05	892	326	1 089	404	876	319
	12–20	0.53	0.05	441	311	535	378	433	306
Banks Pen. South	0–4	0.42	0.03	1 850	354	2 175	416	1 824	350
	4–12	0.42	0.03	1 055	468	1 207	525	1 043	464
	12–20	0.42	0.03						
Timaru	0–4	0.42	0.03	717	260	861	308	706	257
	4–12	0.42	0.03	1 131	510	1 239	551	1 123	507
	12–20	0.42	0.03						
Otago	0–4	0.40	0.05						
	4–12	0.40	0.05						
	12–20	0.40	0.05						
Total				9 334	1 316	10 949	1 608	9 208	1292

Table K.1 (cont): Estimated summer abundance of Hector's dolphins in each stratum ($\hat{N}_k$) and overall obtained from the top-ranked detection function models for the full data set, and using the dive-cycle based estimates of availability. Given is the estimate of availability ($\hat{N}_k$) and the estimated abundance ($\hat{N}_k$) from each detection function model. Column labels indicate the order of the detection function models in Table 4 with the values in parentheses indicating the corresponding adjusted AIC model weight for each detection function model.

Coastal Section	Offshore Stratum (nmi)	All $\hat{P}_{ak}$	SE	4 (0.06) $\hat{N}_k$	SE	5 (0.06) $\hat{N}_k$	SE	6 (0.02) $\hat{N}_k$	SE
Golden Bay North	0–4	0.63	0.12						
	4–12	0.63	0.12						
Golden Bay A	0–4	0.63	0.12						
	4–12	0.63	0.12						
	12–20	0.63	0.12						
Golden Bay B	0–4	0.63	0.12						
	4–12	0.63	0.12						
	12–20	0.63	0.12						
Marlborough Sounds	0–4	0.63	0.12						
	4–12	0.63	0.12						
	12–20	0.63	0.12						
Cloudy/Clifford Bay	0–4	0.63	0.12	465	175	448	168	442	169
	4–12	0.63	0.12	539	195	518	186	512	188
	12–20	0.63	0.12						
Kaikoura	0–4	0.57	0.05	409	214	398	209	394	209
	4–12	0.57	0.05						
	12–20	0.57	0.05						
Clarence	0–4	0.57	0.05	152	126	147	123	146	122
	4–12	0.57	0.05						
	12–20	0.57	0.05						
Pegasus Bay	0–4	0.53	0.05	504	150	480	141	472	146
	4–12	0.53	0.05	316	181	305	175	301	174
	12–20	0.53	0.05	351	333	336	318	331	315
Banks Pen. North	0–4	0.53	0.05	1 017	228	977	215	964	225
	4–12	0.53	0.05	1 061	396	1 014	374	998	379
	12–20	0.53	0.05	521	369	498	352	491	349
Banks Pen. South	0–4	0.42	0.03	2 126	414	2 048	390	2 021	413
	4–12	0.42	0.03	1 182	516	1 145	501	1 133	501
	12–20	0.42	0.03						
Timaru	0–4	0.42	0.03	840	302	805	288	794	292
	4–12	0.42	0.03	1 219	543	1 192	532	1 184	531
	12–20	0.42	0.03						
Otago	0–4	0.40	0.05						
	4–12	0.40	0.05						
	12–20	0.40	0.05						
Total				10 702	1 617	10 311	1 490	10 183	1 643

Table K.2: Estimated summer abundance of Hector's dolphins in each stratum ($\hat{N}_k$) and overall obtained from the top-ranked detection function models for the full data set, and using the circle-back based estimates of availability. Given is the estimate of availability ($\hat{N}_k$) and the estimated abundance ($\hat{N}_k$) from each detection function model. Column labels indicate the order of the detection function models in Table 4 with the values in parentheses indicating the corresponding adjusted AIC model weight for each detection function model.

| Coastal Section | Offshore Stratum (nmi) | 1 (0.50) | | | | 2 (0.27) | | | |
		$\hat{P}_{ak}$	SE	$\hat{N}_k$	SE	$\hat{P}_{ak}$	SE	$\hat{N}_k$	SE
Golden Bay North	0–4	0.56	0.07			0.68	0.08		
	4–12	0.55	0.07			0.66	0.08		
Golden Bay A	0–4	0.56	0.07			0.68	0.08		
	4–12	0.55	0.07			0.66	0.08		
	12–20	0.55	0.07			0.66	0.08		
Golden Bay B	0–4	0.56	0.07			0.68	0.08		
	4–12	0.55	0.07			0.66	0.08		
	12–20	0.55	0.07			0.66	0.08		
Marlborough Sounds	0–4	0.56	0.07			0.68	0.08		
	4–12	0.55	0.07			0.66	0.08		
	12–20	0.55	0.07			0.66	0.08		
Cloudy/Clifford Bay	0–4	0.56	0.07	451	157	0.68	0.08	443	152
	4–12	0.55	0.07	533	176	0.66	0.08	521	171
	12–20	0.55	0.07			0.66	0.08		
Kaikoura	0–4	0.57	0.06	370	199	0.68	0.07	344	181
	4–12	0.56	0.07			0.67	0.08		
	12–20	0.56	0.07			0.67	0.08		
Clarence	0–4	0.57	0.06	136	115	0.68	0.07	128	107
	4–12	0.56	0.07			0.67	0.08		
	12–20	0.56	0.07			0.67	0.08		
Pegasus Bay	0–4	0.57	0.05	392	115	0.69	0.06	403	119
	4–12	0.56	0.06	264	153	0.67	0.06	256	147
	12–20	0.56	0.06	283	267	0.67	0.06	285	271
Banks Pen. North	0–4	0.57	0.05	823	180	0.69	0.06	811	180
	4–12	0.56	0.06	850	313	0.67	0.06	862	322
	12–20	0.56	0.06	420	297	0.67	0.06	423	300
Banks Pen. South	0–4	0.57	0.05	1 364	273	0.69	0.06	1 333	265
	4–12	0.56	0.06	791	356	0.68	0.07	752	331
	12–20	0.56	0.06			0.68	0.07		
Timaru	0–4	0.57	0.05	529	194	0.69	0.06	528	191
	4–12	0.56	0.06	848	387	0.68	0.07	772	347
	12–20	0.56	0.06			0.68	0.07		
Otago	0–4	0.57	0.05			0.69	0.06		
	4–12	0.56	0.06			0.68	0.07		
	12–20	0.56	0.06			0.68	0.07		
Total				8 054	1 224			7 861	1 239

Table K.2 (cont): Estimated summer abundance of Hector's dolphins in each stratum ($\hat{N}_k$) and overall obtained from the top-ranked detection function models for the full data set, and using the circle-back based estimates of availability. Given is the estimate of availability ($\hat{N}_k$) and the estimated abundance ($\hat{N}_k$) from each detection function model. Column labels indicate the order of the detection function models in Table 4 with the values in parentheses indicating the corresponding adjusted AIC model weight for each detection function model.

Coastal Section	Offshore Stratum (nmi)	3 (0.08)				4 (0.06)			
		$\hat{P}_{ak}$	SE	$\hat{N}_k$	SE	$\hat{P}_{ak}$	SE	$\hat{N}_k$	SE
Golden Bay North	0–4	0.54	0.06			0.65	0.08		
	4–12	0.53	0.06			0.64	0.08		
Golden Bay A	0–4	0.54	0.06			0.65	0.08		
	4–12	0.53	0.06			0.64	0.08		
	12–20	0.53	0.06			0.64	0.08		
Golden Bay B	0–4	0.54	0.06			0.65	0.08		
	4–12	0.53	0.06			0.64	0.08		
	12–20	0.53	0.06			0.64	0.08		
Marlborough Sounds	0–4	0.54	0.06			0.65	0.08		
	4–12	0.53	0.06			0.64	0.08		
	12–20	0.53	0.06			0.64	0.08		
Cloudy/Clifford Bay	0–4	0.54	0.06	462	161	0.65	0.08	452	156
	4–12	0.53	0.06	548	181	0.64	0.08	533	176
	12–20	0.53	0.06			0.64	0.08		
Kaikoura	0–4	0.55	0.06	381	206	0.65	0.07	353	186
	4–12	0.54	0.06			0.64	0.08		
	12–20	0.54	0.06			0.64	0.08		
Clarence	0–4	0.55	0.06	140	119	0.65	0.07	131	109
	4–12	0.54	0.06			0.64	0.08		
	12–20	0.54	0.06			0.64	0.08		
Pegasus Bay	0–4	0.55	0.05	400	118	0.66	0.06	410	122
	4–12	0.54	0.05	271	157	0.64	0.06	262	151
	12–20	0.54	0.05	290	273	0.64	0.06	291	276
Banks Pen. North	0–4	0.55	0.05	842	184	0.66	0.06	826	186
	4–12	0.54	0.05	869	320	0.64	0.06	879	331
	12–20	0.54	0.05	430	304	0.64	0.06	431	306
Banks Pen. South	0–4	0.55	0.05	1 395	281	0.66	0.06	1 358	277
	4–12	0.54	0.06	813	367	0.65	0.07	769	341
	12–20	0.54	0.06			0.65	0.07		
Timaru	0–4	0.55	0.05	540	199	0.66	0.06	536	196
	4–12	0.54	0.06	876	401	0.65	0.07	794	358
	12–20	0.54	0.06			0.65	0.07		
Otago	0–4	0.55	0.05			0.66	0.06		
	4–12	0.54	0.06			0.65	0.07		
	12–20	0.54	0.06			0.65	0.07		
Total				8 256	1 254			8 024	1 303

Table K.2 (cont): Estimated summer abundance of Hector's dolphins in each stratum ($\hat{N}_k$) and overall obtained from the top-ranked detection function models for the full data set, and using the circle-back based estimates of availability. Given is the estimate of availability ($\hat{N}_k$) and the estimated abundance ($\hat{N}_k$) from each detection function model. Column labels indicate the order of the detection function models in Table 4 with the values in parentheses indicating the corresponding adjusted AIC model weight for each detection function model.

Coastal Section	Offshore Stratum (nmi)	5 (0.06)				6 (0.02)			
		$\hat{P}_{\alpha k}$	SE	$\hat{N}_k$	SE	$\hat{P}_{\alpha k}$	SE	$\hat{N}_k$	SE
Golden Bay North	0–4	0.62	0.07			0.61	0.07		
	4–12	0.61	0.07			0.60	0.07		
Golden Bay A	0–4	0.62	0.07			0.61	0.07		
	4–12	0.61	0.07			0.60	0.07		
	12–20	0.61	0.07			0.60	0.07		
Golden Bay B	0–4	0.62	0.07			0.61	0.07		
	4–12	0.61	0.07			0.60	0.07		
	12–20	0.61	0.07			0.60	0.07		
Marlborough Sounds	0–4	0.62	0.07			0.61	0.07		
	4–12	0.61	0.07			0.60	0.07		
	12-20	0.61	0.07			0.60	0.07		
Cloudy/Clifford Bay	0–4	0.62	0.07	453	156	0.61	0.07	453	160
	4–12	0.61	0.07	535	176	0.60	0.07	536	181
	12–20	0.61	0.07			0.60	0.07		
Kaikoura	0–4	0.63	0.07	358	190	0.62	0.07	360	192
	4–12	0.62	0.07			0.61	0.07		
	12–20	0.62	0.07			0.61	0.07		
Clarence	0–4	0.63	0.07	132	111	0.62	0.07	133	112
	4–12	0.62	0.07			0.61	0.07		
	12–20	0.62	0.07			0.61	0.07		
Pegasus Bay	0–4	0.63	0.06	407	119	0.62	0.06	406	126
	4–12	0.62	0.06	263	151	0.61	0.06	264	153
	12–20	0.62	0.06	290	275	0.61	0.06	290	276
Banks Pen. North	0–4	0.63	0.06	828	183	0.62	0.06	829	194
	4–12	0.62	0.06	875	325	0.61	0.06	875	335
	12–20	0.62	0.06	430	305	0.61	0.06	430	307
Banks Pen. South	0–4	0.63	0.06	1 363	272	0.62	0.06	1 366	291
	4–12	0.62	0.06	777	345	0.61	0.06	780	350
	12–20	0.62	0.06			0.61	0.06		
Timaru	0–4	0.63	0.06	536	195	0.62	0.06	536	200
	4–12	0.62	0.06	809	366	0.61	0.06	816	371
	12–20	0.62	0.06			0.61	0.06		
Otago	0–4	0.63	0.06			0.62	0.06		
	4–12	0.62	0.06			0.61	0.06		
	12–20	0.62	0.06			0.61	0.06		
Total				8 056	1 257			8 074	1 389

SECTION L

Stratum-specific estimates of summer abundance for the top-ranked detection function models using the reduced data set

Table L.1: Estimated summer abundance of Hector's dolphins in each stratum ($\hat{N}_k$) and overall obtained from the top-ranked detection function models for the reduced data set, and using the dive-cycle based estimates of availability. Given is the estimate of availability ($\hat{P}_{\alpha k}$) and the estimated abundance ($\hat{N}_k$) from each detection function model. Column labels indicate the order of the detection function models in Table 6 with the values in parentheses indicating the corresponding adjusted AIC model weight for each detection function model.

Coastal Section	Offshore Stratum (nmi)	All $\hat{P}_{\alpha k}$	SE	1 (0.39) $\hat{N}_k$	SE	2 (0.16) $\hat{N}_k$	SE	3 (0.14) $\hat{N}_k$	SE
Golden Bay North	0–4	0.63	0.12						
	4–12	0.63	0.12						
Golden Bay A	0–4	0.63	0.12						
	4–12	0.63	0.12						
	12–20	0.63	0.12						
Golden Bay B	0–4	0.63	0.12						
	4–12	0.63	0.12						
	12–20	0.63	0.12						
Marlborough Sounds	0–4	0.63	0.12						
	4–12	0.63	0.12						
	12–20	0.63	0.12						
Cloudy/Clifford Bay	0–4	0.63	0.12	431	151	409	148	415	146
	4–12	0.63	0.12	460	141	435	138	442	135
	12–20	0.63	0.12						
Kaikoura	0–4	0.57	0.05	342	195	335	192	335	191
	4–12	0.57	0.05						
	12–20	0.57	0.05						
Clarence	0–4	0.57	0.05	187	157	180	152	182	152
	4–12	0.57	0.05						
	12–20	0.57	0.05						
Pegasus Bay	0–4	0.53	0.05	459	126	427	127	439	120
	4–12	0.53	0.05	336	192	322	186	325	186
	12–20	0.53	0.05	249	245	234	233	239	236
Banks Pen. North	0–4	0.53	0.05	927	220	878	220	893	211
	4–12	0.53	0.05	998	353	934	342	957	337
	12–20	0.53	0.05	575	396	540	376	551	380
Banks Pen. South	0–4	0.42	0.03	2 030	397	1 924	411	1957	383
	4–12	0.42	0.03	1 272	558	1 221	546	1232	543
	12–20	0.42	0.03						
Timaru	0–4	0.42	0.03	782	304	739	298	752	294
	4–12	0.42	0.03	1 109	536	1 078	529	1 081	525
	12–20	0.42	0.03						
Otago	0–4	0.40	0.05						
	4–12	0.40	0.05						
	12–20	0.40	0.05						
Total				10 159	1 362	9 655	1 488	9 799	1 303

Table L.1 (cont): Estimated summer abundance of Hector's dolphins in each stratum ($\hat{N}_k$) and overall obtained from the top-ranked detection function models for the reduced data set, and using the dive-cycle based estimates of availability. Given is the estimate of availability ($\hat{P}_{\alpha k}$) and the estimated abundance ($\hat{N}_k$) from each detection function model. Column labels indicate the order of the detection function models in Table 6 with the values in parentheses indicating the corresponding adjusted AIC model weight for each detection function model.

Coastal Section	Offshore Stratum (nmi)	$\hat{P}_{\alpha k}$	SE	5 (0.10) $\hat{N}_k$	SE	6 (0.09) $\hat{N}_k$	SE	7 (0.06) $\hat{N}_k$	SE
Golden Bay North	0–4	0.63	0.12						
	4–12	0.63	0.12						
Golden Bay A	0–4	0.63	0.12						
	4–12	0.63	0.12						
	12–20	0.63	0.12						
Golden Bay B	0–4	0.63	0.12						
	4–12	0.63	0.12						
	12–20	0.63	0.12						
Marlborough Sounds	0–4	0.63	0.12						
	4–12	0.63	0.12						
	12–20	0.63	0.12						
Cloudy/Clifford Bay	0–4	0.63	0.12	469	184	431	151	417	146
	4–12	0.63	0.12	505	183	461	141	445	136
	12–20	0.63	0.12						
Kaikoura	0–4	0.57	0.05	354	201	342	194	335	191
	4–12	0.57	0.05						
	12–20	0.57	0.05						
Clarence	0–4	0.57	0.05	199	168	187	157	182	153
	4–12	0.57	0.05						
	12–20	0.57	0.05						
Pegasus Bay	0–4	0.53	0.05	517	187	459	126	441	121
	4–12	0.53	0.05	362	212	336	192	326	187
	12–20	0.53	0.05	276	276	249	246	240	237
Banks Pen. North	0–4	0.53	0.05	1 014	306	928	219	897	211
	4–12	0.53	0.05	1 114	466	999	352	962	338
	12–20	0.53	0.05	637	459	575	397	554	382
Banks Pen. South	0–4	0.42	0.03	2 218	591	2 031	395	1 966	383
	4–12	0.42	0.03	1 359	619	1 272	557	1 236	543
	12–20	0.42	0.03						
Timaru	0–4	0.42	0.03	860	368	783	304	756	295
	4–12	0.42	0.03	1 162	565	1 109	535	1 083	525
	12–20	0.42	0.03						
Otago	0–4	0.40	0.05						
	4–12	0.40	0.05						
	12–20	0.40	0.05						
Total				11 048	2453	10 165	1 348	9 842	1 298

Table L.1 (cont): Estimated summer abundance of Hector's dolphins in each stratum ($\hat{N}_k$) and overall obtained from the top-ranked detection function models for the reduced data set, and using the dive-cycle based estimates of availability. Given is the estimate of availability ($\hat{P}_{\alpha k}$) and the estimated abundance ($\hat{N}_k$) from each detection function model. Column labels indicate the order of the detection function models in Table 6 with the values in parentheses indicating the corresponding adjusted AIC model weight for each detection function model.

Coastal Section	Offshore Stratum (nmi)	All		8 (0.05)	
		$\hat{P}_{\alpha k}$	SE	$\hat{N}_k$	SE
Golden Bay North	0–4	0.63	0.12		
	4–12	0.63	0.12		
Golden Bay A	0–4	0.63	0.12		
	4–12	0.63	0.12		
	12–20	0.63	0.12		
Golden Bay B	0–4	0.63	0.12		
	4–12	0.63	0.12		
	12–20	0.63	0.12		
Marlborough Sounds	0–4	0.63	0.12		
	4–12	0.63	0.12		
	12–20	0.63	0.12		
Cloudy/Clifford Bay	0–4	0.63	0.12	398	142
	4–12	0.63	0.12	422	130
	12–20	0.63	0.12		
Kaikoura	0–4	0.57	0.05	331	191
	4–12	0.57	0.05		
	12–20	0.57	0.05		
Clarence	0–4	0.57	0.05	177	149
	4–12	0.57	0.05		
	12–20	0.57	0.05		
Pegasus Bay	0–4	0.53	0.05	410	116
	4–12	0.53	0.05	314	182
	12–20	0.53	0.05	226	225
Banks Pen. North	0–4	0.53	0.05	854	205
	4–12	0.53	0.05	901	320
	12–20	0.53	0.05	522	361
Banks Pen. South	0–4	0.42	0.03	1 870	380
	4–12	0.42	0.03	1 196	534
	12–20	0.42	0.03		
Timaru	0–4	0.42	0.03	717	287
	4–12	0.42	0.03	1 062	523
	12–20	0.42	0.03		
Otago	0–4	0.40	0.05		
	4–12	0.40	0.05		
	12–20	0.40	0.05		
Total				9 402	1 300

Table L.2: Estimated summer abundance of Hector's dolphins in each stratum ($\hat{N}_k$) and overall obtained from the top-ranked detection function models for the reduced data set, and using the circle-back based estimates of availability. Given is the estimate of availability ($\hat{N}_k$) and the estimated abundance ($\hat{N}_k$) from each detection function model. Column labels indicate the order of the detection function models in Table 6 with the values in parentheses indicating the corresponding adjusted AIC model weight for each detection function model.

Coastal Section	Offshore Stratum (nmi)	1 (0.39)				2 (0.16)			
		$\hat{P}_{ak}$	SE	$\hat{N}_k$	SE	$\hat{P}_{ak}$	SE	$\hat{N}_k$	SE
Golden Bay North	0–4	0.56	0.10			0.53	0.10		
	4–12	0.54	0.10			0.51	0.09		
Golden Bay A	0–4	0.56	0.10			0.53	0.10		
	4–12	0.54	0.10			0.51	0.09		
	12–20	0.54	0.10			0.51	0.09		
Golden Bay B	0–4	0.56	0.10			0.53	0.10		
	4–12	0.54	0.10			0.51	0.09		
	12–20	0.54	0.10			0.51	0.09		
Marlborough Sounds	0–4	0.56	0.10			0.53	0.10		
	4–12	0.54	0.10			0.51	0.09		
	12–20	0.54	0.10			0.51	0.09		
Cloudy/Clifford Bay	0–4	0.56	0.10	481	178	0.53	0.10	489	187
	4–12	0.54	0.10	532	175	0.51	0.09	538	184
	12–20	0.54	0.10			0.51	0.09		
Kaikoura	0–4	0.57	0.09	338	198	0.54	0.09	353	209
	4–12	0.55	0.10			0.52	0.10		
	12–20	0.55	0.10			0.52	0.10		
Clarence	0–4	0.57	0.09	185	157	0.54	0.09	190	163
	4–12	0.55	0.10			0.52	0.10		
	12–20	0.55	0.10			0.52	0.10		
Pegasus Bay	0–4	0.58	0.07	419	119	0.55	0.06	416	128
	4–12	0.57	0.07	318	184	0.53	0.07	324	190
	12–20	0.57	0.07	235	233	0.53	0.07	236	235
Banks Pen. North	0–4	0.58	0.07	847	210	0.55	0.06	856	224
	4–12	0.57	0.07	943	344	0.53	0.07	941	356
	12–20	0.57	0.07	543	378	0.53	0.07	544	382
Banks Pen. South	0–4	0.62	0.08	1 391	314	0.58	0.08	1 401	341
	4–12	0.60	0.09	899	412	0.56	0.09	917	429
	12–20	0.60	0.09			0.56	0.09		
Timaru	0–4	0.62	0.08	536	217	0.58	0.08	538	226
	4–12	0.60	0.09	784	393	0.56	0.09	810	412
	12–20	0.60	0.09			0.56	0.09		
Otago	0–4	0.62	0.08			0.58	0.08		
	4–12	0.60	0.09			0.56	0.09		
	12–20	0.60	0.09			0.56	0.09		
Total				8 449	1 291			8 552	1 463

Table L.2 (cont): Estimated summer abundance of Hector's dolphins in each stratum ($\hat{N}_k$) and overall obtained from the top-ranked detection function models for the reduced data set, and using the circle-back based estimates of availability. Given is the estimate of availability ($\hat{N}_k$) and the estimated abundance ($\hat{N}_k$) from each detection function model. Column labels indicate the order of the detection function models in Table 6 with the values in parentheses indicating the corresponding adjusted AIC model weight for each detection function model.

Coastal Section	Offshore Stratum (nmi)	3 (0.14)				5 (0.10)			
		$\hat{P}_{\alpha k}$	SE	$\hat{N}_k$	SE	$\hat{P}_{\alpha k}$	SE	$\hat{N}_k$	SE
Golden Bay North	0–4	0.54	0.10			0.63	0.11		
	4–12	0.52	0.09			0.61	0.11		
Golden Bay A	0–4	0.54	0.10			0.63	0.11		
	4–12	0.52	0.09			0.61	0.11		
	12–20	0.52	0.09			0.61	0.11		
Golden Bay B	0–4	0.54	0.10			0.63	0.11		
	4–12	0.52	0.09			0.61	0.11		
	12–20	0.52	0.09			0.61	0.11		
Marlborough Sounds	0–4	0.54	0.10			0.63	0.11		
	4–12	0.52	0.09			0.61	0.11		
	12–20	0.52	0.09			0.61	0.11		
Cloudy/Clifford Bay	0–4	0.54	0.10	484	180	0.63	0.11	471	192
	4–12	0.52	0.09	534	176	0.61	0.11	524	199
	12–20	0.52	0.09			0.61	0.11		
Kaikoura	0–4	0.55	0.09	345	203	0.64	0.10	315	184
	4–12	0.53	0.10			0.62	0.11		
	12–20	0.53	0.10			0.62	0.11		
Clarence	0–4	0.55	0.09	187	159	0.64	0.10	177	151
	4–12	0.53	0.10			0.62	0.11		
	12–20	0.53	0.10			0.62	0.11		
Pegasus Bay	0–4	0.56	0.06	418	119	0.65	0.07	426	158
	4–12	0.54	0.07	320	186	0.63	0.08	308	183
	12–20	0.54	0.07	235	233	0.63	0.08	236	237
Banks Pen. North	0–4	0.56	0.06	850	211	0.65	0.07	837	259
	4–12	0.54	0.07	942	343	0.63	0.08	950	407
	12–20	0.54	0.07	543	378	0.63	0.08	543	395
Banks Pen. South	0–4	0.59	0.08	1 396	316	0.68	0.09	1 380	396
	4–12	0.57	0.09	907	418	0.66	0.10	872	412
	12–20	0.57	0.09			0.66	0.10		
Timaru	0–4	0.59	0.08	537	218	0.68	0.09	535	236
	4–12	0.57	0.09	796	401	0.66	0.10	745	375
	12–20	0.57	0.09			0.66	0.10		
Otago	0–4	0.59	0.08			0.68	0.09		
	4–12	0.57	0.09			0.66	0.10		
	12–20	0.57	0.09			0.66	0.10		
Total				8 491	1 289			8 319	1 959

Table L.2 (cont): Estimated summer abundance of Hector's dolphins in each stratum ($\hat{N}_k$) and overall obtained from the top-ranked detection function models for the reduced data set, and using the circle-back based estimates of availability. Given is the estimate of availability ($\hat{N}_k$) and the estimated abundance ($\hat{N}_k$) from each detection function model. Column labels indicate the order of the detection function models in Table 6 with the values in parentheses indicating the corresponding adjusted AIC model weight for each detection function model.

Coastal Section	Offshore Stratum (nmi)	6 (0.09)				7 (0.06)			
		$\hat{P}_{ak}$	SE	$\hat{N}_k$	SE	$\hat{P}_{ak}$	SE	$\hat{N}_k$	SE
Golden Bay North	0–4	0.55	0.10			0.53	0.10		
	4–12	0.53	0.10			0.51	0.09		
Golden Bay A	0–4	0.55	0.10			0.53	0.10		
	4–12	0.53	0.10			0.51	0.09		
	12–20	0.53	0.10			0.51	0.09		
Golden Bay B	0–4	0.55	0.10			0.53	0.10		
	4–12	0.53	0.10			0.51	0.09		
	12–20	0.53	0.10			0.51	0.09		
Marlborough Sounds	0–4	0.55	0.10			0.53	0.10		
	4–12	0.53	0.10			0.51	0.09		
	12–20	0.53	0.10			0.51	0.09		
Cloudy/Clifford Bay	0–4	0.55	0.10	494	183	0.53	0.10	496	184
	4–12	0.53	0.10	547	180	0.51	0.09	548	181
	12–20	0.53	0.10			0.51	0.09		
Kaikoura	0–4	0.56	0.09	347	203	0.54	0.09	352	207
	4–12	0.54	0.10			0.52	0.09		
	12–20	0.54	0.10			0.52	0.09		
Clarence	0–4	0.56	0.09	190	161	0.54	0.09	191	163
	4–12	0.54	0.10			0.52	0.09		
	12–20	0.54	0.10			0.52	0.09		
Pegasus Bay	0–4	0.57	0.06	430	122	0.55	0.06	429	122
	4–12	0.55	0.07	326	189	0.53	0.07	328	190
	12–20	0.55	0.07	242	239	0.53	0.07	242	239
Banks Pen. North	0–4	0.57	0.06	870	215	0.55	0.06	872	216
	4–12	0.55	0.07	969	353	0.53	0.07	967	352
	12–20	0.55	0.07	558	388	0.53	0.07	557	388
Banks Pen. South	0–4	0.60	0.08	1 428	321	0.58	0.08	1 431	323
	4–12	0.58	0.09	923	423	0.56	0.09	929	427
	12–20	0.58	0.09			0.56	0.09		
Timaru	0–4	0.60	0.08	551	223	0.58	0.08	551	224
	4–12	0.58	0.09	805	403	0.56	0.09	814	410
	12–20	0.58	0.09			0.56	0.09		
Otago	0–4	0.60	0.08			0.58	0.08		
	4–12	0.58	0.09			0.56	0.09		
	12–20	0.58	0.09			0.56	0.09		
Total				8 680	1 316			8 708	1 314

Table L.2 (cont): Estimated summer abundance of Hector's dolphins in each stratum ($\hat{N}_k$) and overall obtained from the top-ranked detection function models for the reduced data set, and using the circle-back based estimates of availability. Given is the estimate of availability ($\hat{N}_k$) and the estimated abundance ($\hat{N}_k$) from each detection function model. Column labels indicate the order of the detection function models in Table 6 with the values in parentheses indicating the corresponding adjusted AIC model weight for each detection function model.

| Coastal Section | Offshore Stratum (nmi) | 8 (0.05) | | | |
		$\hat{P}_{\alpha k}$	SE	$\hat{N}_k$	SE
Golden Bay North	0–4	0.49	0.09		
	4–12	0.47	0.09		
Golden Bay A	0–4	0.49	0.09		
	4–12	0.47	0.09		
	12–20	0.47	0.09		
Golden Bay B	0–4	0.49	0.09		
	4–12	0.47	0.09		
	12–20	0.47	0.09		
Marlborough Sounds	0–4	0.49	0.09		
	4–12	0.47	0.09		
	12–20	0.47	0.09		
Cloudy/Clifford Bay	0–4	0.49	0.09	509	193
	4–12	0.47	0.09	559	188
	12–20	0.47	0.09		
Kaikoura	0–4	0.50	0.09	374	222
	4–12	0.48	0.09		
	12–20	0.48	0.09		
Clarence	0–4	0.50	0.09	199	171
	4–12	0.48	0.09		
	12–20	0.48	0.09		
Pegasus Bay	0–4	0.51	0.06	427	125
	4–12	0.50	0.06	338	198
	12–20	0.50	0.06	243	243
Banks Pen. North	0–4	0.51	0.06	889	224
	4–12	0.50	0.06	970	356
	12–20	0.50	0.06	562	392
Banks Pen. South	0–4	0.54	0.07	1 452	341
	4–12	0.53	0.08	958	448
	12–20	0.53	0.08		
Timaru	0–4	0.54	0.07	556	232
	4–12	0.53	0.08	850	435
	12–20	0.53	0.08		
Otago	0–4	0.54	0.07		
	4–12	0.53	0.08		
	12–20	0.53	0.08		
Total				8 887	1 390

SECTION M

Stratum-specific estimates of winter abundance for the top-ranked detection function models using the full data set

Table M.1: Estimated winter abundance of Hector's dolphins in each stratum ($\hat{N}_k$) and overall obtained from the top-ranked detection function models for the full data set, and using the dive-cycle based estimates of availability. Given is the estimate of availability ($\hat{P}_{ak}$) and the estimated abundance ($\hat{N}_k$) from each detection function model. Column labels indicate the order of the detection function models in Table 10 with the values in parentheses indicating the corresponding adjusted AIC model weight for each detection function model.

Coastal Section	Offshore Stratum (nmi)	All $\hat{P}_{ak}$	SE	1 (0.77) $\hat{N}_k$	SE	2 (0.10) $\hat{N}_k$	SE
Golden Bay North	0–4	0.46	0.03				
	4–12	0.46	0.03				
Golden Bay A	0–4	0.46	0.03				
	4–12	0.46	0.03	152	163	158	170
	12–20	0.46	0.03				
Golden Bay B	0–4	0.46	0.03				
	4–12	0.46	0.03				
	12–20	0.46	0.03				
Marlborough Sounds	0–4	0.46	0.03				
	4–12	0.46	0.03				
	12-20	0.46	0.03				
Cloudy/Clifford Bay	0–4	0.46	0.03	115	67	123	72
	4–12	0.46	0.03	377	148	406	158
	12–20	0.46	0.03	207	145	227	158
Kaikoura	0–4	0.33	0.08	228	111	251	122
	4–12	0.33	0.08				
	12–20	0.33	0.08				
Clarence	0–4	0.33	0.08	405	211	427	221
	4–12	0.33	0.08				
	12–20	0.33	0.08				
Pegasus Bay	0–4	0.62	0.06	42	34	46	37
	4–12	0.62	0.06	499	245	545	264
	12–20	0.62	0.06	410	165	443	177
Banks Pen. North	0–4	0.62	0.06	276	82	295	87
	4–12	0.62	0.06	474	108	518	118
	12–20	0.62	0.06	479	222	514	235
Banks Pen. South	0–4	0.56	0.05	470	133	505	141
	4–12	0.56	0.05	256	68	276	73
	12–20	0.56	0.05	129	98	141	107
Timaru	0–4	0.56	0.05	263	90	284	97
	4–12	0.56	0.05	1 818	389	1 930	414
	12–20	0.56	0.05	1 027	283	1 103	302
Otago	0–4	0.56	0.05				
	4–12	0.56	0.05				
	12–20	0.56	0.05				
Total				7 627	902	8 194	972

Table M.1 (cont): Estimated winter abundance of Hector's dolphins in each stratum ($\hat{N}_k$) and overall obtained from the top-ranked detection function models for the full data set, and using the dive-cycle based estimates of availability. Given is the estimate of availability ($\hat{P}_{\alpha k}$) and the estimated abundance ($\hat{N}_k$) from each detection function model. Column labels indicate the order of the detection function models in Table 10 with the values in parentheses indicating the corresponding adjusted AIC model weight for each detection function model.

Coastal Section	Offshore Stratum (nmi)	All		3 (0.09)		4 (0.04)	
		$\hat{P}_{\alpha k}$	SE	$\hat{N}_k$	SE	$\hat{N}_k$	SE
Golden Bay North	0–4	0.46	0.03				
	4–12	0.46	0.03				
Golden Bay A	0–4	0.46	0.03				
	4–12	0.46	0.03	154	165	164	176
	12–20	0.46	0.03				
Golden Bay B	0–4	0.46	0.03				
	4–12	0.46	0.03				
	12–20	0.46	0.03				
Marlborough Sounds	0–4	0.46	0.03				
	4–12	0.46	0.03				
	12–20	0.46	0.03				
Cloudy/Clifford Bay	0–4	0.46	0.03	117	69	131	77
	4–12	0.46	0.03	385	150	437	173
	12–20	0.46	0.03	213	148	249	174
Kaikoura	0–4	0.33	0.08	235	114	277	136
	4–12	0.33	0.08				
	12-20	0.33	0.08				
Clarence	0–4	0.33	0.08	411	213	451	233
	4–12	0.33	0.08				
	12-20	0.33	0.08				
Pegasus Bay	0–4	0.62	0.06	43	35	50	40
	4–12	0.62	0.06	513	249	595	288
	12–20	0.62	0.06	420	168	479	194
Banks Pen. North	0–4	0.62	0.06	281	83	315	94
	4–12	0.62	0.06	487	109	565	137
	12–20	0.62	0.06	489	225	552	253
Banks Pen. South	0–4	0.56	0.05	480	135	543	156
	4–12	0.56	0.05	262	69	298	81
	12–20	0.56	0.05	132	101	153	117
Timaru	0–4	0.56	0.05	269	91	307	106
	4–12	0.56	0.05	1 849	393	2 050	455
	12–20	0.56	0.05	1 049	287	1 185	333
Otago	0–4	0.56	0.05				
	4–12	0.56	0.05				
	12–20	0.56	0.05				
Total				7 789	889	8 800	1 206

Table M.2: Estimated winter abundance of Hector's dolphins in each stratum ($\hat{N}_k$) and overall obtained from the top-ranked detection function models for the full data set, and using the circle-back based estimates of availability. Given is the estimate of availability ($\hat{N}_k$) and the estimated abundance ($\hat{N}_k$) from each detection function model. Column labels indicate the order of the detection function models in Table 10 with the values in parentheses indicating the corresponding adjusted AIC model weight for each detection function model.

Coastal Section	Offshore Stratum (nmi)	1 (0.77)				2 (0.10)			
		$\hat{P}_{ak}$	SE	$\hat{N}_k$	SE	$\hat{P}_{ak}$	SE	$\hat{N}_k$	SE
Golden Bay North	0–4	0.43	0.11			0.46	0.13		
	4–12	0.42	0.09			0.44	0.10		
Golden Bay A	0–4	0.43	0.11			0.46	0.13		
	4–12	0.42	0.09	167	183	0.44	0.10	163	179
	12–20	0.42	0.09			0.44	0.10		
Golden Bay B	0–4	0.43	0.11			0.46	0.13		
	4–12	0.42	0.09			0.44	0.10		
	12–20	0.42	0.09			0.44	0.10		
Marlborough Sounds	0–4	0.43	0.11			0.46	0.13		
	4–12	0.42	0.09			0.44	0.10		
	12–20	0.42	0.09			0.44	0.10		
Cloudy/Clifford Bay	0–4	0.43	0.11	123	79	0.46	0.13	122	79
	4–12	0.42	0.09	414	184	0.44	0.10	419	186
	12–20	0.42	0.09	227	166	0.44	0.10	235	171
Kaikoura	0–4	0.26	0.21	296	275	0.27	0.23	312	295
	4–12	0.25	0.21			0.25	0.22		
	12–20	0.25	0.21			0.25	0.22		
Clarence	0–4	0.26	0.21	525	499	0.27	0.23	531	510
	4–12	0.25	0.21			0.25	0.22		
	12–20	0.25	0.21			0.25	0.22		
Pegasus Bay	0–4	0.67	0.13	39	32	0.73	0.14	39	31
	4–12	0.66	0.12	466	240	0.72	0.13	466	237
	12–20	0.66	0.12	384	166	0.72	0.13	379	163
Banks Pen. North	0–4	0.67	0.13	254	86	0.73	0.14	247	84
	4–12	0.66	0.12	443	123	0.72	0.13	443	123
	12–20	0.66	0.12	447	219	0.72	0.13	439	213
Banks Pen. South	0–4	0.60	0.09	436	135	0.65	0.10	432	133
	4–12	0.59	0.09	242	72	0.64	0.10	243	72
	12–20	0.59	0.09	122	95	0.64	0.10	123	95
Timaru	0–4	0.60	0.09	244	89	0.65	0.10	243	88
	4–12	0.59	0.09	1 719	432	0.64	0.10	1 695	431
	12–20	0.59	0.09	971	297	0.64	0.10	969	296
Otago	0–4	0.60	0.09			0.65	0.10		
	4–12	0.59	0.09			0.64	0.10		
	12–20	0.59	0.09			0.64	0.10		
Total				7 519	1 170			7 499	1 186

Table M.2 (cont): Estimated winter abundance of Hector's dolphins in each stratum ($\hat{N}_k$) and overall obtained from the top-ranked detection function models for the full data set, and using the circle-back based estimates of availability. Given is the estimate of availability ($\hat{N}_k$) and the estimated abundance ($\hat{N}_k$) from each detection function model. Column labels indicate the order of the detection function models in Table 10 with the values in parentheses indicating the corresponding adjusted AIC model weight for each detection function model.

Coastal Section	Offshore Stratum (nmi)	3 (0.09)				4 (0.04)			
		$\hat{P}_{ak}$	SE	$\hat{N}_k$	SE	$\hat{P}_{ak}$	SE	$\hat{N}_k$	SE
Golden Bay North	0–4	0.44	0.12			0.51	0.17		
	4–12	0.43	0.09			0.47	0.10		
Golden Bay A	0–4	0.44	0.12			0.51	0.17		
	4–12	0.43	0.09	166	181	0.47	0.10	160	175
	12–20	0.43	0.09			0.47	0.10		
Golden Bay B	0–4	0.44	0.12			0.51	0.17		
	4–12	0.43	0.09			0.47	0.10		
	12–20	0.43	0.09			0.47	0.10		
Marlborough Sounds	0–4	0.44	0.12			0.51	0.17		
	4–12	0.43	0.09			0.47	0.10		
	12–20	0.43	0.09			0.47	0.10		
Cloudy/Clifford Bay	0–4	0.44	0.12	122	78	0.51	0.17	118	80
	4–12	0.43	0.09	415	184	0.47	0.10	425	191
	12–20	0.43	0.09	230	167	0.47	0.10	242	177
Kaikoura	0–4	0.26	0.22	302	283	0.28	0.24	329	316
	4–12	0.25	0.21			0.26	0.24		
	12–20	0.25	0.21			0.26	0.24		
Clarence	0–4	0.26	0.22	528	504	0.28	0.24	536	522
	4–12	0.25	0.21			0.26	0.24		
	12–20	0.25	0.21			0.26	0.24		
Pegasus Bay	0–4	0.69	0.13	39	32	0.81	0.16	38	31
	4–12	0.68	0.13	465	238	0.79	0.15	462	237
	12–20	0.68	0.13	381	164	0.79	0.15	372	163
Banks Pen. North	0–4	0.69	0.13	251	85	0.81	0.16	240	82
	4–12	0.68	0.13	442	121	0.79	0.15	439	129
	12–20	0.68	0.13	443	215	0.79	0.15	429	209
Banks Pen. South	0–4	0.62	0.10	433	134	0.71	0.11	427	135
	4–12	0.61	0.10	241	71	0.68	0.12	245	76
	12–20	0.61	0.10	122	94	0.68	0.12	126	98
Timaru	0–4	0.62	0.10	243	88	0.71	0.11	241	89
	4–12	0.61	0.10	1 705	427	0.68	0.12	1 685	451
	12–20	0.61	0.10	967	294	0.68	0.12	974	310
Otago	0–4	0.62	0.10			0.71	0.11		
	4–12	0.61	0.10			0.68	0.12		
	12–20	0.61	0.10			0.68	0.12		
Total				7 494	1151			7 488	1 310

SECTION N

Stratum-specific estimates of winter abundance for the top-ranked detection function models using the reduced data set

Table N.1: Estimated winter abundance of Hector's dolphins in each stratum ($\hat{N}_k$) and overall obtained from the top-ranked detection function models for the reduced data set, and using the dive-cycle based estimates of availability. Given is the estimate of availability ($\hat{P}_{\alpha k}$) and the estimated abundance ($\hat{N}_k$) from each detection function model. Column labels indicate the order of the detection function models in Table 12 with the values in parentheses indicating the corresponding adjusted AIC model weight for each detection function model.

Coastal Section	Offshore Stratum (nmi)	All $\hat{P}_{\alpha k}$	SE	1 (0.55) $\hat{N}_k$	SE	2 (0.39) $\hat{N}_k$	SE	3 (0.06) $\hat{N}_k$	SE
Golden Bay North	0–4	0.46	0.03						
	4–12	0.46	0.03						
Golden Bay A	0–4	0.46	0.03						
	4–12	0.46	0.03	238	255	218	234	238	256
	12–20	0.46	0.03						
Golden Bay B	0–4	0.46	0.03						
	4–12	0.46	0.03						
	12–20	0.46	0.03						
Marlborough Sounds	0–4	0.46	0.03						
	4–12	0.46	0.03						
	12–20	0.46	0.03						
Cloudy/Clifford Bay	0–4	0.46	0.03	65	71	56	62	66	73
	4–12	0.46	0.03	329	123	279	105	338	127
	12–20	0.46	0.03	212	125	178	107	219	129
Kaikoura	0–4	0.33	0.08	198	133	164	112	206	138
	4–12	0.33	0.08						
	12–20	0.33	0.08						
Clarence	0–4	0.33	0.08	332	208	303	193	335	209
	4–12	0.33	0.08						
	12–20	0.33	0.08						
Pegasus Bay	0–4	0.62	0.06	74	59	62	50	77	61
	4–12	0.62	0.06	673	419	559	358	697	432
	12–20	0.62	0.06	403	146	338	126	417	151
Banks Pen. North	0–4	0.62	0.06	350	117	294	101	362	121
	4–12	0.62	0.06	583	147	483	125	604	155
	12–20	0.62	0.06	551	279	479	249	565	284
Banks Pen. South	0–4	0.56	0.05	535	170	458	149	550	175
	4–12	0.56	0.05	320	105	271	91	329	108
	12–20	0.56	0.05	64	47	51	37	67	49
Timaru	0–4	0.56	0.05	229	85	189	71	237	89
	4–12	0.56	0.05	2196	525	1914	466	2246	540
	12–20	0.56	0.05	1363	430	1185	380	1394	442
Otago	0–4	0.56	0.05						
	4–12	0.56	0.05						
	12–20	0.56	0.05						
Total				8 715	1 266	7 483	1 145	8 948	1 334

Table N.2: Estimated winter abundance of Hector's dolphins in each stratum ($\hat{N}_k$) and overall obtained from the top-ranked detection function models for the reduced data set, and using the circle-back based estimates of availability. Given is the estimate of availability ($\hat{N}_k$) and the estimated abundance ($\hat{N}_k$) from each detection function model. Column labels indicate the order of the detection function models in Table 12 with the values in parentheses indicating the corresponding adjusted AIC model weight for each detection function model.

Coastal Section	Offshore Stratum (nmi)	1 (0.55)				2 (0.39)			
		$\hat{P}_{\alpha k}$	SE	$\hat{N}_k$	SE	$\hat{P}_{\alpha k}$	SE	$\hat{N}_k$	SE
Golden Bay North	0–4	0.59	0.21			0.49	0.15		
	4–12	0.55	0.14			0.49	0.12		
Golden Bay A	0–4	0.59	0.21			0.49	0.15		
	4–12	0.55	0.14	198	218	0.49	0.12	204	224
	12–20	0.55	0.14			0.49	0.12		
Golden Bay B	0–4	0.59	0.21			0.49	0.15		
	4–12	0.55	0.14			0.49	0.12		
	12–20	0.55	0.14			0.49	0.12		
Marlborough Sounds	0–4	0.59	0.21			0.49	0.15		
	4–12	0.55	0.14			0.49	0.12		
	12–20	0.55	0.14			0.49	0.12		
Cloudy/Clifford Bay	0–4	0.59	0.21	50	58	0.49	0.15	52	60
	4–12	0.55	0.14	273	123	0.49	0.12	261	117
	12–20	0.55	0.14	176	113	0.49	0.12	166	108
Kaikoura	0–4	0.43	0.32	152	145	0.38	0.26	141	132
	4–12	0.40	0.33			0.39	0.27		
	12–20	0.40	0.33			0.39	0.27		
Clarence	0–4	0.43	0.32	253	235	0.38	0.26	261	236
	4–12	0.40	0.33			0.39	0.27		
	12–20	0.40	0.33			0.39	0.27		
Pegasus Bay	0–4	0.91	0.16	50	41	0.75	0.16	51	42
	4–12	0.91	0.16	457	293	0.75	0.14	458	303
	12–20	0.91	0.16	274	107	0.75	0.14	277	113
Banks Pen. North	0–4	0.91	0.16	237	87	0.75	0.16	241	94
	4–12	0.91	0.16	396	116	0.75	0.14	396	122
	12–20	0.91	0.16	374	197	0.75	0.14	393	214
Banks Pen. South	0–4	0.79	0.14	378	133	0.66	0.12	386	141
	4–12	0.77	0.13	234	85	0.66	0.11	228	84
	12–20	0.77	0.13	47	35	0.66	0.11	43	32
Timaru	0–4	0.79	0.14	162	65	0.66	0.12	160	66
	4–12	0.77	0.13	1 605	455	0.66	0.11	1610	458
	12–20	0.77	0.13	996	349	0.66	0.11	998	352
Otago	0–4	0.79	0.14			0.66	0.12		
	4–12	0.77	0.13			0.66	0.11		
	12–20	0.77	0.13			0.66	0.11		
Total				6 312	1 099			6 328	1 153

Table N.2 (cont): Estimated winter abundance of Hector's dolphins in each stratum ($\hat{N}_k$) and overall obtained from the top-ranked detection function models for the reduced data set, and using the circle-back based estimates of availability. Given is the estimate of availability ($\hat{N}_k$) and the estimated abundance ($\hat{N}_k$) from each detection function model. Column labels indicate the order of the detection function models in Table 12 with the values in parentheses indicating the corresponding adjusted AIC model weight for each detection function model.

| Coastal Section | Offshore Stratum (nmi) | 3 (0.06) | | | |
		$\hat{P}_{ak}$	SE	$\hat{N}_k$	SE
Golden Bay North	0–4	0.60	0.22		
	4–12	0.56	0.14		
Golden Bay A	0–4	0.60	0.22		
	4–12	0.56	0.14	195	215
	12–20	0.56	0.14		
Golden Bay B	0–4	0.60	0.22		
	4–12	0.56	0.14		
	12–20	0.56	0.14		
Marlborough Sounds	0–4	0.60	0.22		
	4–12	0.56	0.14		
	12–20	0.56	0.14		
Cloudy/Clifford Bay	0–4	0.60	0.22	50	58
	4–12	0.56	0.14	277	124
	12–20	0.56	0.14	179	115
Kaikoura	0–4	0.44	0.33	155	149
	4–12	0.41	0.34		
	12–20	0.41	0.34		
Clarence	0–4	0.44	0.33	251	235
	4–12	0.41	0.34		
	12–20	0.41	0.34		
Pegasus Bay	0–4	0.93	0.16	51	41
	4–12	0.93	0.16	463	294
	12–20	0.93	0.16	277	107
Banks Pen. North	0–4	0.93	0.16	240	87
	4–12	0.93	0.16	401	116
	12–20	0.93	0.16	375	195
Banks Pen. South	0–4	0.81	0.14	380	133
	4–12	0.78	0.14	235	85
	12–20	0.78	0.14	48	36
Timaru	0–4	0.81	0.14	164	66
	4–12	0.78	0.14	1 605	458
	12–20	0.78	0.14	997	351
Otago	0–4	0.81	0.14		
	4–12	0.78	0.14		
	12–20	0.78	0.14		
Total				6 343	1 122

SECTION O

Comparison with DISTANCE results

Given that the entire width of the transect is being surveyed from both observer positions with the reduced summer data set, regular distance sampling methods of analysis can be applied as a comparison to the results gained with the current analysis methods. Two brief DISTANCE-style analyses are considered here:

1. Conventional distance sampling (CDS; e.g., Buckland et al. 2001) where detections from both observer positions are pooled and treated as if there was a single observer. This assumes that detection on the track line is perfect.
2. Mark-recapture distance sampling using a CDS detection function for the probability of detection from either observer position, and a mark-recapture component using the detections from each observer position to estimate detection probability on the track line (e.g., Laake & Borchers 2004). This is the same basic intent as the current methods, but uses an alternative parameterisation and assumes point independence.

Both analyses were conducted in R using the *mrds* package, which is an R implantation of the routines used by DISTANCE. Note that this is not intended to be an alternative, in-depth analysis, but a simple comparison to illustrate that the abundance estimates provided by the current methods are realistic.

For both sets of analyses, the CDS component was modelled with either a half-normal or hazard rate key function with no adjustment. The mark-recapture component was modelled on the logit-scale as a linear-function of distance with a different relationship for each observer position and an additive effect of group size on detection.

The estimated number of dolphin groups in the covered region using the DISTANCE-style analyses are comparable to those using the current methods, producing estimates and standard errors that are of a very similar magnitude (Tables O.1 and O.2). Adjustments due to group size, fraction of the survey area covered and availability when estimating overall abundance would be the same for any of these analyses. This demonstrates that abundance estimates from these newer, more flexible methods for modelling the detection function should not be considered unreasonable. The advantage of the new approaches over the present DISTANCE-style analyses is that a wider range of dependence structures can be considered (i.e., constant and limiting independence) and partial overlap of the observers' search areas.

References

Buckland, S.T.; Laake, J.L.; Borchers, D.L. (2010). Double-observer line transect methods: levels of independence. *Biometrics 66*: 169–177.

Laake, J.L.; Borchers, D.L. (2004). Methods for incomplete detection at distance zero. Pp. 108–189 in Advanced Distance Sampling, eds S.T. Buckland, D.R. Anderson, K.P. Burnham, J.L. Laake, D.L. Borchers and L. Thomas. Oxford University Press, Oxford.

Table O.1: Estimated number of dolphin groups in covered region ($\hat{N}_{cg}$, and standard error; SE) using DISTANCE-style analysis. Analysis-type is either conventional distance sampling (CDS) or mark-recapture distance sampling (MRDS) and key function is either half-normal (HN) or hazard rate (HR). For MRDS models, the mark-recapture recapture component was modelled on the logit-scale as a linear-function of distance with a different relationship for each observer position, and an additive effect of group size on detection.

Analysis-type	Key	$\hat{N}_{cg}$	SE
CDS	HN	389	27
CDS	HR	341	18
MRDS	HN	424	33
MRDS	HR	372	23

Table O.2: Estimated number of dolphin groups in covered region ($\hat{N}_{cg}$, and standard error; SE) using current analysis methods. Given is the AIC-based rank of the models in the analysis of the reduced summer data set (Table 6). The 37th ranked model is most comparable to the MRDS models considered in Table O.1 as detection was modelled as a linear function of distance in both cases.

Model Rank	$\hat{N}_{cg}$	SE
1	382	28
2	357	44
3	366	25
37	418	36

SECTION P

Sighting rates around Banks Peninsula

At the AEWG meeting of 11 October 2013, S. Dawson commented that the sighting rates achieved during the summer and winter surveys around Banks Peninsula were high compared to their experience in the area. A request for access to the aerial survey data they collected during the summers and winters of 2002, 2004 and 2005 to ensure an accurate comparison was declined, although Rayment (2008) was supplied with the comment from S. Dawson "Luckily, all the material you need is in Will's PhD thesis." Unfortunately this was incorrect as raw sighting rates may differ for a whole host of reasons that may be of little biological consequence, e.g., transect width searched, average detection rates, observer ability, etc., and without access to the original data it is impossible to make an accurate, meaningful comparison. Therefore, any comparison of the sighting rates reported below should be made with extreme caution and should not be interpreted as any indication of differences in Hector's dolphin abundance as differences in sighting rates may be due to differences in sampling protocols that we are unable to account for with the information supplied.

Rayment (2008) used a similar setup to that used in our surveys with two observers on each side of a fixed-wing aircraft. The rear observer had a bubble window enabling a view between 40 and 90 degrees from the horizontal (although focusing effort near the trackline, i.e., 90 degrees), and the front observer had a flat window enabling a view from 60 degrees, outwards (with no lowest search angle specified). Sightings made by either observer within the 40–60 degree area of overlap were retained in their sighting data with the information of the rear observer used if the sighting was between 50–90 degrees from the horizontal, and the information from the front observer used if the sighting was less than 50 degrees. No details are provided on the matching criteria used to determine whether sightings made within the overlap zone were potentially duplicate sightings of the same dolphin group or unique sightings of different groups. Sighting rates (number of dolphins per nmi) have been calculated from table 2.2 of Rayment (2008). Note that although the purpose of the aerial surveys by Rayment (2008) was to detail Hector's dolphin distribution, based upon the description of the field protocols, all the necessary information to estimate the abundance of available dolphins appears to have been collected.

In an effort to match survey areas, only the sightings from the transects of our 2013 surveys conducted within the area indicated in Figure P.1 were used. As no lowest search angle was specified by Rayment (2008), no right truncation was used for our data. Groups sighted by both observers are only counted as a single sighting. The number of dolphins seen and total length of transects flown within each 1 nmi band offshore in summer and winter are given in Tables P.1 and P.2 respectively. The resulting sighting rates by offshore band are presented in Figures P.2 and P.3.

While there are some offshore bands for which the 2013 sighting rates are highest, overall the 2013 sighting rates are not atypically high and there are many instances where the sighting rates from Rayment (2008) are much higher, particularly during the winter. Claims made during the AEWG meeting on 11 October 2013 are clearly unsubstantiated. Note that the 2013 sighting rates reported here are larger than those presented at the AEWG meeting of 29 November 2013 as an incorrect unit of measurement was used at that time. This correction does not alter the overall conclusions presented at that meeting.

References

Rayment. W. (2008). Distribution and ranging of Hector's dolphins: implications for protected area design. PhD Dissertation. University of Otago, Dunedin, New Zealand. 221 p.
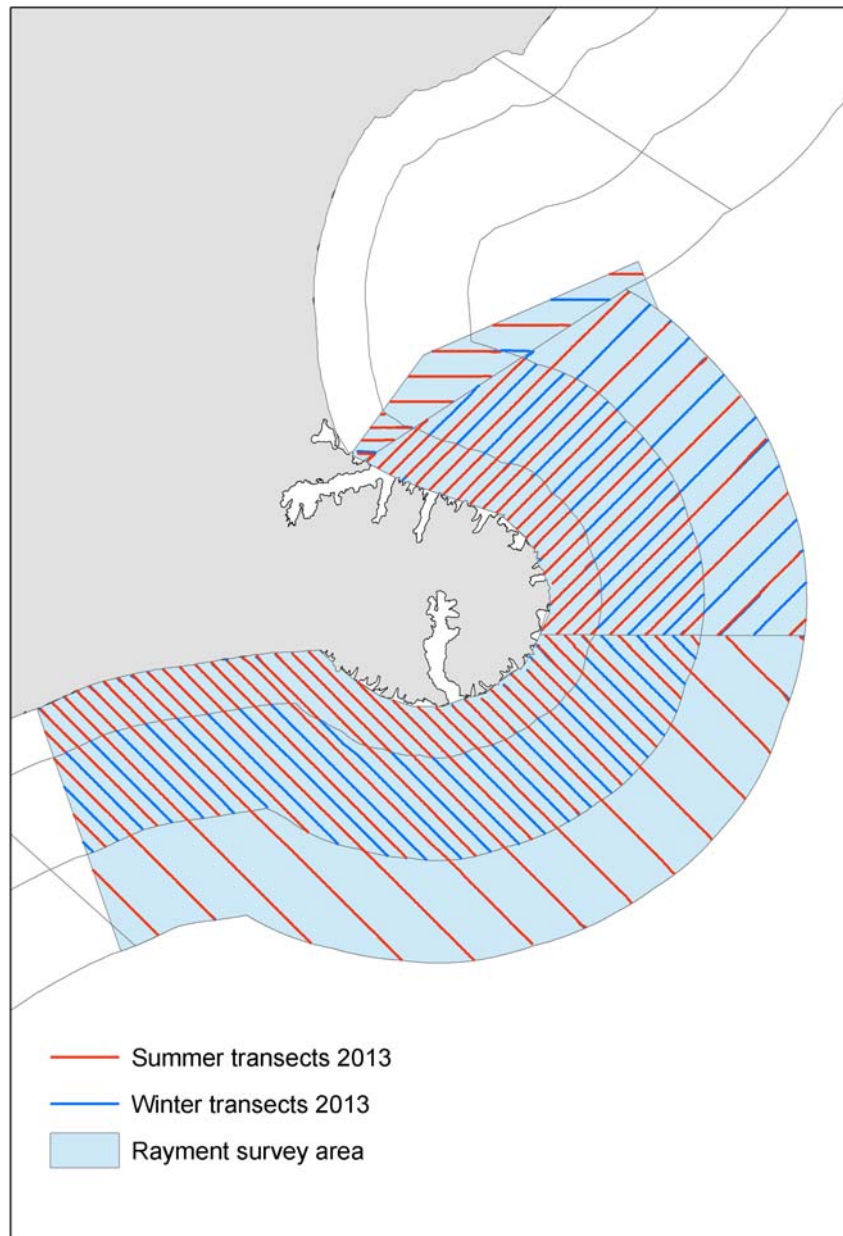
Figure P.1: The limits of survey area used to calculate sighting rates for comparison with those of Rayment (2008).

Table P.1: Number of dolphins seen and survey effort (nmi) within each 1 nmi band offshore in the summer of each survey year. Data for 2002, 2004 and 2005 comes from table 2.2 of Rayment (2008).

Offshore (nmi)	2002 Dolphins	Effort (nmi)	2004 Dolphins	Effort (nmi)	2005 Dolphins	Effort (nmi)	2013 Dolphins	Effort (nmi)
0 to 1	17	24.37	27	14.54	51	13.95	109	65.73
1 to 2	12	24.66	25	16.11	34	16.01	48	70.23
2 to 3	9	22.63	39	17.55	13	18.04	56	73.36
3 to 4	12	23.62	0	21.96	19	22.30	88	73.43
4 to 5	5	25.35	0	16.32	4	17.42	44	38.02
5 to 6	0	24.40	0	16.43	5	16.12	37	39.88
6 to 7	0	25.40	8	19.60	2	20.30	16	40.87
7 to 8	2	25.47	2	24.60	7	23.63	6	40.27
8 to 9	0	25.35	0	20.55	5	20.59	1	42.22
9 to 10	1	25.45	2	17.60	2	17.94	4	46.04
10 to 11	0	27.03	0	20.42	5	19.56	11	42.42
11 to 12	1	26.68	0	29.16	0	29.02	11	47.10
12 to 13	4	27.68	0	24.34	1	22.85	6	19.80
13 to 14	0	28.16	0	19.26	3	19.53	2	24.88
14 to 15	1	24.12	0	21.89	1	21.51	6	27.44
15 to 16			0	6.52	1	6.61	10	25.56
16 to 17			0	6.58	1	6.54	0	23.40
17 to 18			0	6.62	0	6.73	1	23.72
18 to 19			0	7.19	0	7.13	0	26.06
19 to 20			0	6.36	0	6.48	0	25.48

Table P.2: Number of dolphins seen and nm of survey effort within each 1nm band offshore in the winter of each survey year. Data for 2002, 2004 and 2005 comes from table 2.2 of Rayment (2008).

Offshore (nmi)	2002 Dolphins	Effort (nmi)	2004 Dolphins	Effort (nmi)	2005 Dolphins	Effort (nmi)	2013 Dolphins	Effort (nmi)
0 to 1	16	20.19	2	13.87	7	14.22	9	67.18
1 to 2	8	15.52	3	15.75	12	15.99	39	68.73
2 to 3	11	20.06	16	17.70	26	17.79	39	72.19
3 to 4	0	19.88	8	22.65	13	22.64	15	73.67
4 to 5	5	18.87	1	16.92	12	17.03	8	75.95
5 to 6	7	17.97	5	16.01	14	16.06	22	76.45
6 to 7	4	23.31	3	19.89	9	19.46	8	80.58
7 to 8	11	19.66	2	24.10	6	24.47	19	80.43
8 to 9	9	20.69	8	20.55	7	20.34	10	83.21
9 to 10	3	19.35	7	17.95	3	17.84	13	86.00
10 to 11	4	22.94	0	20.70	3	20.66	7	84.84
11 to 12	7	23.19	3	28.63	3	28.95	15	87.71
12 to 13	4	23.74	0	22.76	0	22.62	7	30.02
13 to 14	3	24.67	4	19.37	2	19.20	4	31.30
14 to 15	2	24.60	3	22.42	0	21.22	2	33.96
15 to 16			0	6.69	0	6.77	10	32.05
16 to 17			0	6.56	0	6.52	5	31.53
17 to 18			1	6.73	1	6.62	10	34.48
18 to 19			1	7.04	0	7.02	5	35.60
19 to 20			0	6.93	0	6.27	2	33.23
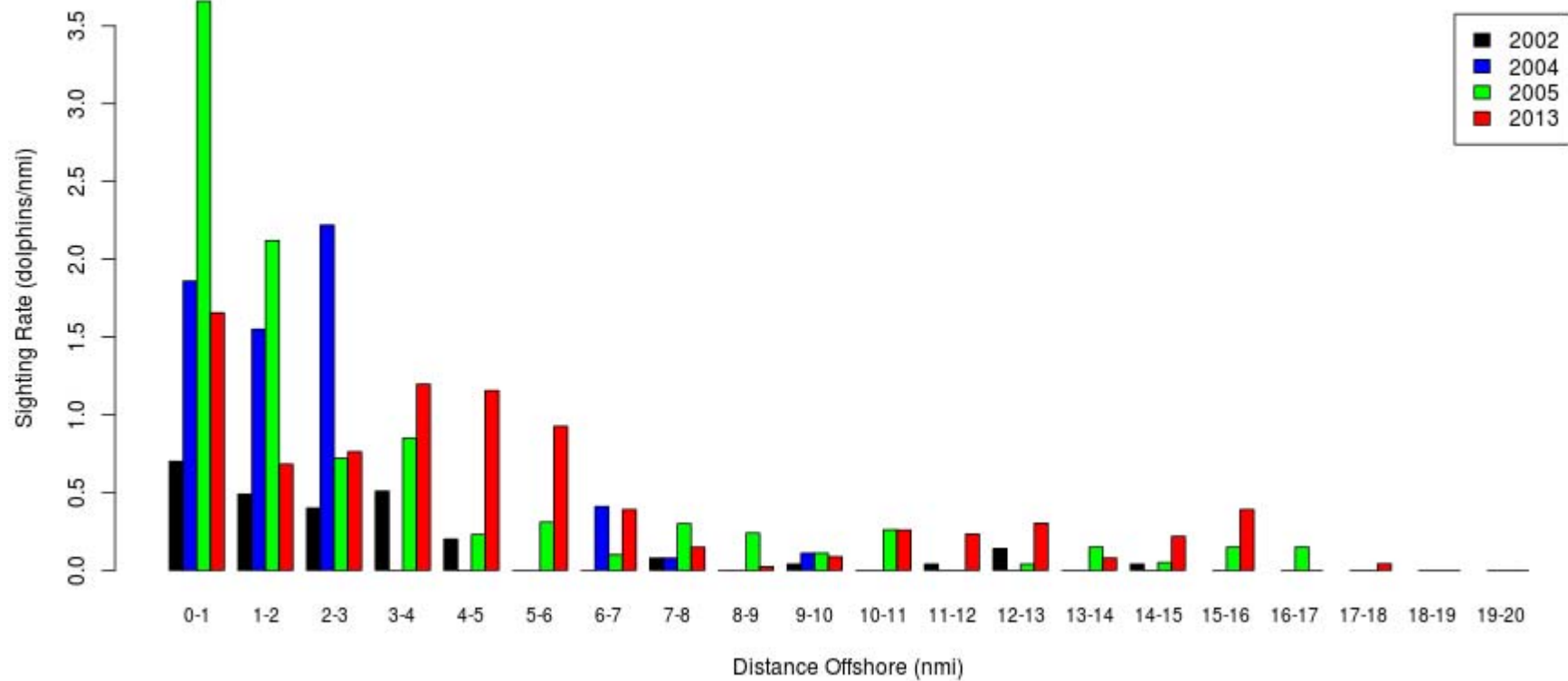
Figure P.2: Number of dolphins sighted per nmi within each 1 nmi band offshore during summer surveys.
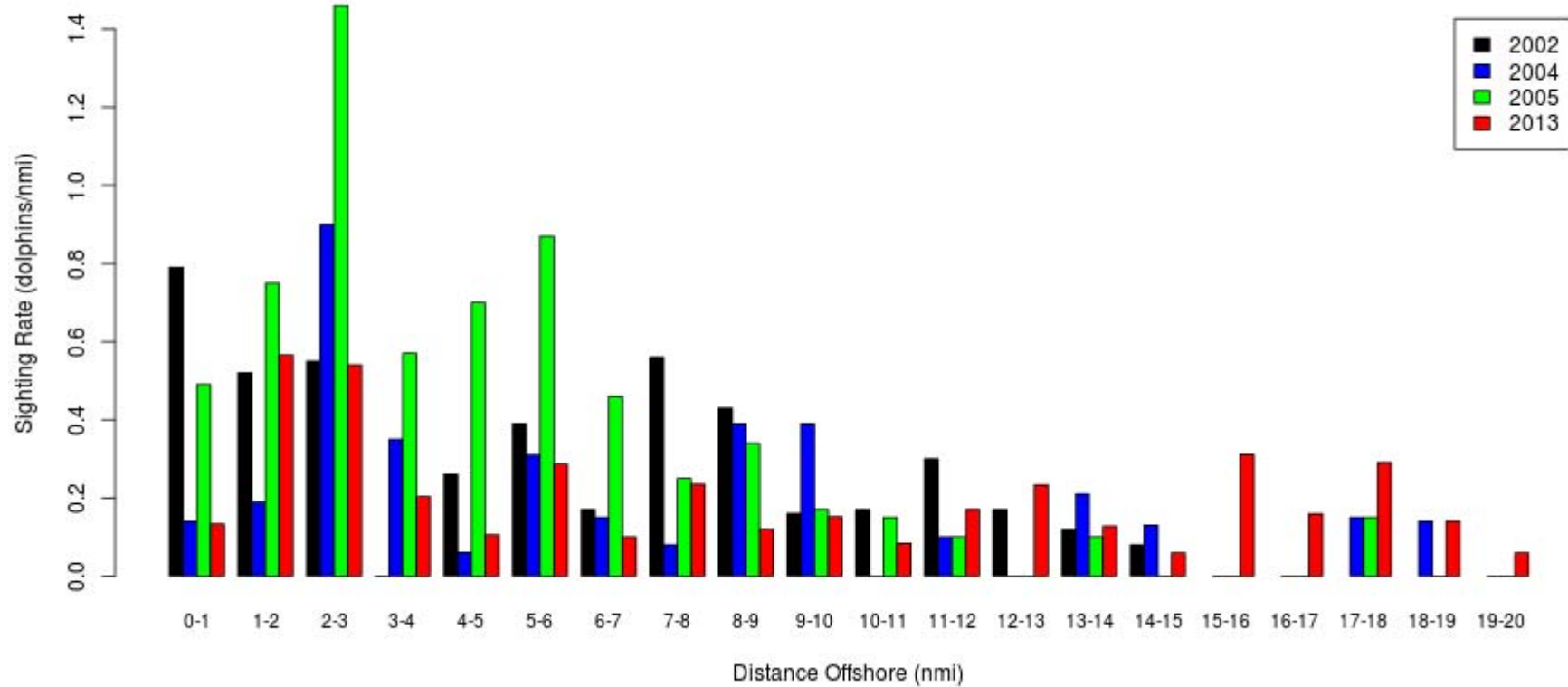
Figure P.3: Number of dolphins sighted per nmi within each 1 nmi band offshore during winter surveys.

SECTION Q

Addressing independent reviewer comments

MPI solicited independent reviews of the draft final report from Professor Steve T. Buckland (School of Mathematics and Statistics, University of St Andrews) and Professor Philip S. Hammond (School of Biology, University of St Andrews). Their review comments are detailed below along with our responses to their comments. Note that Prof. Buckland's comments were made directly onto a PDF of the draft report and have been transcribed below.

Overall, while some comments made by both reviewers are valid and could lead to small changes in the estimated abundance for ECSI Hector's dolphins, the resulting differences could be in opposite directions given the aspects the reviewers have noted. Our opinion is that such changes are not warranted at this point given the level of work that would be required to implement them and that they are extremely unlikely to substantially alter the main findings of this project, especially considering the wide range of the confidence intervals. We note that both reviewers classified the report as a sound piece of work as it currently stands.

Prof. Buckland's comments and our responses:
SB: Pg 5; Thomas et al. 2010 not in refs
DM/DC: reference added

SB: Pg 5; optimal allocation can also lead to low sample sizes in areas of low density, forcing a common detection function model across low and high density strata. (This issue is less important though when covariates are included in the detection function.)
DM/DC: a common detection function was assumed regardless across all strata given consistent field methods were used.

SB: Pg 11, so how was group size used? From statement below, it is clear that a duplicate might have 2 different recorded group sizes.
DM/DC: the procedure used to determine duplicate sightings, including the use of observed group size has been clarified.

SB: Pg 11; suggests perhaps that a correction should be used for detections seen by just one observer.
DM/DC: the implication of the comment here is that if the groups sighted by a single observer had actually been seen by 2 observers, then some of the group sizes used in the analysis would be larger. From the duplicate sightings, the average difference in the recorded group sizes was 0.27 in summer and 0.17 in winter. 56% of total group sightings in summer were made by a single observer, and 69% in winter. Assuming that 50% of the recorded group sightings by a single observer would be too small, an approximate correction to the average group size would be: $0.27 \times 0.56 \times 0.5 = 0.07$ in summer and $0.17 \times 0.69 \times 0.5 = 0.06$ in winter. Compared to the current average group sizes of 2.30 and 1.64 respectively, any correction would lead to an approximate increase in estimated abundance of 3-4%. To incorporate any correction properly would require a complete reworking of the entire analysis and lead to a possible change that will be small relative to the width of the current confidence intervals and not substantially alter the overall results. We do not believe it is worthwhile pursuing such a correction at this point in time.

SB: Pg 15; as ubar and bbar are sample estimates, then P_a should be an estimate, not the true probability
DM/DC: text and equation adjusted to reflect P_a is an estimate

SB: Pg 24; typo highlighted
DM/DC: 0.701 km corrected to 0.071 km.

SB: Pg 31; typo highlighted
DM/DC: theoretically corrected to theoretical

SB: Pg 45; I was confused by this until I realised this is bottom depth, not animal depth! Clarify?
DM/DC: clarified that we are referring to seabed depth not depth of dolphin group

SB: Pg 60: typo highlighted
DM/DC: previous corrected to previously

Prof. Hammond's comments and our responses

Main points:
PH: The designation of duplicate sightings in the main survey is not well justified. Why 5 seconds, 5 degrees and what was the group size tolerance? How sensitive were the results to variation in these threshold values? This could make a considerable difference to the perception correction.
DM/DC: a range of criteria were used to decide whether a sighting was a duplicate sighting of a group already recorded by the other observer, including time between sightings, recorded angles, group size and observer comments. 5 seconds and 5 degrees were used as guidelines, but were not strictly adhered to with experience playing a leading role in the process (note that all matching was done manually). The following text has been added to the report to clarify how the matching was done.

"Duplicate sightings were those in which the same group of animals was recorded by both the front and rear observer (on the same side of the plane). Duplicates were manually identified by comparing three different sighting variables; sighting time (within ± 5 seconds), sighting angle (within ± 5 degrees) and group size (± 1 individual), in line with criteria from previous Hector's dolphin aerial surveys (e.g. DuFresne & Mattlin 2009, Clement et al. 2011). Matching criteria helped identified those sightings with agreement in at least two of the three variables while observer experience and any distinguishing comments recorded by observers at the time (e.g. mother/calf pair) were also important factors considered in final duplicate decisions, particularly in cases where a sighting fell just outside one or more of the matching criteria."

The likely effects of errors in duplicate matching had been discussed at previous Aquatic Environment Working Group meetings when interim summer results had been discussed, with the conclusion that any effects are likely to be small. Here, to quickly explore the likely effects of misidentifying duplicates on estimated abundance using MRDS, we considered the simpler case of the Lincoln-Petersen estimator for mark-recapture studies which has the same underlying logic of MRDS methods to account for perception bias. Table Q.1 considers the case where there are truly 500 groups, and the probability of a group being detected by one of

the observers is 0.5, under various levels of misidentification. The misidentification rate was defined here as the proportion of sightings of individual groups by different observers that were incorrectly assigned as duplicates (i.e. 2 unique groups incorrectly assigned as 1 group seen by both observers). Clearly, as the misidentification rate increases, the negative bias in estimated bias also increases. The level of bias in estimated abundance depends on the true level of detection, as indicated by Table Q.2, with the scenario of p=0.5 closest to the situation found in this study (in terms of the overall probability of detecting a group in the transect width, not just perception bias).

Table Q.1: Effect of incorrectly assigning sightings of groups by different observers as duplicate sightings of a group. Duplicates is the number of groups recorded as sighted by both observers, Front only is the number of groups recorded as sighted by the front observer only, Rear only is the number of groups recorded as sighted by the rear observer only, Unique is the recorded number of groups sighted at least once, N is the estimated abundance, p is the apparent detection probability for each observer and $p*$ is the apparent probability of a group being detected at least once. p and $p*$ are similar to perception bias.

				Misidentification Rate	
	0.00%	1.00%	5.00%	10.00%	20.00%
Duplicates	125	126	131	138	150
Front only	125	124	119	113	100
Rear only	125	124	119	113	100
Unique	375	374	369	363	350
N	500	495	476	455	417
p	0.50	0.51	0.53	0.55	0.60
$p*$	0.75	0.75	0.77	0.80	0.84

Table Q.2: Percent relative bias in estimated abundance for different true levels of detection and misidentification rates.

				Misidentification Rate	
p	0.00%	1.00%	5.00%	10.00%	20.00%
0.3	0.00%	-2.00%	-10.00%	-19.00%	-32.00%
0.5	0.00%	-1.00%	-5.00%	-9.00%	-17.00%
0.7	0.00%	0.00%	-2.00%	-4.00%	-8.00%

By contrast, when there is the potential for misidentifying a duplicate sighting as unique sightings for each observer (i.e., 1 group incorrectly recorded as 2), abundance tends to be overestimated (Table Q.3), although in this case the percent relative bias is consistent for different true levels of detection.

Table Q.3: Effect of incorrectly assigning duplicate sightings as unique group sightings for each observer. Duplicates is the number of groups recorded as sighted by both observers, Front only is the number of groups recorded as sighted by the front observer only, Rear only is the number of groups recorded as sighted by the rear observer only, Unique is the recorded number of groups sighted at least once, N is the estimated abundance, % RB is the percent relative bias, p is the apparent detection probability for each observer and p^* is the apparent probability of a group being detected at least once. p and p^* are similar to perception bias.

				Misidentification Rate	
	0.00%	1.00%	5.00%	10.00%	20.00%
Duplicates	125	124	119	113	100
Front only	125	126	131	138	150
Rear only	125	126	131	138	150
Unique	375	376	381	388	400
N	500	505	526	556	625
% RB	0.00%	1.00%	5.00%	11.00%	25.00%
p	0.50	0.50	0.48	0.45	0.40
p^*	0.75	0.74	0.72	0.70	0.64

Clearly there is the potential for bias to be introduced through the misidentification of duplicates, and in some circumstances the bias can be quite extreme. However, the biases may be either negative or positive, and given the protocols used during the surveys, in duplicate matching and DC's experience in aerial survey work for Hector's dolphin (dating from the early 2000s as an observer on surveys on the South Island's West Coast), it is hard to imagine misidentification rates in excess of 5%, especially given the low frequency of any dolphin sightings during the surveys. On balance, it is our opinion that if anything, decisions regarding determination of duplicates likely erred on the side of incorrectly combining two groups as a single duplicate sighting in which case, estimates may be conservative (i.e., slightly too low).

The process of duplicate matching was done manually and as such is not a simple task. Investigating what effect slightly different criteria may have on estimated abundance is therefore a substantial undertaking. Given that it is an issue that has been discussed previously, and that any effect is likely to be relatively minor and not practically alter the overall conclusions (particularly when the width of the confidence intervals are considered), we do not believe a reworking of the data and reanalysis is worthwhile at this stage.

PH: It is conventional to use mean group size estimates if more than one independent value is available. The decision to use the maximum is not well justified and causes estimates to be higher than they otherwise would be.

DM/DC: as noted in the report, we believe that undercounting of the group size was potentially more likely than overcounting; hence the use of the maximum. Furthermore, observers were instructed to record the minimum group size they were certain of rather than approximating group size. In this situation, your detailed comment on this issue (see below) would suggest you do not think the use of the maximum recorded group size is unreasonable.

PH: In the circle-back analysis, it is assumed that groups stay in the survey strip; however, some may move out of view in the time taken to circle back (a few minutes). This could potentially cause resightings to be missed, availability to be underestimated and abundance to be overestimated. Uncertainty in resighting is referred to but otherwise apparently ignored in analysis.
and
It is not clear that availability as determined from the helicopter dive time experiments is the same as availability on the surveys themselves. This is critical to avoid bias in the use of this correction. Bias that could potentially result could be in either direction.

DM/DC: we agree wholeheartedly with your comments regarding availability measures and their shortcomings. We are fully aware of the issues you raised, have voiced similar concerns ourselves during meetings and long noted that there is insufficient emphasis on making resources available for studies into a robust method for estimating availability. Indeed, it was concerns about how accurately availability estimated from helicopter surveys of dive cycles hovering near groups (as had been previously used) reflected availability for observers in fixed-wing aircraft flying transects that led us to trialling, and implementing, the circle-back methodology. Given the resources available these were the best, but imperfect, options open to us. That both methods give similar results is encouraging, although it's impossible to determine whether both are ok, or both are badly wrong, without information from a better method for assessing availability. While you have noted there is the potential for biases, you do not appear to be making any clear recommendations on what could be done differently to improve the analysis given the data that is available.

We have reworded some sections to ensure the appropriate caveats concerning availability are more apparent.

Detailed comments:
PH: P8: Cueing
If cueing were a problem despite attempts to avoid it, this would cause there to be more duplicates than there should be, an underestimate in the number of groups missed and an underestimation of abundance.
DM/DC: allowing for a lack of independence between sightings from each observer position is one possible way of accounting for any cueing that may occur (noted in report). As would be expected, these models typically provided a higher estimate of abundance than those models that assumed sightings were fully independent. In some situations cueing could also represent a form of heterogeneity and if it could be considered as additional random variation then the simulation results would suggest that that does not lead to a major bias in the estimates.

PH: P11: Rounding to zero perpendicular distance
If these angles were genuinely greater than 90 (i.e. on the other side of the track line), this would cause rounding to zero perpendicular distance, which is undesirable. However, since it only happened twice, this is unimportant.
DM/DC: agreed.

PH: P11: Duplicates
Front and Rear sightings were considered duplicates if they were within 5 seconds, and within 5 degrees but what about group size? How close did this have to be?

5 degrees seems OK but 5 seconds seems long given that objects were only in view on average 6 seconds (t=6, below). Why 5 seconds? How sensitive is the number of duplicates to this choice (or indeed the choice of 5 degrees and whatever the group size difference was allowed to be)? This seems potentially important in relation to bias and precision (see also below).

For example, if 5 seconds is too long and leads to too many duplicates being designated, the perception bias correction will be overestimated and abundance underestimated.
There seems to be no consideration of uncertainty in duplicate identification. There must be some and if this is not considered then variability in final estimates is likely underestimated.
DM/DC: see response to major comment

PH: P11: Larger value of group size used
If the group sizes were observed minimum group sizes, OK. But if they were best estimates then I don't think this is justified. What difference does it make if the average group size is used?
DM/DC: see response to major comment. Observers were instructed to record minimum group size they were certain of, hence the use of the maximum.

PH: P17: Circle back assumption that groups remain in the strip
But some may move out of the strip; how is this accounted for? If some groups move out of the strip between circles, they would be classed as non-resightings whereas if they hadn't moved they could be classed as a resighting. Unless the probability that the group would be unavailable to be resighted because of movement out of the strip is somehow incorporated, surely this introduces bias in the form of too few duplicates, an underestimation of availability and an overestimation of abundance? And the probability of having moved out of the strip would presumably be greater in the second circle than the first (for the original sighting).
DM/DC: see response to major comment. This is an acknowledged assumption of the approach and one that is difficult to relax without dolphin movement data, which we don't have.

PH: P18: The initial detection of the group that initiated the circle-backs is not used to estimate availability

I don't understand this. What is then used to estimate availability? On p16 it says, for example, "To aid in the re-identification of the original sightings ..."
DM/DC: the modelling of the circle-back availability is conditional upon the sightings of the group that initiates the circle-backs. If the initial detection was included in the availability estimate (using the approach that was implemented), that would lead to an overestimate of availability because there must always be at least one detection for that group. That is, with two additional passes the possible number of sightings for that group would be 1, 2 or 3, but not 0. The modelling of the circle-back data essentially assumed the number of sightings followed a binomial distribution, which assumes a value of 0 is possible.

PH: P19: Misidentification will likely lead to some bias in the availability estimates though sound protocols should minimise the potential for misidentification.

This is rather cryptic and it isn't clear what it means. Is it referring to recording a resighting of the wrong group, or to erroneously not recording a resighting of the right group, or both? Depending on what is meant by misidentification, this could cause bias in either direction. The following sentence points out that the potential for misidentification is much less for the helicopter work, which implies it is a problem for the circle-back implementation used.

DM/DC: text has been clarified on what we regarded as potential misidentification (in this case, both the examples you note). We agree that this is a potential source of bias (which may go in either direction) but is a caveat of the approach that we are unable to do much about without additional information or with the resources available for this project. Also see our response to your major comments on availability.

PH: P24: Sighting data in winter and summer, full and truncated
There seems to be a difference in how the sightings are distributed in summer and winter. In summer, front observers (left truncated at 0.071km) saw 83% as many as the rear observers but in winter this was only 73%. The left truncation of rear observer sightings leaves 71% of sightings in summer but only 58% in winter. Is this an effect of worse weather in winter? Or were the observers searching differently? I don't think this affects the analysis but it does seem curious.
DM/DC: we agree is doesn't affect the analysis and as such haven't pursued this aspect of the data analysis.

PH: P31: Naïve estimates:
It is important to present these estimates because they set a baseline that depends only on the data and not on analysis to estimate detection probability and availability.
DM/DC: agreed.

PH: P31: Detection function not monotonically non-increasing is OK
That may be so theoretically but it goes against good practice for line transect surveying.
DM/DC: while convention and practicality would often suggest detection probability should be higher nearer the trackline, why should that be regarded as better practice than having higher detection rates elsewhere within the transect width? From an estimation perspective, it makes no difference provided sufficient flexibility is included in the form of the detection function that is fit to the data. From a design perspective, accepting that g(0)<1, good practice would be to maximise the overall probability of detecting a group if it's within the survey transect, not just ensuring it's highest along the trackline. For example, guarding the trackline and having a very high detection rate there is not very helpful if little effort is devoted elsewhere within the transect width so that the detection function drops of very quickly as distance increases.

PH: P36: Additional covariates not considered further in detection function analysis
An additional reason is to improve precision. For the top model, precision is the same for the best (full) model(CV=0.0818) as the base model (CV-0.0813) [Table 8] but improves from CV=0.0965 to 0.0905 for the second ranked model [Table 9].
DM/DC: an improvement in precision is not guaranteed. For example, a number of the more complex models ranked higher than the base model in Tables 8 and 9 have larger CV's for estimated abundance. Indeed, typically SE's for parameter estimates increase as a greater number of parameters are estimated because the information in the data is being spread more thinly.

PH: P42: Dive data availability correction – time within field of view

This is rather vague. As mentioned above, t varies as a function of perpendicular distance. Usually, in such calculations, t is the time in view on the transect line because g(0) is being considered. Here, however, for the left truncated datasets, it is effectively g(0.071km). At the least, the authors should give a bit more information for what 6 seconds on average means and also how sensitive the estimated probability (Pa) is to variation in t.

DM/DC: t=6 was the average for objects at different distances from the trackline. This value was used given that availability is applied to all groups within the transect regardless of their perpendicular distance. The effects of alternative values were considered in a previous interim report, with a difference of about 0.02-0.03 for every 3 seconds. As the previous value of t=6 had been accepted it was the only value used and reported on in the final analysis. While not perfect, it is likely more realistic than the instantaneous availability estimate (i.e., t=0) that has been used previously for Hector's dolphins.

PH: P42: Time at or near the surface:
This is also rather vague. It is critical that the definition for "available" is the same as realized on the surveys themselves. Telemetry data for harbour porpoise in the North Atlantic (a not dissimilar species) show that there is a sharp increase in the proportion of time spent at 0m (visible on the surface) to 0-1m, 1-2m, etc.

No information is given on what "on or near the surface" means, nor on the proportion of sightings on the surface or just under the surface. A mismatch in the application of this probability could potential cause considerable bias. Which direction the bias is depends on whether the availability correction was too much or too little, compared to what was seen on the survey.

DM/DC: we have clarified our definition in the text. Basically it is the time for which a dolphin is visible to an observer in the helicopter. We are fully aware of the caveats around such data and concerns about how representative that information is about availability relative to the actual survey. Indeed, it was such concerns that lead us to trial the circle-back procedure in an attempt to more closely replicate actual survey conditions. Also see our response to your major comments.

PH: P44: Availability estimates from dive cycles
This regional variability seems quite high given the SEs. Is there any information about what could cause this? Presumably methods used to collect the data were the same in all regions.
DM/DC: consistent methods were used in all regions. The effects may be due to differences in water depth, temperature or local ecosystems. Understanding why such differences might exist, however, was outside of the contract and have not been explored.

PH: P50: Availability estimates from circle-back
The range of values over the different regions is much higher in winter than in summer. It is even wider for the reduced winter dataset. The Appendices show that CVs were also higher for winter than summer, but the sample size is not much less in winter than summer. Why so much more variability in winter?
DM/DC: greater regional variation in the estimates in winter are due to a more pronounced regional effect in the data resulting in the models that included a regional effect having higher model weights compared to the summer circle-back data (e.g., see Tables J.1 and J.14). As such, the regional effect models have a greater contribution to the model averaged estimates in winter, resulting in more defined regional differences.

PH: P55: Abundance estimates

There generally seems to be a bigger difference between full and reduced datasets in winter than in summer. Why should this be? Because there is more variability in the winter estimates (bigger CVs)?

DM/DC: this aspect has not been fully explored (beyond error checking) as seeking an explanation will not change the results.